AD-A186 774 INTERACTION OF THE COLD CONVEYOR BELT WITH POLAR JET STREAKS(U) AIR FORCE INST OF TECH WRIGHT-PATTERSON AFB OH W D NICHOLAS 1987 AFIT/CI/NR-87-44T 1/2

UNCLASSIFIED F/G 4/2 NL

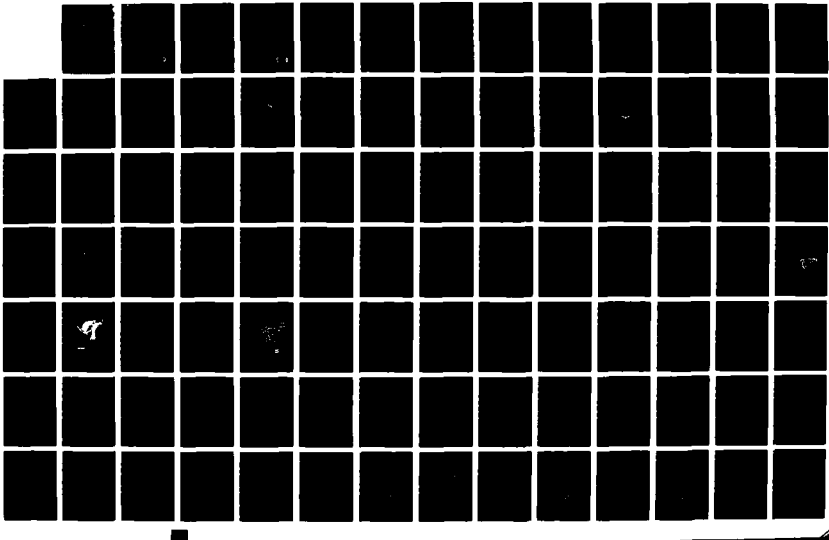

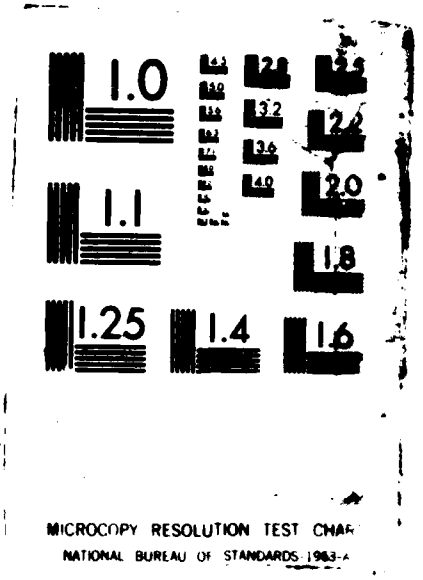
1.0
1.1
1.25
1.4
1.6
1.8
2.0
2.2
2.8
3.2
3.6
4.0
MICROCOPY RESOLUTION TEST CHAR
NATIONAL BUREAU OF STANDARDS 1963-A

INTERACTION OF THE COLD CONVEYOR BELT WITH POLAR JET STREAKS

WILLIAM DOUGLAS NICHOLS, B. S.

A Thesis Presented to the Faculty of the Graduate School
of Saint Louis University in Partial Fulfillment of
the Requirements for the Degree of
Masters of Science (Research)

1987

SECURITY CLASSIFICATION OF THIS PAGE (When Data Entered)

REPORT DOCUMENTATION PAGE

READ INSTRUCTIONS BEFORE COMPLETING FORM

1. REPORT NUMBER: AFIT/CI/NR 87-44T	2. GOVT ACCESSION NO.
3. RECIPIENT'S CATALOG NUMBER	
4. TITLE (and Subtitle): Interaction Of The Cold Conveyor Belt With Polar Jet Streaks	5. TYPE OF REPORT & PERIOD COVERED: THESIS/DISSERTATION
	6. PERFORMING ORG. REPORT NUMBER
7. AUTHOR(s): William Douglas Nichols	8. CONTRACT OR GRANT NUMBER(s)
9. PERFORMING ORGANIZATION NAME AND ADDRESS: AFIT STUDENT AT: Saint Louis University	10. PROGRAM ELEMENT, PROJECT, TASK AREA & WORK UNIT NUMBERS
11. CONTROLLING OFFICE NAME AND ADDRESS: AFIT/NR WPAFB OH 45433-6583	12. REPORT DATE: 1987
	13. NUMBER OF PAGES: 149
14. MONITORING AGENCY NAME & ADDRESS(if different from Controlling Office)	15. SECURITY CLASS. (of this report): UNCLASSIFIED
	15a. DECLASSIFICATION/DOWNGRADING SCHEDULE

16. DISTRIBUTION STATEMENT (of this Report)

APPROVED FOR PUBLIC RELEASE; DISTRIBUTION UNLIMITED

17. DISTRIBUTION STATEMENT (of the abstract entered in Block 20, if different from Report)

18. SUPPLEMENTARY NOTES

APPROVED FOR PUBLIC RELEASE: IAW AFR 190-1

Lynn Wolaver 17 May 87

LYNN E. WOLAVER
Dean for Research and
Professional Development
AFIT/NR

19. KEY WORDS (Continue on reverse side if necessary and identify by block number)

20. ABSTRACT (Continue on reverse side if necessary and identify by block number)

ATTACHED

DD FORM 1 JAN 73 1473 EDITION OF 1 NOV 65 IS OBSOLETE

SECURITY CLASSIFICATION OF THIS PAGE (When Data Entered)

(1)

INTERACTION OF THE COLD CONVEYOR BELT WITH POLAR JET STREAKS

WILLIAM DOUGLAS NICHOLS, B. S.

A Thesis Presented to the Faculty of the Graduate School
of Saint Louis University in Partial Fulfillment of
the Requirements for the Degree of
Masters of Science (Research)

1987

INTERACTION OF THE COLD CONVEYOR BELT WITH POLAR JET STREAKS

WILLIAM DOUGLAS NICHOLS, B. S.

A Digest Presented to the Faculty of the Graduate School
of Saint Louis University in Partial Fulfillment of
the Requirements for the Degree of
Masters of Science (Research)

1987

DIGEST

Evaluation of the interaction of the low level Cold Moist Conveyor Belt (CMCB) with upper level jet streaks is accomplished using isentropic surfaces. Primary goals are: 1) to assess where the CMCB flows with respect to the low level flow and upper level jet streak; 2) to demonstrate that the CMCB plays a part in the transverse circulations for the upper level jet streak entrance and exit regions; and 3) to isolate which physical parameters play an important role in modifying the low level transverse circulations of the CMCB as related to upper level jet streaks.

Three case studies illustrate the relationship of the CMCB with jet streaks. Isentropic cross-sections and soundings in the CMCB determine an appropriate isentropic surface within in the CMCB. Streamline analysis and selected trajectories taken from isentropic surfaces in the CMCB reveal two branches to the CMCB.

Langrangian computations of potential energy, psi, and omega, along with Eularian computations of omega for isentropic surfaces in the CMCB, are taken. Results

reveal a positive correlation between the easterly CMCB with the lower level of the indirect thermal circulation for exit regions of jet streaks. The entrance region of the jet streaks also showed evidence of a direct thermal circulation in lower levels as the CMCB turned south and recrossed the jet axis trough.

Attempts to identify certain physical forcing mechanisms related to jet streaks revealed mixed results. Comparisons of the orientation of vertical motion fields in CMCB to jet streaks indicated varied contributions by diffluence, warm advection, jet streaks, and curvature in jet exit region. In jet entrance region, more consistent contributions by cold air advection, confluence, and curvature were observed compatable with several theoretical and observational studies on curved jet streaks in the entrance region.

COMMITTEE IN CHARGE OF CANDIDACY:

Associate Professor James T. Moore,
Chairperson and Advisor

Professor Gandikota V. Rao

Assistant Professor Lawrence Coy

ACKNOWLEDGEMENTS

The author wishes to express his deepest thanks and appreciation to Dr. James T. Moore for his caring guidance and support during this project. He also extends his appreciation to Dr. Gandikota V. Rao and Dr. Lawrence Coy for their helpful comments and suggestions. Special thanks go to Captain Harold Elkins (USAF) and Rich Molinaro for their help in computer programming along with all the other members in the Gold Team room.

Appreciation is also extended to the United States Air Force, particularly the Air Force Institute of Technology and Air Weather Service for their financial, technical, and moral support. In particular, the author would like to thank Major James P. Millard and Captain Miklos Varsanyi of the United States Air Force Environmental Technical Applications Center. Finally, the author would like to express his deepest appreciation and gratitude to his wife, Patricia and his family for their prayers and continued support, without which this study would not have been possible.

TABLE OF CONTENTS

TABLE OF CONTENTS (CONTINUED)

TABLE OF CONTENTS (CONTINUED)

LIST OF FIGURES

LIST OF FIGURES (CONTINUED)

LIST OF FIGURES (CONTINUED)

LIST OF FIGURES (CONTINUED)

1. INTRODUCTION

1.1 Historical Background of Conveyor Belts

The concept of conveyor belts transporting momentum, heat, and moisture within the circulations of an extratropical cyclone stems from the English school during the late 1960's. Using a combination of radar and synoptic data Harrold (1973) and Browning (1974) described conveyor belts as being primarily responsible for the formation and distribution of precipitation in English cyclones. Harrold used isentropic analyses based on the earlier work of Green, et al. (1966) to portray the flow through cyclones. He identified three fields of motion (Fig. 1). He didn't label each flow but preferred to describe their kinematic features and apply them to six synoptic cyclone situations in Great Britain.

Carlson (1980) applied the theory of conveyor belts to the United States which had earlier been labeled as warm and cold conveyor belts by Browning (1974). Including them into a schematic model of airflow for a midlatitude cyclone, Carlson used relative-wind isentropic techniques to explore the relationship and configuration of the two belts for a single Eastern

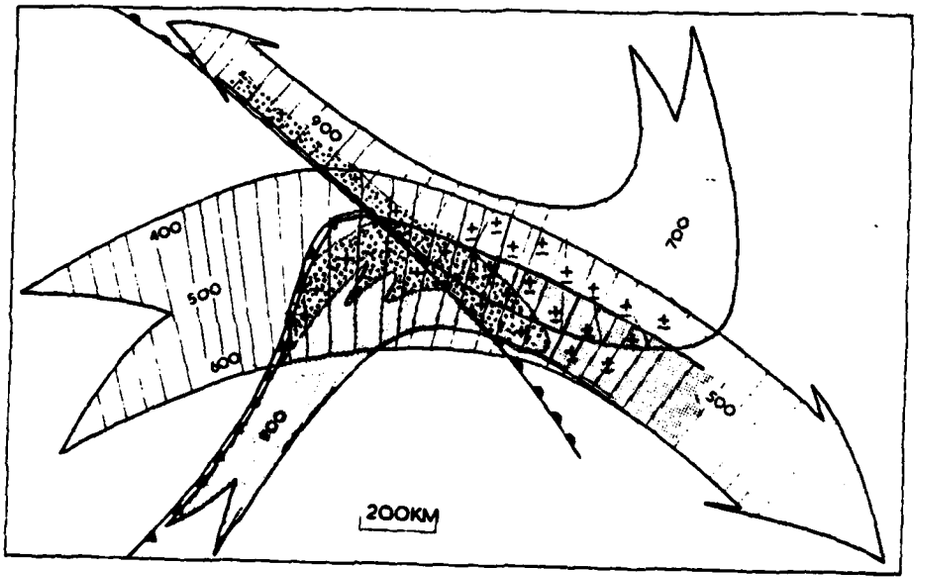

Figure 1. Schematic representation of the features of the large-scale flow which determine the distribution of precipitation at the surface. Two westerly flows are ascending with stippled area indicating precipitation. Descending dry easterly flow ahead of cold front results in evaporation of leading edge of precipitation before it reaches the ground. (Harrold, 1973).

U. S. extratropical cyclone. He labeled the westward flowing stream the cold conveyor belt and the northward flowing stream the warm conveyor belt (Fig. 2). His model relates boundaries to each belt while describing the vertical motion encountered during their evolution. Carlson's purpose was to account for the sharp boundaries of cloud and weather patterns seen on satellite and to explain conceptually the westward expansion of a comma cloud as indicated by satellite studies (Weldon, 1979). Carlson accomplished this by contending that the cold conveyor belt passed under the warm conveyor belt northeast of the low turning anticyclonically northeast away from the low resulting in an "open" wave.

Browning (1986) applied conveyor belts to a wider range of European synoptic cyclones illustrating the vertical motion and precipitation fields of the belts for each type of cyclone and comparing them with observed radar and satellite data. One specific type of cyclone, the cold air vortex, was shown as a "closed" system with the cold conveyor belt turning cyclonically around the low to the west. Also of note was Browning's inclusion of fallen precipitation into the cold conveyor belt. He based this upon growing observational evidence

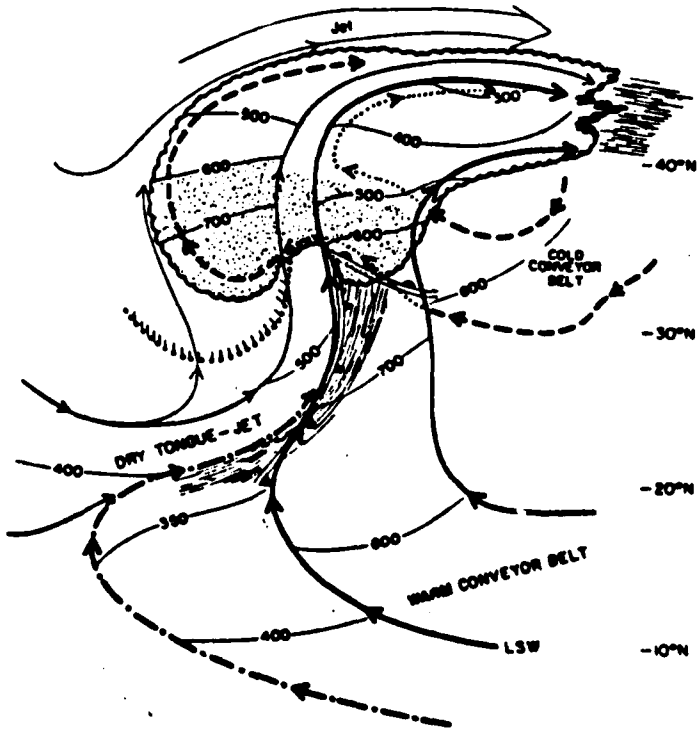

AIRFLOW THROUGH MID-LATITUDE WAVE CYCLONE

Figure 2. Schematic composite of airflow through midlatitude cyclone. Heavy dotted lines depict airflow at top of warm conveyor belt. Dashed flow is the cold conveyor belt with dotted lines where it lies underneath the warm conveyor belt. Dot-dashed flow is air from tropical midlevels with thin solid streamlines indicating dry air originating at upper levels west of trough. Thin solid lines are heights of airstream (mb). Scalloping is the border of mid and high level clouds with sustained precipitation shown by stippling. The edge of low level stratus is shown by curved border of small dots with tails and streaks indicate high thin cirrus. (Carlson,1980).

of this phenomenon by Matsumoto (1982), Browning and Hill (1985), and others. All previous models had described the warm conveyor belt as the main producer of precipitation.

1.2 Historical Background of Jet Streaks

With the advent of high altitude aircraft and radiosondes in the 1930's came the discovery of jet streams near the tropopause along with areas of associated wind maxima called jet streaks. In the ensuing years considerable research was done to explain their dynamics. Several authors, including Bjerknes (1951), Riehl (1952), Murray and Daniels (1953), Newton (1959), Uccellini and Johnson (1979), and Shapiro and Kennedy (1981) were able to identify ageostrophic motion through jet streaks resulting in a satisfactory explanation of how air flows through a finite-length, straight jet streak (Fig. 3). Their results revealed areas of convergence and divergence caused by the cross-contour component of the ageostrophic wind as air parcels first accelerated and then decelerated through a jet streak. Later, airflow through a curved jet was schematically illustrated by Shapiro and Kennedy (1981)

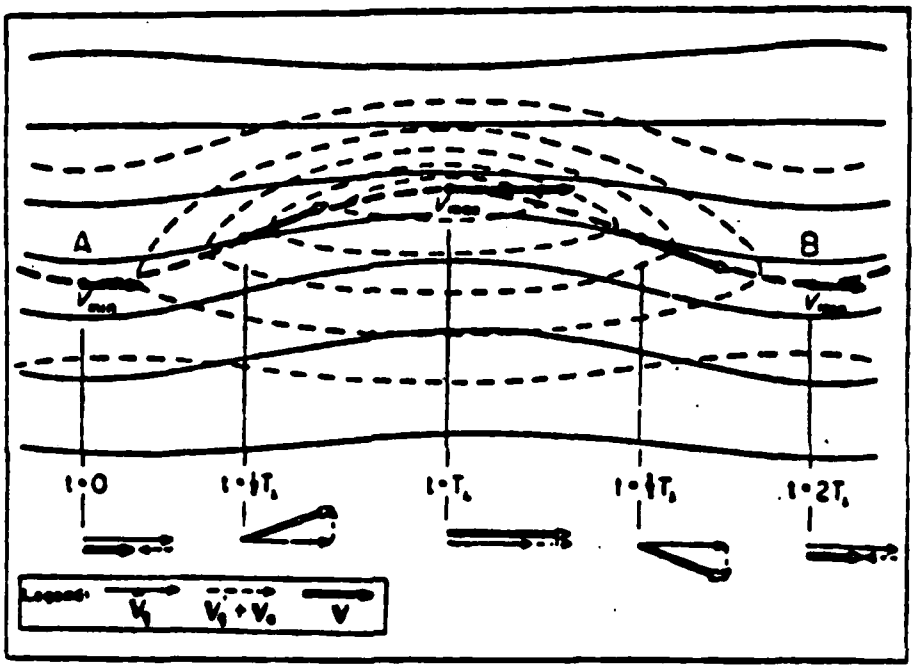

Figure 3. Schematic contours (solid), isotachs (thin dashed) and vector winds illustrating an ageostrophic oscillation for an air parcel propagating through a jet streak (Newton, 1959).

who described how air parcels develop along-contour ageostrophic components due to changes in curvature in an infinite-length of constant speed jet streak. From this, corresponding areas of divergence and convergence associated with wind maxima could be explained (Fig. 4).

1.3 Historical Background of Jet Streak Numerical Modeling

Relating these theoretical ideas to observational studies is a primary objective of meteorology and one way to do this is through the use of numerical models. Several recent upper-level frontogenetical models by Buzzi et al. (1977), Mudrick (1974), and Newton and Trevisan (1984) have yielded favorable results relating the simulated kinematic fields of upper level jet streaks to those corresponding to conventional synoptic cyclone models such as Bergeron (1952) and Palmen and Newton (1969). Other studies by Newton (1956), Reiter (1959), and Hovanec and Horn (1975) have indicated that jet streaks play an important role in the development of cyclones.

Recently, several studies indicated that under

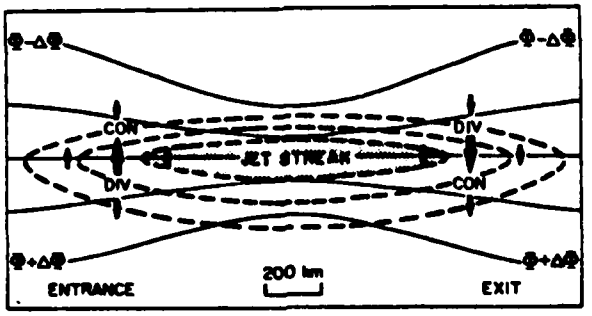

(a)

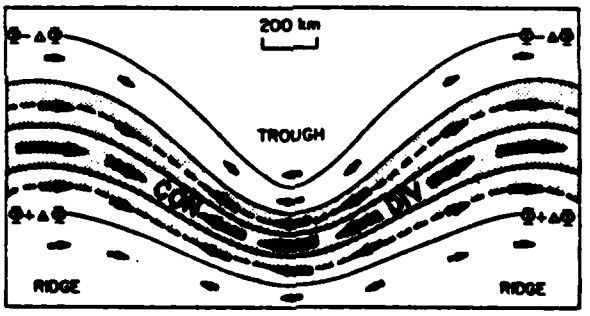

(b)

Figure 4. Schematic representation of the ageostrophic motions (heavy arrows) and associated patterns of convergence (CON) and divergence (DIV) in the vicinity of (a) a straight jet streak in the absence of along-contour thermal advection and (b) a uniform jet stream within a stationary synoptic-scale wave. Solid lines indicate geopotential height of a constant pressure surface. Dashed lines are isotachs with maximum wind speed shaded (Shapiro and Kennedy, 1981).

certain favorable conditions, upper-level fronts and jets may be directly related. Cahir (1971), Uccellini and Johnson (1979), and Uccellini (1980) couple upper and lower level jets dynamically using the transverse circulations created by jet streaks. They consider the interaction of the low level jet with these transverse circulations important to the initial organization of severe convective storms. Shapiro (1983) presents a hypothetical schematic illustration of superimposed surface fronts and their associated transverse ageostrophic circulations showing areas favorable and unfavorable for the formation of convective storms.

1.3 Statement of the Problem

Relating theoretical and conceptual ideas has been of prime importance in meteorology since it helps us to better understand the complex non-linear processes in the atmosphere. Some research into the mechanisms and dynamics associated with convective storms in the warm sector of extratropical cyclones has been done, by Uccellini (1980), Shapiro (1983), and Wetzal et al. (1983). However, studies into the relationship between cold air flow in an extratropical cyclone and jet

streaks has been very limited. Satellite observational studies by Leese (1962), Weldon (1979), and Barr et al. (1966) have indicated that cold air flow in the comma cloud rotates cyclonically around the low center. However, Harrold (1973) and Browning (1974) conveyor belt models give no indications as to what happens to the cold air flow after it passes by the low center. Carlson's (1980) schematic model indicates that the top portion of the cold conveyor belt turns anticyclonically away from the low after passing by to the north but gives no direct explanation as to what happens to the bottom half. Later, Browning (1986) modified the cold conveyor belt for a variety of synoptic situations indicating that the cold conveyor belt could "wrap" around the cyclone center in the case of cold air vortices.

Air motion within the cold conveyor belt (CCB) was considered to be descending toward the low by Browning (1971) and Harrold (1973) for maritime English cyclones. Browning (1986) indicated that rising motion could occur in the CCB for European cold air vortices which agreed with the vertical motion satellite studies by Leese (1962) and Barr et. al. (1966). Carlson (1980) indicated that a rising CCB occurs for U. S. cyclones.

Interaction between upper and lower level jet streaks as related to convective storms has been studied by Fawbush and Miller (1953, 1954), Petterson (1956), Newton (1967), Whitney (1977), and Uccellini and Johnson (1979) among others. Meanwhile, documentation into the relationship of the cold conveyor belt flow to upper-level jet streaks has been limited. Carlson (1980) relates the southern edge of the comma cloud shield as being somewhere north of the jet streak axis but makes no attempt to relate any interaction between the two.

1.4 Objectives of this Study

We intend to use isentropic analysis to identify the CCB for three occluded synoptic cases in the eastern U. S.. After identifying the belts we will determine and follow the evolution of the cold conveyor belts as the cyclones mature noting possible changes in its structure using soundings analysis and isentropic cross sections. Using isentropic trajectories and streamline analysis we will determine where the conveyor belt goes as it passes by the low center. Also we wish to determine and describe various kinematic motions within

the flow of the CCB at different locations and periods of time.

After identifying the CCB and computing specific kinematic parameters, these results will be applied to answer three specific questions:

1. Where does the CCB go and what is its relationship with respect to the position of the upper-level jet streak?

2. What role does the CCB play in the transverse circulations associated within jet streaks?

3. What modifying roles do the physical processes of warm and cold air advection and confluence/diffluence, play in the lower half (CCB) transverse circulations of jet streaks?

To accomplish these objectives, after identifying the CCB and describing where it goes, we will compare its position with the location of the upper level jet streak(s) of the storm. Then we will attempt to correlate the position of the CCB with the entrance and exit regions of the upper level jet streak. Using computed results of changes in potential energy, pressure, and Montgomery Streamfunction (psi) derived from isentropic trajectories within the CCB, we will show how the CCB is a positive contributor to the direct

(indirect) thermal circulations associated with jet streak entrance (exit) regions. Then, by comparing computed Eularian vertical motion fields on an isentropic surface in the CCB to the various corresponding vertical motion fields related to upper-level jet streaks, we will determine how closely these relationships compare with various modifying aspects of along-front thermal variations to the four-quadrant thermal variation of jet streak theory as explained by Keyser and Shapiro (1986).

We also intend to show the coupling of the CCB with jet streaks by calculating changes in the Montgomery streamfunction using trajectories and following streamlines. From these changes, we intend to relate the implied ageostrophic components in the cold conveyor belt to the corresponding ageostrophic components of the transverse circulations processes of jet streaks. This will help show that the cold conveyor belt is a possible participant of the transverse circulation process of jet streaks as identified by Riehl (1952), Reiter (1969), Cahir (1971), Uccellini and Johnson (1979), and Keyser and Shapiro (1986). To accomplish these tasks, we must familiarize ourselves with jet streaks.

2. BACKGROUND

2.1 Transverse circulations related to jet streaks

Transverse circulations develop in straight jet streaks due to the acceleration and deceleration of air parcels as they enter and exit jet streaks as shown by Riehl (1963), Johnson (1970), and Cahir (1971). In the entrance region of a jet (Fig. 5a) an air parcel approaches the confluent Montgomery streamfunctions (psi) resulting in an increasing geostrophic wind. For the parcel to adjust to this imbalance it crosses to lower values of psi to accelerate and match its speed with that of the environment. This results in a cross-stream ageostrophic component to the left creating convergence to the left of the jet axis and divergence to the right (Fig. 5b) in the entrance region. This process creates a direct transverse circulation as cold air descends to the left and warm air rises to the right of the jet axis, thereby converting potential energy to kinetic energy. As the parcel reaches the exit region, diffluent heights result in a decreasing geostrophic

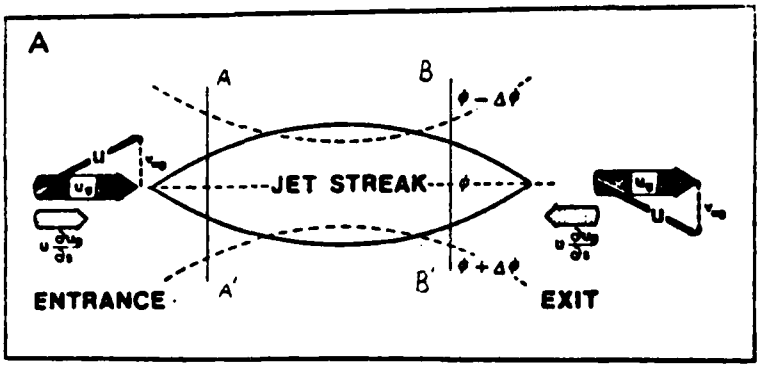

(b) (c)

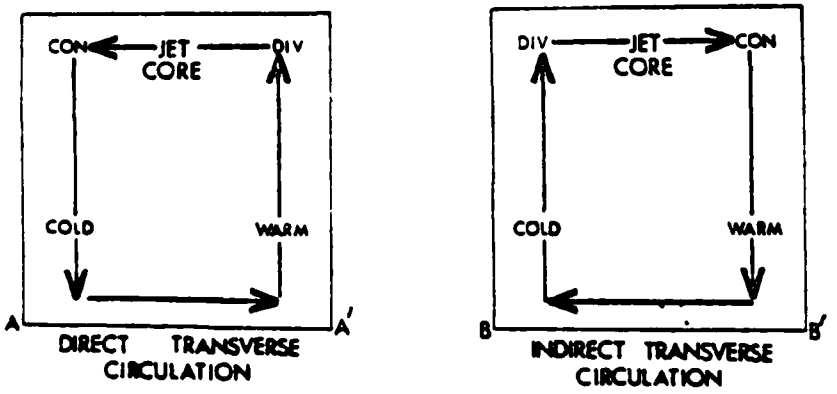

Figure 5. Schematic of transverse component (v_{ag}) forced by the along-stream variations of pressure gradient force at jet streak level. (b), (c) normal plane across jet entrance (exit) region from A-A'(B-B') showing showing respective direct (indirect) transverse circulation (Johnson, 1970).

wind. For the parcel to match this deceleration it must cross to higher heights creating an ageostrophic cross-contour component to the right with reversed areas of convergence and divergence (Fig. 5c). Due to this reversed pattern, an indirect circulation develops as cold air rises and warm air sinks converting kinetic energy to potential energy. Both the direct and indirect circulations are caused by imbalances of the air parcels as they move through the entrance then exit regions. This process has been proved to exist by the work of Rossby (1949), Cahn (1945), and Sawyer (1956).

In a more recent study of transverse circulations and sub-synoptic scale precipitation bands, Cahir (1971) simulated direct and indirect circulations using a two-dimensional primitive equation model mapped on a vertical plane normal to a propagating jet streak. Applying this model to an actual case study (Fig. 6), Cahir showed quantitatively the upper and lower components of the indirect circulation using horizontal transverse components across the jet axis and opposing vertical motions to the right and left of the jet axis. By increasing the relative humidity by 30%, he showed that the added latent heat released nearly doubled the magnitude of the upward vertical motion on the cyclonic

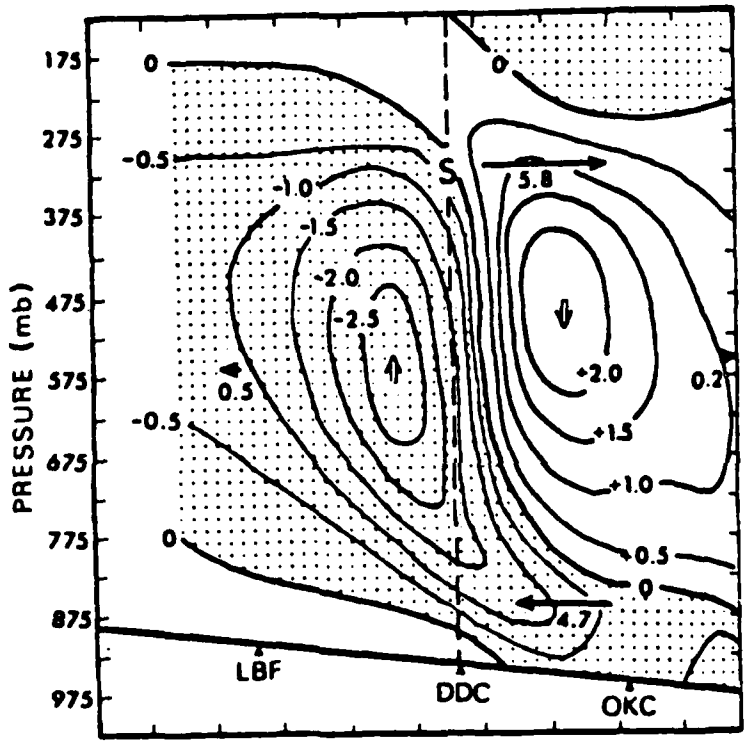

Figure 6. Indirect circulation simulated by primitive equation model mapped on cross section through exit region of a jet streak. Solid isopleths are vertical motion (μb s^{-1}) with upward vertical motion stippled. Arrows with centered magnitudes indicate horizontal transverse components (m s^{-1}) (Cahir, 1971).

side of the jet, thus enhancing the indirect circulation. Cahir applied his model to numerous case studies and emphasized that sub-synoptic scale precipitation bands are caused by the upward vertical branches of both direct and indirect circulations associated with jet streaks.

Uccellini and Johnson (1979) coupled the low level jet with the exit region of a propagating straight jet streak using an application of the isallobaric wind equation with the restrictive assumption of frictionless, adiabatic flow in isentropic coordinates. The ageostrophic velocity can be written as:

$$\vec{V}_{AG} = f^{-1}\left[\underbrace{\hat{k} \times \frac{\partial \vec{V}_G}{\partial t_\theta}}_{\text{Term A}} + \underbrace{\vec{V} \cdot \nabla_\theta (\hat{k} \times \vec{V}_G)}_{\text{Term B}}\right] \qquad (1)$$

From a hybrid isentropic-sigma coordinate numerical model, developed by Uccellini et. al. (1979), the isallobaric wind in the lower troposphere, term A, dominates (Fig. 7a), representing the ageostrophic components of the lower troposphere return flow while at upper levels, term B, the inertial advective ageostrophic component of the wind dominates (Fig. 7b)

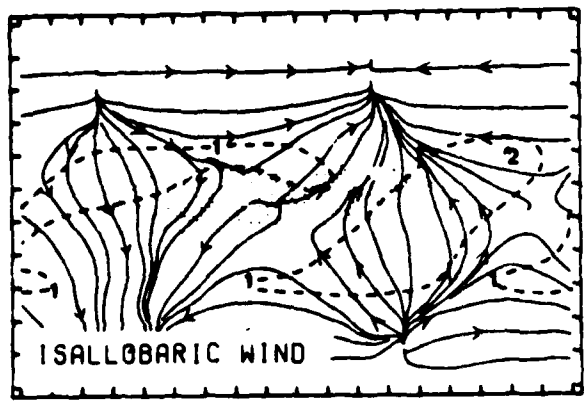

(a)

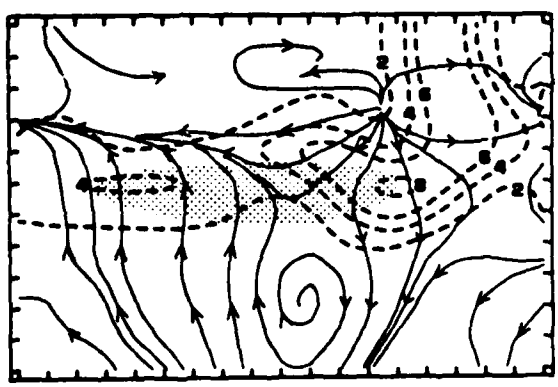

(b)

Figure 7. (a) Model simulated ageostrophic component related to the isallobaric wind term (Term A, Eq. (1)) on 340°K surface. Shaded region represents jet streak (u component >40 m s^{-1}), (b) Same as (a) except for inertial-advective term (Term B, Eq. (1). Marks along border represent 275 km spacing (Uccellini and Johnson, 1979)

giving the main portion of the upper troposphere ageostrophic flow. The total mass-momentum adjustments through jet streaks are composed of both geostrophic and ageostrophic components creating the total mass flux divergence profile throughout a jet streak (Fig. 8). These match the four quadrant divergence pattern shown in Fig. 5a for a straight jet streak thus indicating that the transverse circulations related to jet streaks involve both the ageostrophic and geostrophic component at any one time.

To the author's knowledge, application of the isallobaric wind equation at low levels for curved flow has not yet been applied. Using the two cell divergence pattern at upper levels for purely curved flow as shown in Fig. 4b. and assuming the isallobaric component dominates at low levels, the ageostrophic wind is now composed of the along-contour component caused by curvature. Conceptually then, if both terms in (1) retained their respective magnitudes, for lower levels this would create a northeasterly isallobaric-dominated wind from the top of the ridge in Fig. 5 to the area of divergence at the inflection point ahead of the trough. Also, a southwest wind would occur from the inflection point behind trough axis to the divergence area ahead

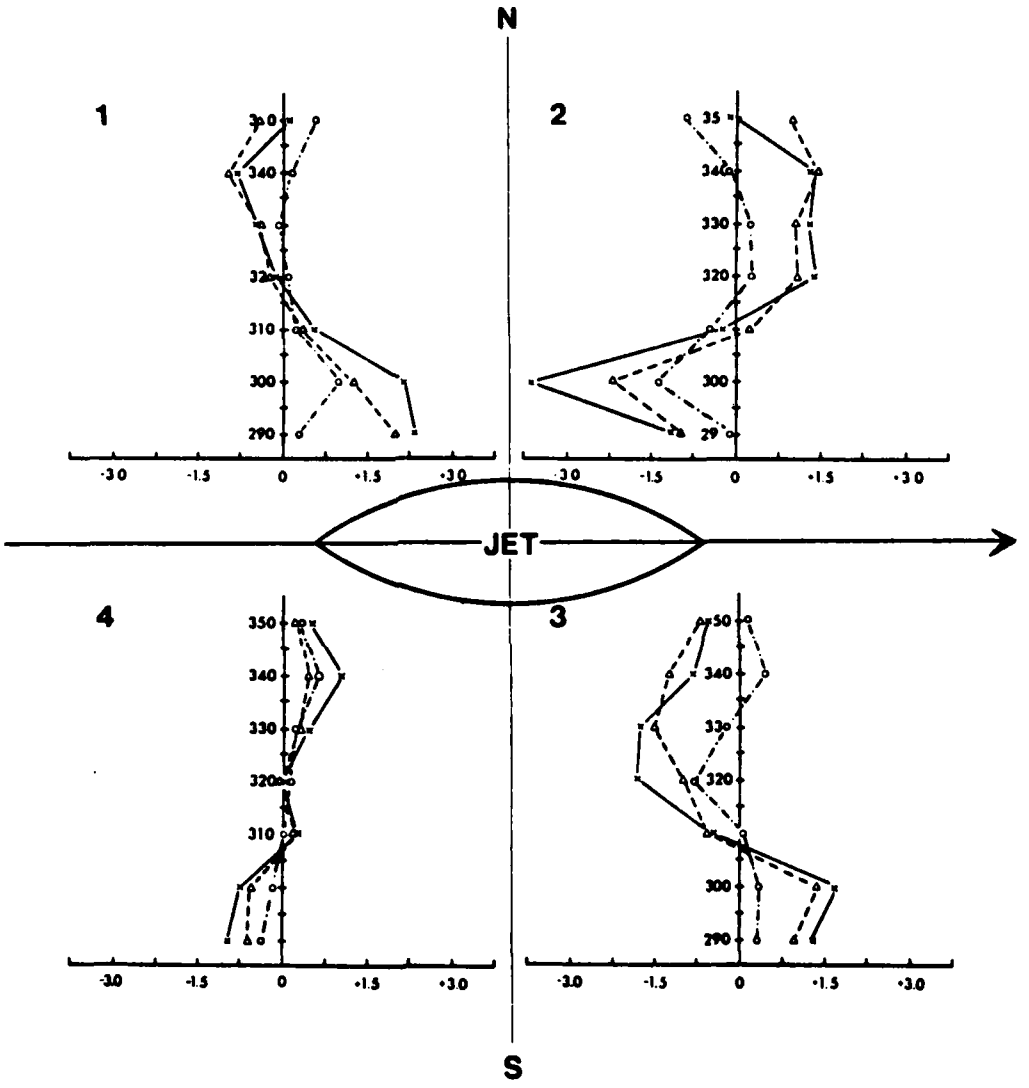

Figure 8. Modeled vertical profiles for averaged mass flux divergence (x10^1 g $m^{-2}s^{-1}$)[total (solid), ageostrophic (dashed), geostrophic (dot-dashed)] in four quadrants surrounding jet streak (Uccellini and Johnson, 1979).

of the trough. At upper levels, if the inertial-advective term still dominated, the flow would be reversed, showing the upper portion of the ageostrophic flow with a southwesterly/northeasterly component overlaying the low level northeasterly/southwesterly ageostrophic flow. This upper level ageostrophic flow for a curved jet was shown to exist and was measured in studies using aircraft at over 60 m/s by Newton and Persson (1962) and over 100 m/s by Shapiro and Kennedy (1981). From this we can create a net flow isallobaric wind for a curved jet streak as shown by Fig. 9.

The isallobaric component of the ageostrophic wind can be written on an isentropic surface as:

$$\vec{V}_{AG} = -f^{-2} \nabla_\theta \frac{\partial \Psi}{\partial t_\theta} \qquad (2)$$

Uccellini and Johnson (1979) used (2) to determine the ageostrophic wind component for a particular parcel by computing changes in the Montgomery Streamfunction for the parcel's trajectory. From this, Uccellini et al. (1984) was able to show the transverse circulation in the President's Day cyclone of 1981.

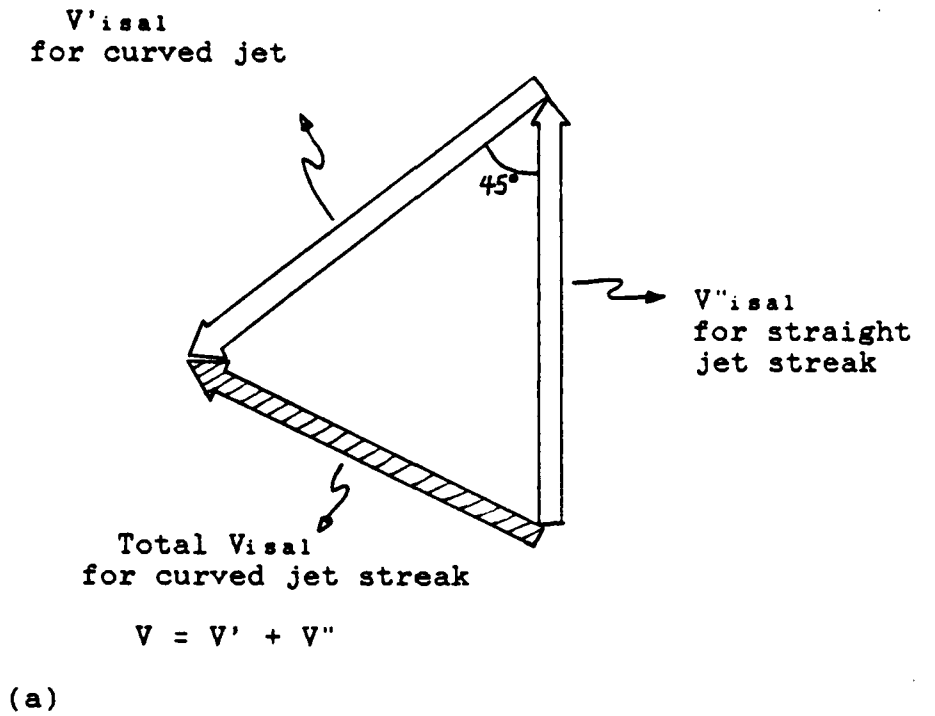

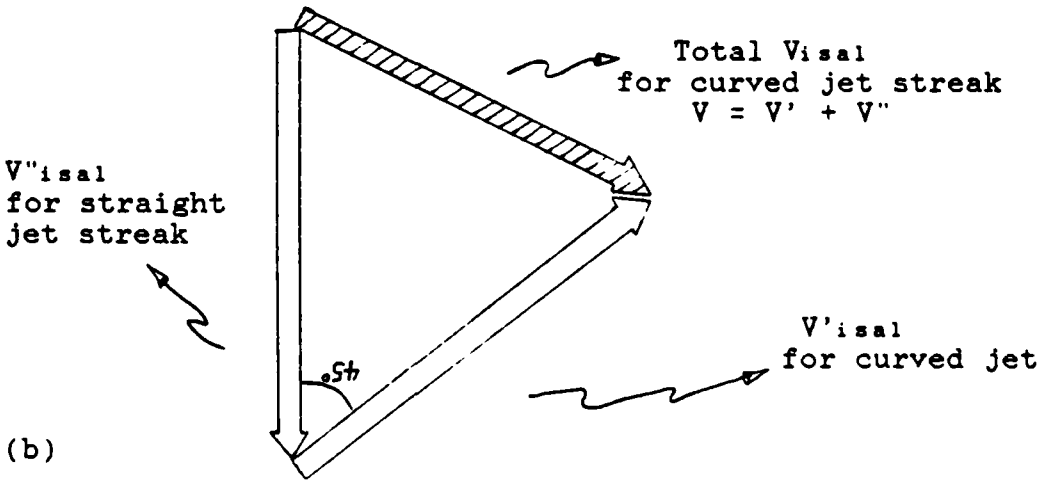

Figure 9. Schematic illustration of the resultant isallobaric wind (stippled) at lower levels for a curved jet streak with jet max at bottom of trough in the (a) jet exit (b) jet entrance region. Taken from combining the along-front and across-front ageostrophic wind components shown in Fig. 4.

2.2 Modifications to transverse circulations

In describing jet-front secondary circulations, the diagnostic ageostrophic circulation equation of Sawyer (1956) and Eliasson (1962) can be utilized to show the various patterns of vertical circulations of ageostrophically-forced secondary circulations. Using the restrictive assumptions of the geostrophic momentum approximation with negligible along-front ageostrophic advection, adiabatic, frictionless conditions and constant Coriolis force, the Sawyer-Eliasson equation can be described for cross-front and vertical gradients of m and theta in a y-p plane as:

$$\left(-\gamma\frac{\partial\theta}{\partial p}\right)\frac{\partial^2\psi}{\partial y^2}+\left(2\frac{\partial m}{\partial p}\right)\frac{\partial^2\psi}{\partial y\partial p}+\left(-\frac{\partial m}{\partial y}\right)\frac{\partial^2\psi}{\partial p^2}+\left(\frac{\partial m}{\partial p}\frac{d\ln\gamma}{dp}\right)\frac{\partial\psi}{\partial y}=-2J_{yp}(u_g,v_g)+\frac{\partial F_x}{\partial p}-\gamma\frac{\partial\dot{\theta}}{\partial y} \qquad (3)$$

where γ is a function of pressure $\gamma=\frac{R}{f\rho_0}\left(\frac{p_0}{p}\right)^{c_v/c_p}$ and the ageostrophic streamfunction ψ is the response which can be determined by the distribution of m and theta (the forcing) where the second order terms of (3) refer to static stability, baroclinity, and inertial

instability, respectively. The response of is a relative minima (maxima) when the forcing terms are positive (negative) and are associated with thermally direct (indirect) circulations (Fig. 10).

From a corresponding analysis of Green's function for a given latitude, it can be determined that only variation in static stability affects the ellipticity of the circulation. Keyser and Shapiro (1986) determined that changes in the transverse circulation, (the response), are due to four physical processes: 1) confluence, 2) diffluence, 3) cold air advection, and 4) warm air advection. A schematic illustration of the effects of these processes are shown in Fig. 11 where the influence of one or more of the above processes affects the classic transverse circulation pattern either to the warm or cold side of the jet streak. Fig. 11c closely approximates the flow near the trough axis with cold air advection. Note how the transverse circulation has been shifted toward the anticyclonic side where the CCB crosses the jet entrance region. Fig. 11d represents warm air advection which occurs as the CCB crosses the jet exit region. Here, again, the transverse circulation has been shifted to the anticyclonic side. Also, as seen in Fig. 11a,

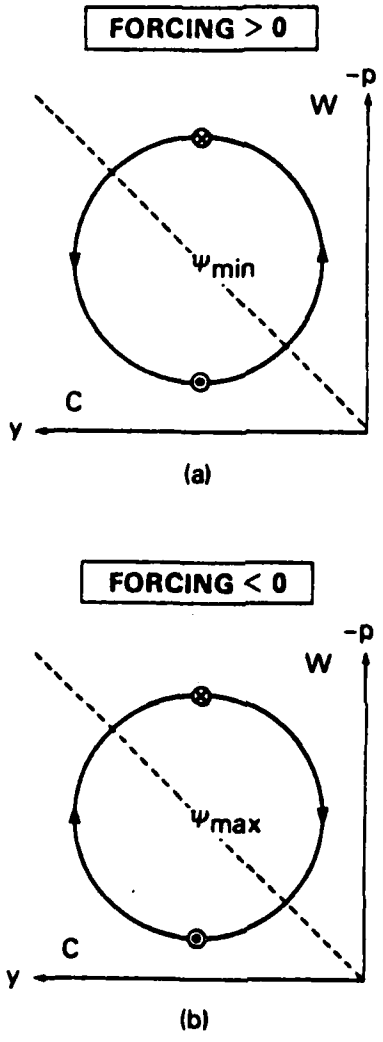

Figure 10. Schematic illustration of sign of forcing and sense of transverse ageostrophic circulation from diagnostic Sawyer-Eliassen equation. Ageostrophic circulation is denoted by solid lines. Dashed lines depict an isentrope separating potentially colder from warmer air. Small circles enclosing x and dot, respectively, indicate along-front wind into and out of the cross section. Transverse circulation is thermodynamically direct in (a), indirect in (b). (Keyser and Shapiro, 1986)

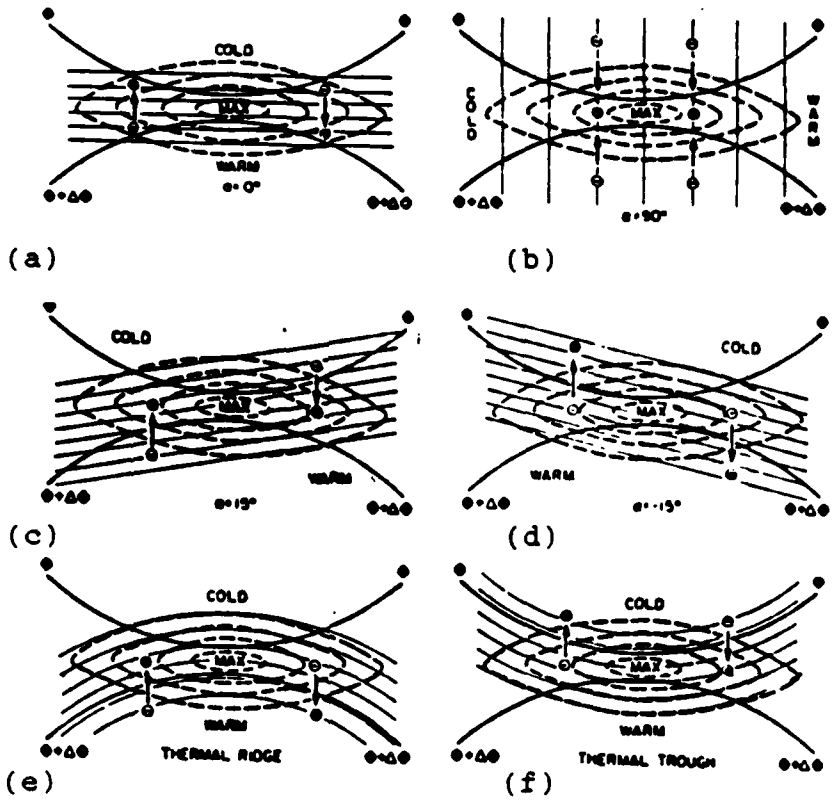

Figure 11. Schematic illustration on a constant pressure surface of various idealized configurations of potential temperature and along-front geostrophic wind for a straight upper-tropospheric jet maximum. Thick solid lines, geopotential height contours; thick dashed lines, isotachs of along-front wind component; solid thin lines, isotherms; thick solid arrows, sense of cross-front ageostrophic wind component; plus and minus signs, vertical velocity, positive downward. (a) pure confluence and diffluence; (b) pure horizontal shear (c)-(f) mixed cases of confluence/diffluence and horizontal shear; (c) along-jet cold advection, (d) along-jet warm advection, (e)jet in thermal ridge, (f) jet in thermal trough. (Shapiro, 1983)

confluence/diffluence in the jet entrance/exit region play a role as do the effects of the thermal ridge/trough shown in Fig. 11e and 11f for an occluded cyclone. The effects of the thermal ridge and trough for an occluded cyclone as specified in Fig. 11 by Keyser and Shapiro (1986) is shown in Fig. 12c of the propagation of a jet streak through a baroclinic wave. It is important to note that at the occluded stage (Fig. 12c) there is cold air advection and confluence in the jet entrance region with slight confluence in the jet core and warm air advection and diffluence in the jet exit region.

Cross sections across the jet axis in the jet entrance region were simulated by a two-dimensional primitive equation model produced by Keyser and Pecnick (1985) to show the total predicted effects across the jet and are shown in Fig. 13 a-c where the transverse ageostrophic circulation and potential temperature for the entrance region of a jet streak are illustrated from a 24-hour integration of a two-dimensional primative equation model of frontogenesis from Keyser and Pecnic (1985). In Fig. 13a, pure confluence shows weak sinking (rising) motion north (south) of the jet. At the level of the cold conveyor belt (below 700mb),

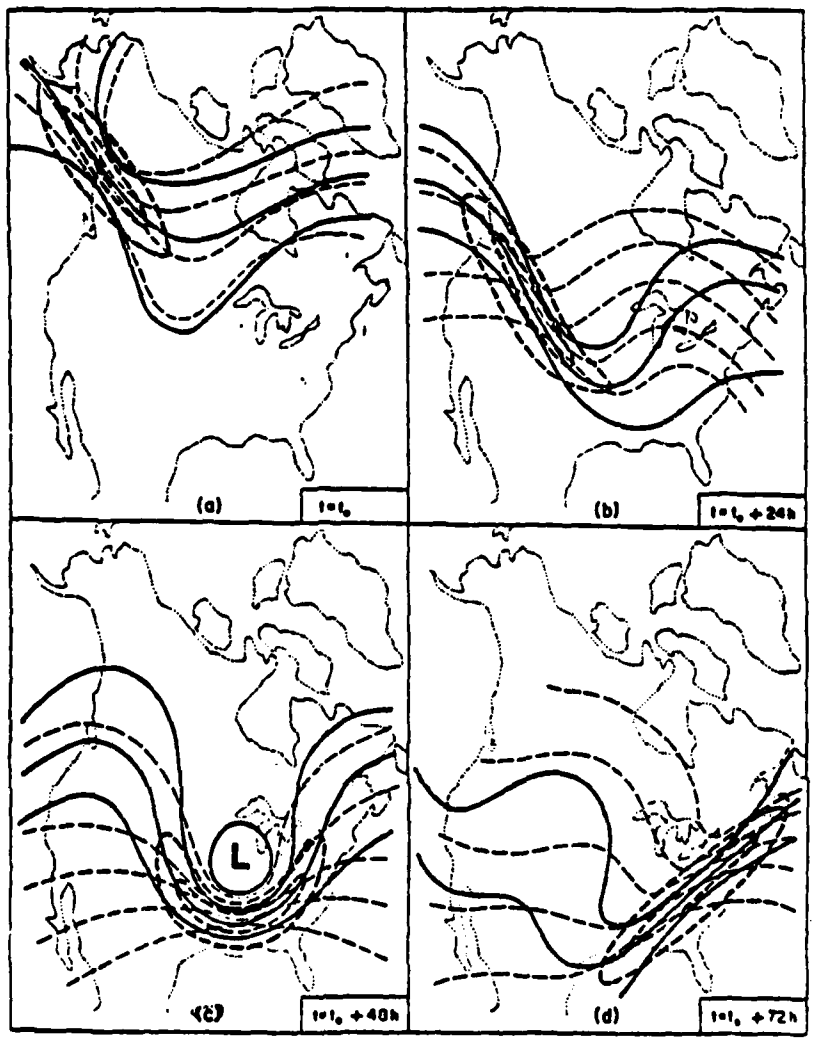

Figure 12. Idealized schematic depiction on a constant pressure surface of the propagation of an upper-tropospheric jet-front system through a midlatitude baroclinic wave over a 72 h period: (a) formation of jet-front in the confluence between mid- and high-latitude currents; (b) jet-front situated in northwesterly flow inflection of amplifying wave; (c) jet-front at the base of the trough of fully developed wave; (d) jet-front situated in southwesterly flow inflection of damping wave. Geopotential height contours, thick solid lines; isotachs, thick dashed ines; isentropes, thin dashed lines. (Shapiro, 1983).

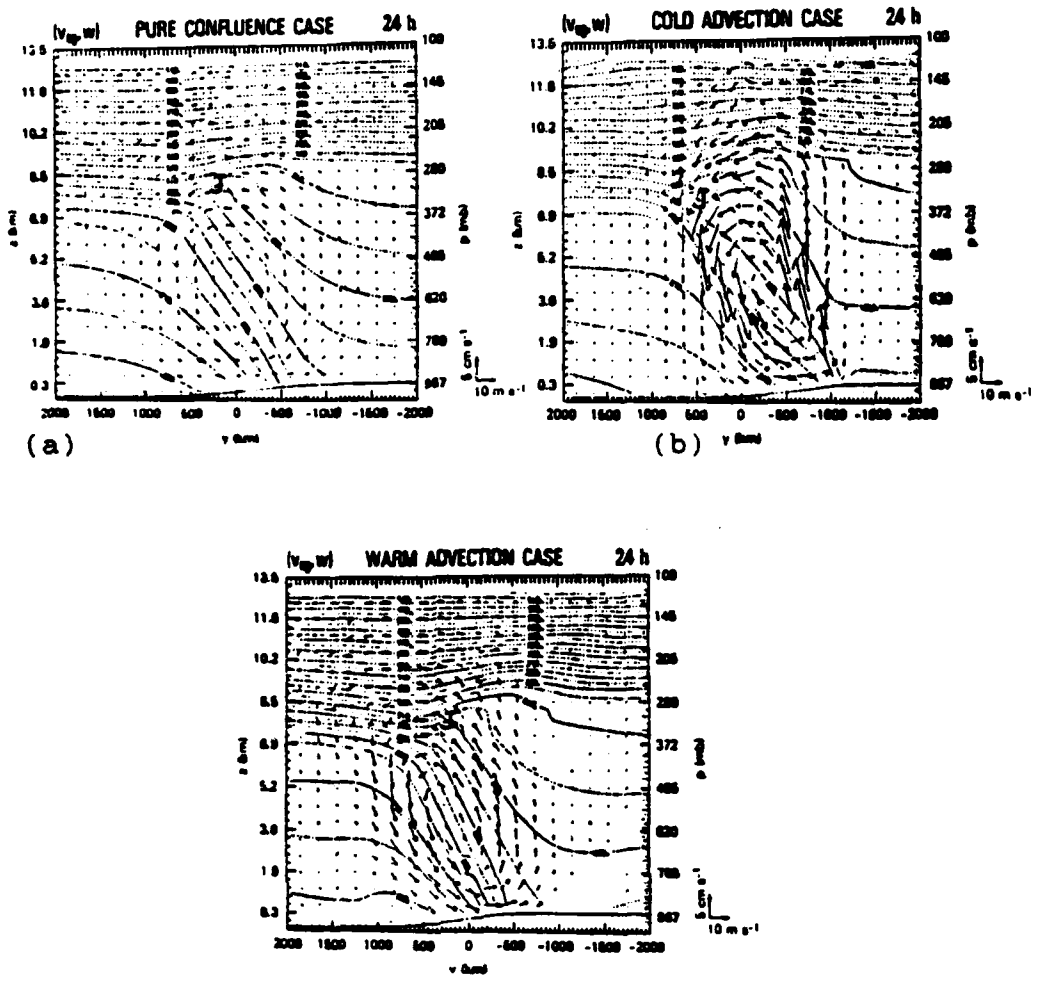

Figure 13. Cross sections of the transverse ageostrophic circulation (v^{ag}, w) and potential temperature in the jet entrance zone after 24 h integration of a two dimensional primitive equation model of frontogenesis; (a) for pure confluence; (b) confluence in the presence of cold air advection; (c) warm air advection with diffluence. Location of Jet axis along-front velocity indicated by J. (Keyser and Pecnic, 1985).

At the level of the cold conveyor belt (below 700mb), the strongest downward motion occurs just to the cyclonic side of the jet axis (y defined as positive for the cyclonic side of the jet). In Fig. 13b, we have strong downward motion under the jet with the strongest downward vertical motion in lower layers south of jet axis and upward vertical motion well south of the jet. Note how the whole transverse circulation has been shifted anticyclonically from its normal position. Hence, cold air advection can increase significantly the sinking motions in jet streaks. Finally in Fig. 13c, warm advection with the transverse circulation straddles the jet axis. Combining these three figures relates well with Fig. 11 a, c, and d, respectively.

2.3 Dynamic modeling of upper-level frontogenesis

So far we have discussed various physical mechanisms in two dimensions. To relate these to the atmosphere's complex three dimensional physical mechanisms we need the use of numerical models. From these models we can relate the relative importance of each mechanism in various parts of the cyclone. An added aspect of modeling can be relating the added affects of

ageostrophic along-contour transverse circulation produced by curvature (Fig. 4b). This can be done using the change in the wind produced by curvature and using:

$$\vec{V}_{GR} - \vec{V}_{G} = - \left(\frac{K V_{GR}}{f} \right) \vec{V}_{GR} \qquad (4)$$

where K is the the curvature parameter (positive for cyclonic turning). The resulting along-contour ageostrophic flow is directed against V_{gr} in a trough (K>0) with subgeostrophic flow, while in the ridge (K>0) the V_{ag} is directed with V_{gr} giving supergeostrophic flow. Curvature vanishes (K=0) at the two inflection points ahead and behind the trough resulting in divergence and convergence at each point, respectively. This results in the two cell pattern produced by curvature versus the four cell pattern for a straight jet streak in Fig. 4a.

From this, we can infer in a qualitative sense the possible three dimensional ageostrophic circulation from a combination of the cross-contour ageostrophic flow caused by changes in wind speed in Fig. 4a and along-contour ageostrophic flow caused by curvature changes (Fig. 4b). For example, in the cyclonically

curved jet in Fig. 12c at the base of a trough, the total ageostrophic transverse circulation and convergence-divergence pattern would be a linear combination of Fig. 4a and 4b since the two patterns are independent of each other in a dynamic sense resulting in a pattern simular to Fig. 11e.

Numerical simulations by Buzzi et al. (1977) of a jet streak in the base of a trough demonstrated the superimposition of these two fields. Using a beta-plane unstable wave for adiabatic, frictionless conditions the model developed a curved jet after intergration of 48 hours. It confirmed that the areas of convergence and divergence were enhanced ahead of and following a trough respectively due to the superimposition of the fields for curved and straight flow simular to that shown in Fig. 11e. Strong sinking motions were located along the jet entrance axis with strong rising motion near the jet exit axis region. This is due to positive contributions of convergence (divergence), cold advection (warm) at the jet entrance (exit) region of a cyclonically curved jet streak.

Another numerical study was done by Newton and Trevisan (1984) similar to the Buzzi et. al. (1977) model. In their model they assumed a curved jet of

constant velocity with only the properties of strong lateral and vertical shear, hence, they were isolating the frontogenetical nature of curved flow as shown in Fig. 4b. Their results are shown in Fig. 14 after integration of 72 hours showing the familiar two cell curved flow pattern with a hint of "wrapping" of upward motion around the closed low due to the cross contour agrostrophic wind effects and the added effects of diffluence and warm air advection. This was operationally measured in strongly occluded cyclones by Matsumoto (1982). These results compare favorably with earlier numerical results by Mudrick (1974) who postulated that the frontogenesis encountered in his upper level beta-plane model was due to the strong subsidence along the jet entrance region along the northwesterly flow inflection point. This process enhanced the vorticity gradient along the north and south sides of jet axis as vorticity was tilted from the horizontal plane to the vertical plane in the midtroposphere resulting in an increased contour vorticity gradient. The results of these upper level frontogenetical models can be compared favorably with conventional cyclone models shown in Bergeron (1952) and Palmen and Newton (1969) which illustrate the air flow

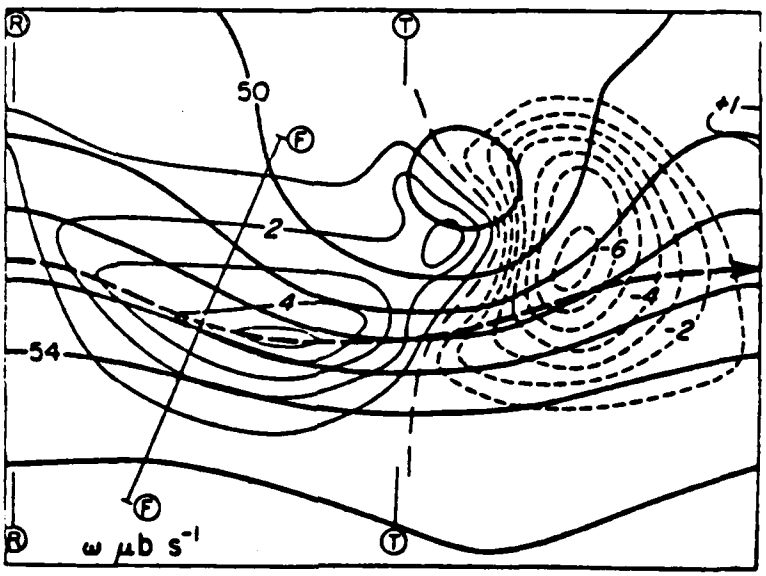

Figure 14. Analysis at 500 mb illustrating the results of a 72 h numerical simulation of a barotropically unstable wave in a beta-plane primitive equation channel model. Thick solid lines are height contours with interval of 100 m, thin solid and dashed lines are pressure-coordinate vertical velocity in interval of 1 microbar per second, thick dashed arrow indicates axis of jet stream at 500mb level. (Newton and Trevisan, 1984)

through an extratropical cyclone (Fig. 15). The air flow is shown to be descending from near a cyclonically curved 600mb level to near the surface and turning right crossing higher heights, indicative of cold advection. This compares favorably with upper-level frontogenetical models which indicate strong descent along the jet axis caused by cold air advection and strongly cyclonically curved flow. An analogous condition exists ahead of the trough as the air flow rises ahead of the frontal zone and veers to the right toward lower heights indicative of warm advection simular to the rising motion described in the frontogenetical jet streaks.

2.4 Hypothesized relationship of conveyor belts with cyclones and jet streaks

Palmen and Newton (1969) described in Fig. 15 air flow through a developing wave cyclone showing air parcel flow ahead of and behind the trough. Comparing these two pictured flows with the conveyor belt theory described by Carlson (1980), Harrold (1973), and Browning (1980) in Fig. 1 and 2 shows that the warm conveyor belt illustrated for those figures is very

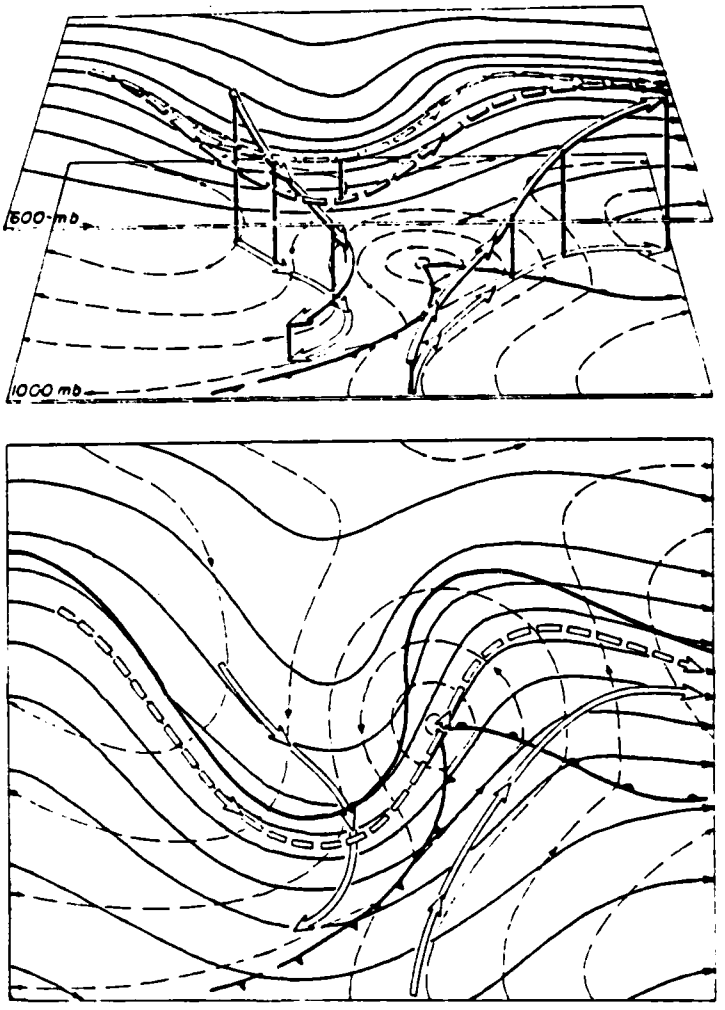

Figure 15. Schematic illustration of three-dimensional flow through an extratropical cyclone: thin lines, contours; thick dashed lines, jet axis; light arrow, flow behind trough; darker arrow, flow ahead of trough; streamlines, flow around surface low (Palmen and Newton, 1969).

similar to the rising air flow described by Palmen and Newton. In the case of the descending air flow behind the trough in Fig. 15 no analogy exists since until now the only flow responsible for the formation and distribution of precipitation and clouds has been explored in conveyor belt theory. Also of note is the absence of specific mention as to what happens to the cold air flow north of the low described in Fig. 15 even though this is shown to exist in earlier cyclone models of Bjerknes (1922) and Bergeron (1952).

Fig. 16 represents an incorporation of cold conveyor belt into Palmen and Newton Cyclone model and is derived from isentropic analysis of 13 synoptic midlatitude cyclones. Instead of a 600 mb surface a 300mb surface is displayed in a two and three dimensional view to relate this flow with upper level frontogenetical flow. Arrow 1 represents the warm, moist, conveyor belt (WMCB) and is analogous to flow ahead of the trough in Palmen and Newton. Arrow 2 corresponds to the flow behind the trough in Palmen and Newton which I shall call the "cold dry conveyor belt" (CDCB) since it is characterized by dry descending cold air flow on isentropic surfaces. Arrow 3 is the "cold moist conveyor belt" (CMCB) analogous to the cold conveyor belt in conveyor belt

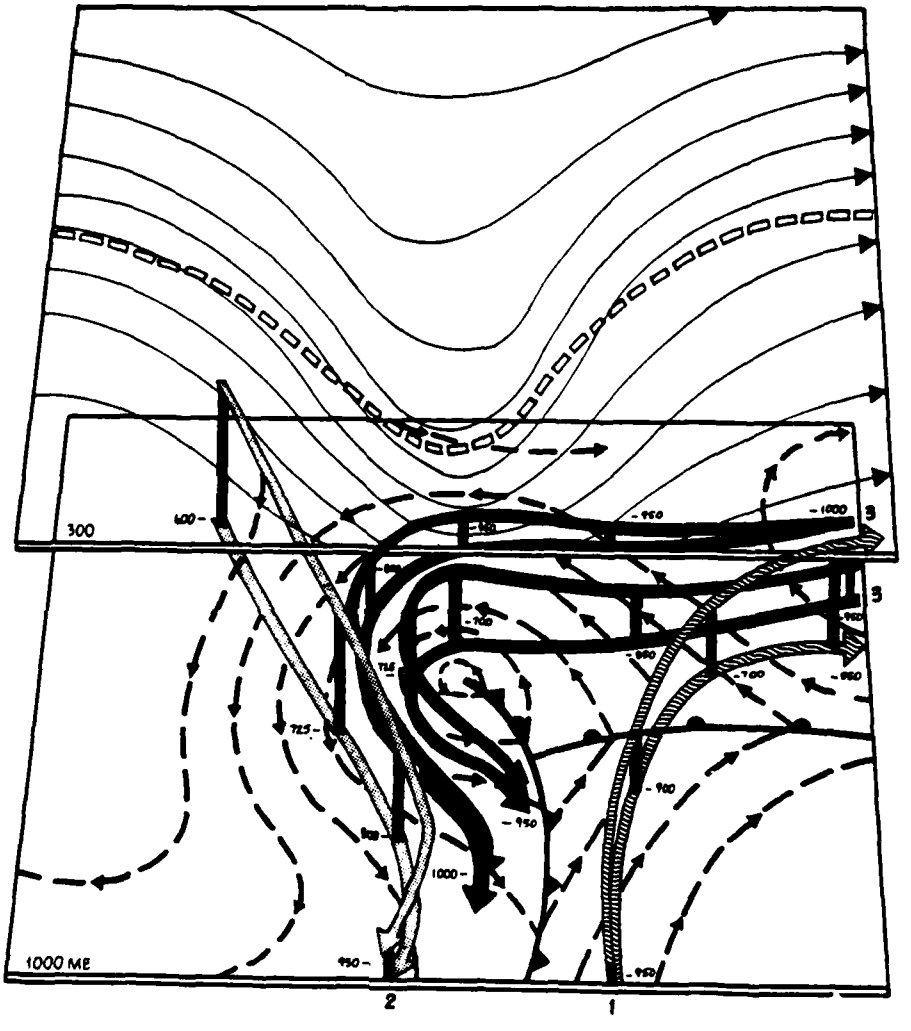

Figure 16. Three dimensional flow through an extratropical cyclone: dark stippled arrow, trajectory of CMCB; lighter stippled arrow, trajectory of CDCB; wavy stippled arrow, trajectory flow of WMCB.

theory. It is encorporated into the cyclone flow with rising motion and flow toward lower heights ahead of the trough. It then turns to either descend behind the trough to merge with the CDCB or rise and veer anticyclonically away to become part of the upper level flow north of the jet axis as described by Carlson (1980). Hence the CMCB works as a "bridge" between the flow ahead of and behind the trough displaying both characteristics depending on its relative location to the trough and jet stream axis.

Fig. 17 is a two dimensional view of the conveyor belts and their relationship to a cyclonically curved jet streak axis for a mature extratropical cyclone. The relationship of the jet streak at this point in the cyclone's life was illustrated by Shapiro (1983) and is related by Fig. 12c to the cycle of a jet streak through a baroclinic trough. This is an attempt to show some of the possible "coupling" of lower tropospheric flow with upper level jet streaks. Note the flow across the jet axis exit region by the cold moist conveyor belt representing part of the transverse circulation for the lower troposphere for the jet streak exit. For the jet streak entrance region we have descending cold moist and

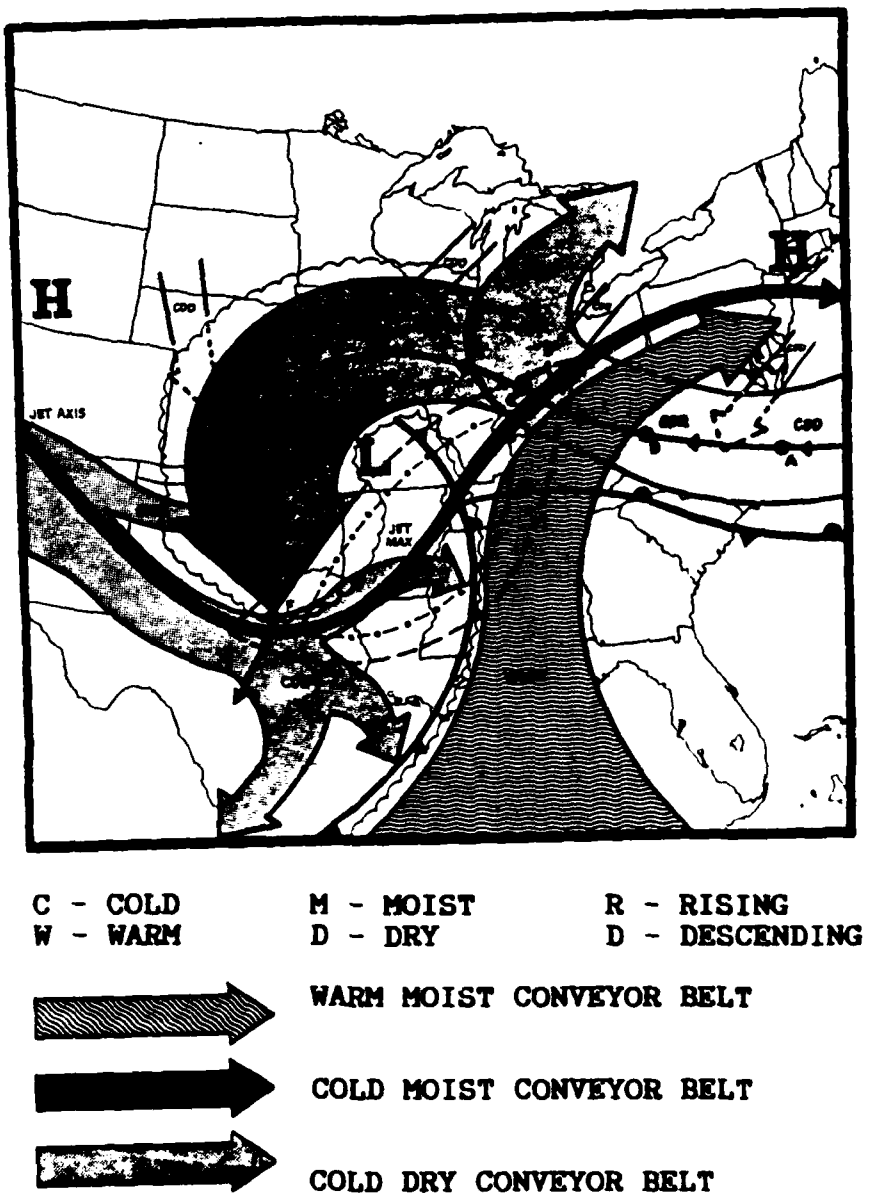

Figure 17. Schematic illustration of the two dimensional flow for the three conveyor belts in an extratropical cyclone. Dark line with arrow and dots, streamline of cold moist conveyor belt; heavy dark line, jet axis; scolloped line, edge of cloud cover; dash and dash dotted lines, isotachs for accompanying jet streak.

dry conveyor belts crossing the jet axis illustrating part of the transverse circulation of the jet entrance region.

An elementary attempt will be be made to describe flow along the CMCB since it appears to be a "bridge" for the two transverse circulations of the jet streak. At point A, the flow of the CMCB starts with air descending arounding the base of the cold anticyclone east or northeast of the cyclone. As it rises it reaches it's saturation point and clouds form. At point B meanwhile, at lower layers it is replaced by colder air originally northwest of the saturated rising air. This "newer" air is flowing from the north or northeast and has yet to saturate. This gives the familiar veering winds with height seen on soundings with cold dry air below the saturated layer and moist air above due to the WMCB. By point C, the airflow reaches the region of strongest upward vertical motion near the crossing of the jet axis exit region. Here, the saturation process has reached it's peak with precipitation falling through the layer with near saturated conditions to high levels indicating presence of both the WMCB and the CMCB. Reaching point D, the

parcels flow around the low at the lower and mid levels as they reach an area of nearly neutral vertical motion as shown by Astling (1982), Carr and Millard (1985), and others. Some drying is noted above the conveyor belt caused by the beginning of the intrusion of thee cold dry air (CNCB) from the norhwest. This area of weak vertical motion corresponds to Fig. 13a of pure confluence charcteristic of the jet streak core. At point E, just north of the jet axis the conveyor belt encounters stronger downward vertical motion at mid and upper levels associated with thee jet entrance region (Fig. 13c). A strong drying is prevelant as the CDCB pushes the CMCB to lower levels leaving only a relatively thin layer of moist air at loower levels (Fig. 16 and 18). Also some drying is noted close to the surface due to the CDCB intruding in at this level as well. This is shown in Fig. 17 as the CDCB pushes underneath the CMCB near the surface along the boundaries of the cold moist conveyor belt. Finally, by point F, along the jet streak entrance axis, the CMCB is dispersed and mixed with the large amounts of descending CDCB air and is characterized by strong downward vertical motion throughout the layer as evidenced by Fig. 13c.

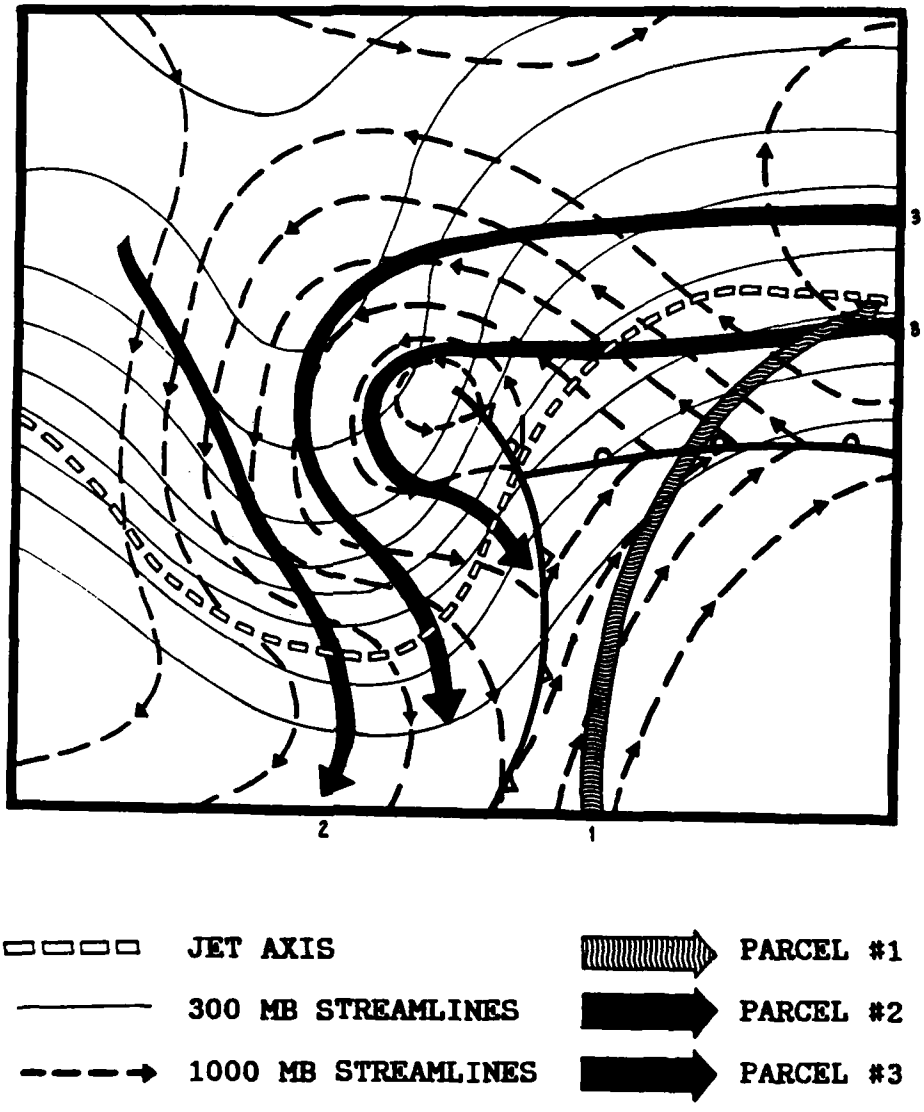

Figure 18. Two dimensional crosssectional view of the three conveyor belts as related to the 1000 mb surface and 300 mb jet. Smaller arrows, surface streamlines; thin solid lines, 300mb contours. Three arrows have same connotation as Fig. 16.

Figures 19a - f represent typical upper air soundings for points A-F in Fig. 18 describing the basic properties associated with each respective point. Averages were taken for the 13 cyclone cases studied giving composite illustrations of the basic properties of temperature, dewpoint, wind speed and direction. Relating the properties associated with each conveyor belt we can identify where in the vertical each belt is located. For point A in Fig. 19a dry air extends up to about 500 mb, and wind veers with height. These represent the end/beginning of the CDCB/CMCB with the moisture above representing the near final stages of the WMCB. Fig. 19b demonstrates more moisture both at middle and upper levels along with a weak inversion near 600 mb separating the CMCB and WMCB along with a sharper change in wind direction. Fig. 19c illustrates the deep moisture available to upper levels caused by significant vertical motions associated with CMCB and WMCB. Some drying is evident above 400 mb as we approach the western boundary of the WMCB as described by Carlson (1980). Note the general easterly wind flow to 650 mb of the CMCB. Fig. 19d shows pronounced drying above 700 mb at point D as the CDCB dominates at high levels. Also important is the weak inversion and sharp backing

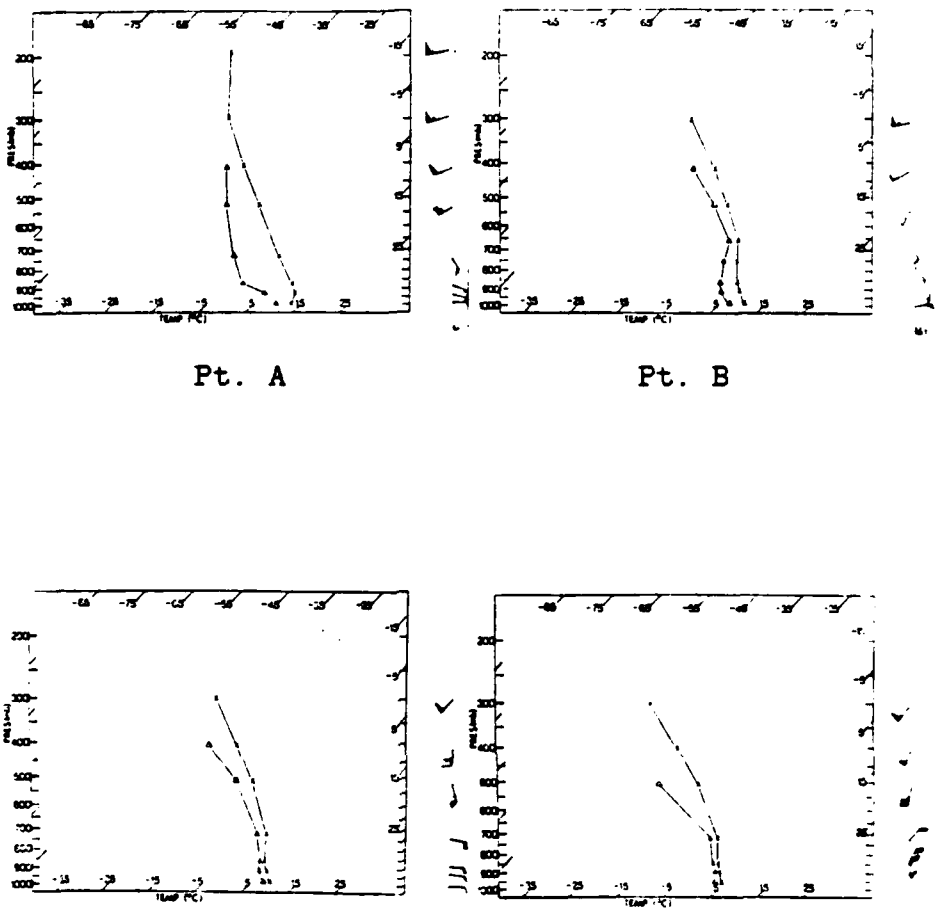

Pt. A

Pt. B

Pt. C

Pt. D

Figure 19. Composite soundings for points A-D in Fig. 17 taken from 13 synoptic cases. Crosses represent temperature; triangles are dewpoint; windbarbs are in knots. Pressure in mb with temperature in Celsius.

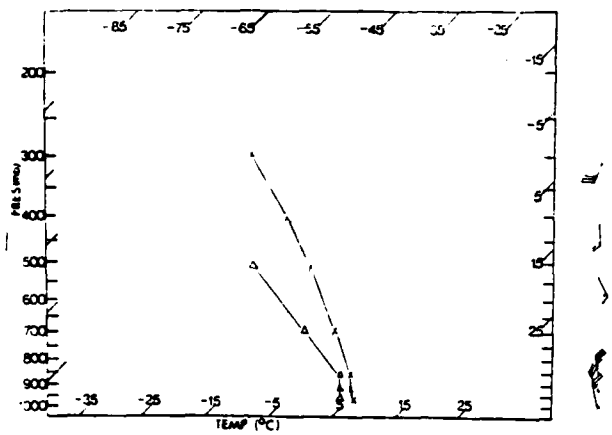

Pt. E

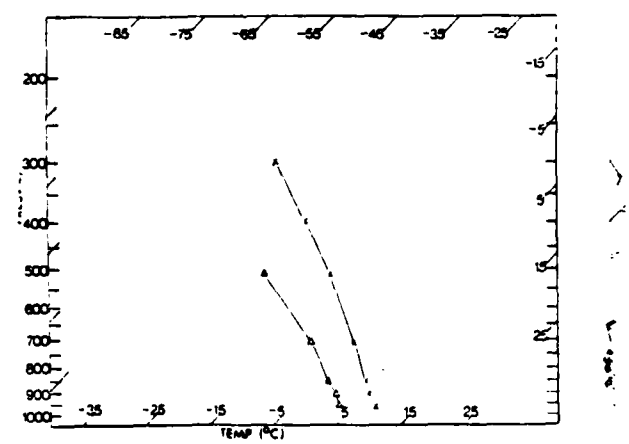

Pt. F

Figure 19 (cont.). Same as preceding page except for points E and F.

of the wind at this level. By Fig. 19e, point E, the area of reduced (lower) lapse rate and associated moisture separating the lower CMCB with the upper CDCB has descended to near 770 mb. Finally, in Fig. 19f, we see the drying evident at all levels due to the CDCB.

3. Methodology

3.1 Gathering Data and Isentropic Transformation

Data for twelve of the thirteen cyclones studied were obtained from the National Climatic Data Center in Asheville, North Carolina. The remaining cyclone data were obtained from the FAA-604 data line which is fed into the Saint Louis University Department of Earth and Atmospheric Sciences Masscomp computer, where all data was stored for computational analysis. Surface and upper air data for all reporting rawinsonde stations in the U.S. were utilized and consisted of temperature, dewpoint depression, pressure, height, wind speed and direction for all significant and mandatory levels. Data were interpolated on to a rectangular grid covering the central and eastern United States which included a total of 50 rawinsonde stations (Fig. 20). Orientation of the grid maxized the number of rawinsonde stations throughout the area in question with an average spacing interval of approximately 400 km. Two exceptions were the extreme eastern and southeastern border due to the Atlantic Ocean and Gulf of Mexico. This sparsity of data had little effect on the analysis since all

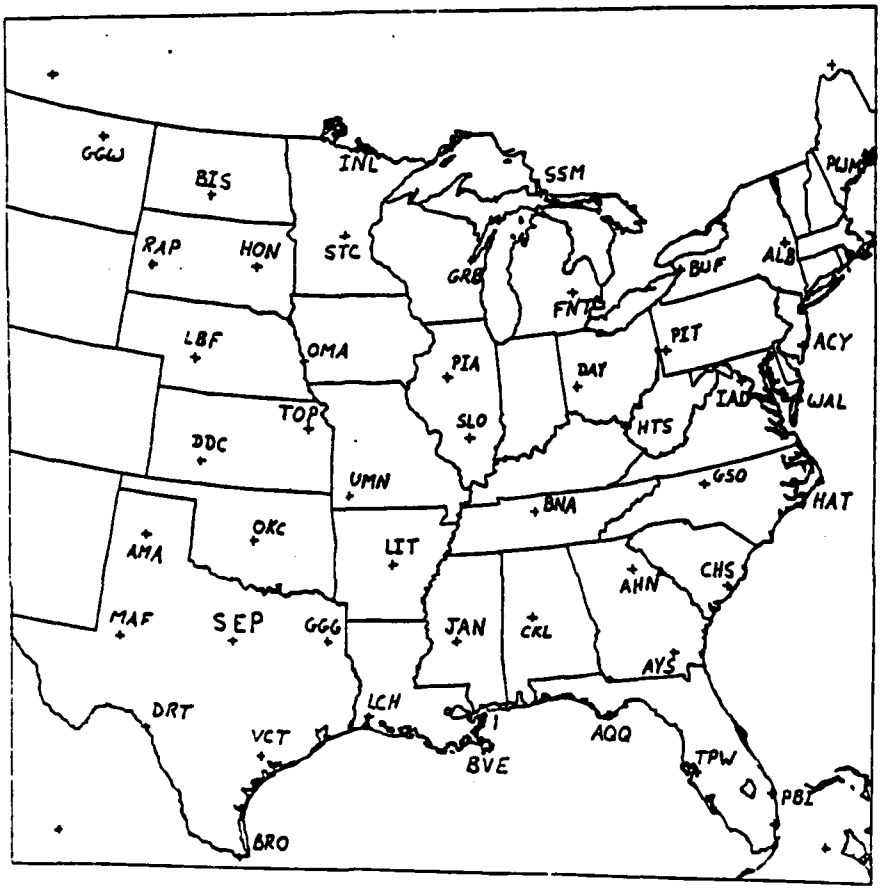

Figure 20. Schematic illustration of the spatial coverage for the upper air network used for data analysis. Crosses represent locations of a particular station; with three letter station identifyer, four extreme corner points represent four corner boundary points of gridded map.

cyclones in question occurred in the central part of grid where resolution was good and far removed from the two border areas.

The data were then converted to isentropic coordinates using the Duquet (1964) isentropic program. In this program, soundings are interpolated vertically to potential temperature levels from the surface every 2° K to the 350° K level and then every 10° K thereafter.

Interpolation of all parameters except winds was carried out assuming linearity with respect to P^k where $k = R/C_p = 0.286$. Winds are interpolated linearly with respect to height; speed and direction are interpolated seperately. The Montgomery Streamfunction ($\Psi = C_pT + gz$) is computed through the vertical integration of the hydrostatic equation in isentropic coordinates computed upward from the ground.

3.2 Objective Analysis Scheme

Objective analysis of the desired kinematic variables was obtained through the use of a Barnes (1973) scheme. This scheme employs the use of two Gaussian weight functions c and g to generate the gridded values. The

former, c, is used as part of the weighting function applied to raw data where the influence of the data point to a gridded point is a function of its distance to the grid point. Outside a specific radius, a weight of zero is assigned to the observation, limiting its radius of influence. The latter, g, employed along with c is used as a "smoothing" parameter to determine the amount of amplitude to be recovered for a particular wave. This effectively reduces the amount of "noise" caused by short wavelengths in the calculations.

Gridded data were placed on to a 26 (x-axis) by 26 (y-axis) grid with a spacing of 127 km. This spacing was selected because it is about 1/2 of the spacing of the rawinsonde observational network and was shown by the work of Koch et al. (1980) as desirable for maximum resolution of the computational process. Gridded data were projected onto a polar stereographic map with a standard longitude of 94°W. Since the gridded spatial interval was 0.5 inches (127km), only about 10% of the two delta (800km) wavelength's amplitude was resolved, while about 96% or greater of a 2000 km plus wave's amplitude were resolved (Fig. 21). This procedure enables us to resolve the wavelengths (2000 - 3000 km) associated with the extratropical

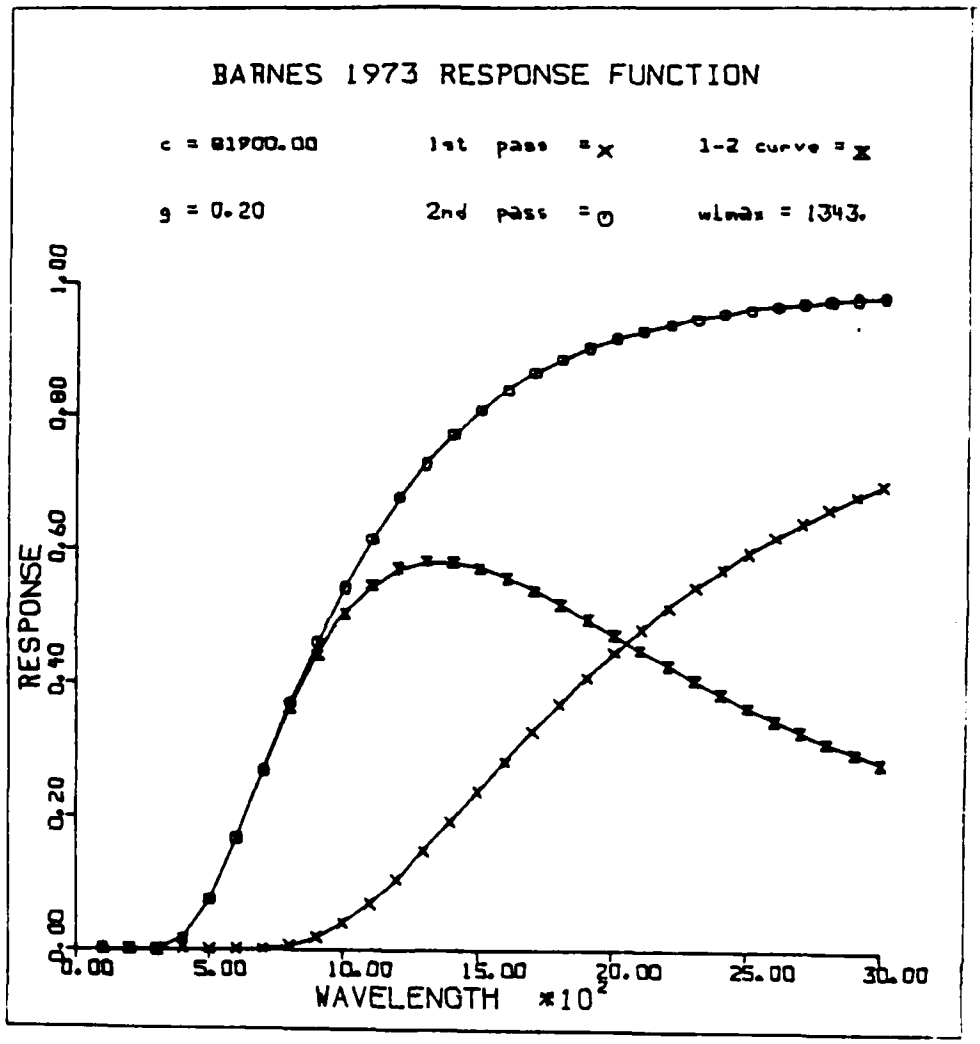

Figure 21. Barnes (1973) response function for a c and g of 81900.00 and 0.20 respectively used for the computation of all upper air data.

cyclones in question while reducing the noise of shorter wavelengths and some of the inherent error in rawinsonde data. It is important to note that a different objective analysis scheme with a different grid and weighting function would produce a different response function.

3.3 Computation of Isentropic Kinematic Values

The Barnes (1973) objective analysis scheme was used to create gridded fields of u, v, q, psi, and P on selected isentropic surfaces. Streamlines were computed from the gridded u and v components and plotted on a corresponding map using an NCAR streamline program. Trajectories for pre-selected points within the grid were calculated from 2 consecutive time periods (covering 12h) of gridded values for the same isentropic surface. Locations of the parcel starting points (Fig. 22) were chosen to cover motions in the CMCB as they crossed near the jet entrance and exit regions for the three specific cyclones studied. Trajectories that reached the borders of the grid were reassigned values near the border inside the grid to keep them on the gridded map. Individual trajectories

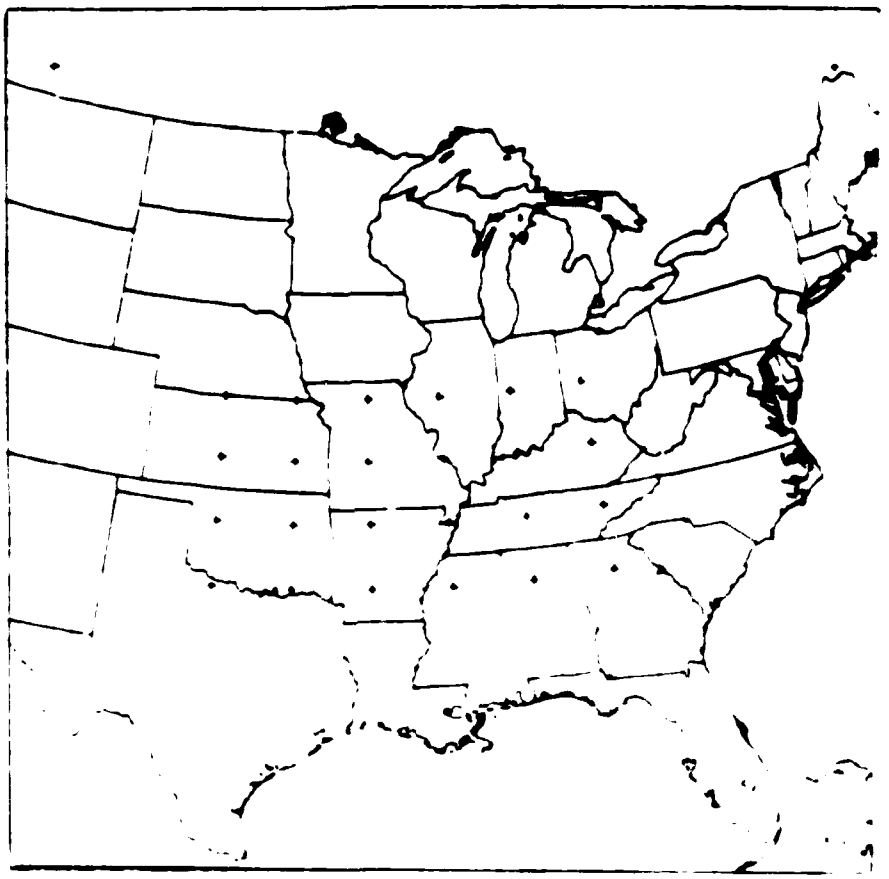

Figure 22. Selected initial locations of trajectories

were calculated from initial and final values of u, v, q, psi, and P using a procedure developed by Peterson and Uccellini (1979). Lagrangian fields of the changes in psi, potential energy (PE), and omega can be calculated for each selected trajectory. Each value was calculated in the following manner:

$$\Delta PE = gz = (\psi_f - \psi_i) - (C_p T_f + C_p T_i)$$

$$\Delta\psi = \psi_f - \psi_i$$

$$\omega = dp/dt = P_f - P_i / 12hrs$$

where the subscripts f and i represent the initial and final values of the appropriate parameters and psi, potential energy are in units of m^2/s^2 and omega is in microbars per second.

Eulerian divergence and omega fields were calculated from gridded Barnes data on a specified isentropic surface at a specific time. Divergence was calculated from centered finite differencing of the u and v wind components in the x and y direction respectively using:

$$Div = \frac{\partial u}{\partial x} + \frac{\partial v}{\partial y} \qquad (5)$$

Omega was calculated from second order finite differencing of the advection of P at a specific point. Diabatic effects were assumed to be zero since parcels

were constrained to an isentropic surface. The local change in pressure $\frac{\partial p}{\partial t}$ was also assumed to be small as this term was shown to be insignificant for synoptic scale events by Uccellini (1976). Hence the equation for omega:

$$\omega = \frac{dp}{dt} = \frac{\partial p}{\partial t} + \vec{V}_\theta \cdot \nabla p + \frac{d\theta}{dt}\frac{\partial p}{\partial \theta} \qquad (6)$$

becomes for our calculations:

$$\omega \approx \vec{V}_\theta \cdot \nabla p \qquad (7)$$

3.4 Identification of CMCB

The cold conveyor belt (CMCB) was diagnosed using a combination of soundings and isentropic cross-sections for the areas normal to the jet streak entrance and exit regions. From the work of Harrold (1973), Carlson (1980), and Browning (1986), the CMCB was identified as the easterly flowing air below the temperature inversion in the jet exit region and the moist northerly to northwesterly flow below the dry northwesterly flow also seperated by a temperature inversion in the jet entrance region. Once the CMCB had been identified, isentropic

cross-sections were taken parallel with the flow (Fig. 23) with winds shown normal to the plane to identify relative position of the jet.

Temperature inversions, and wind direction changes are used in soundings to identify the top of the CMCB. For Fig. 23 this would near 680 mb. Then this height would be used at that station on a corresponding isentropic cross-section. Using Fig. 24, this yields an isentropic temperature of 297°K. Note the inversion marking the boundary of the two conveyor belts shows up as the area of enhanced vertical gradients of isentropic temperatures. Comparison of the values at the jet entrance and exit regions are made to insure they yield approximately the same temperature. This is done to check the comtinuity of the two airflows as outlined in Palmen and Newton (1969) and Byers (1974). Then a representative isentropic level was selected inside (below) the inversion where streamline and trajectories and kinematic values were computed. To limit diurnal effects, selection of the isentropic surface for trajectories occurred just under the top layer of the CMCB providing values in the upper portion of the isentropic flow. Isentropic values below the level selected intersected ground surfaces on 0000 GMT

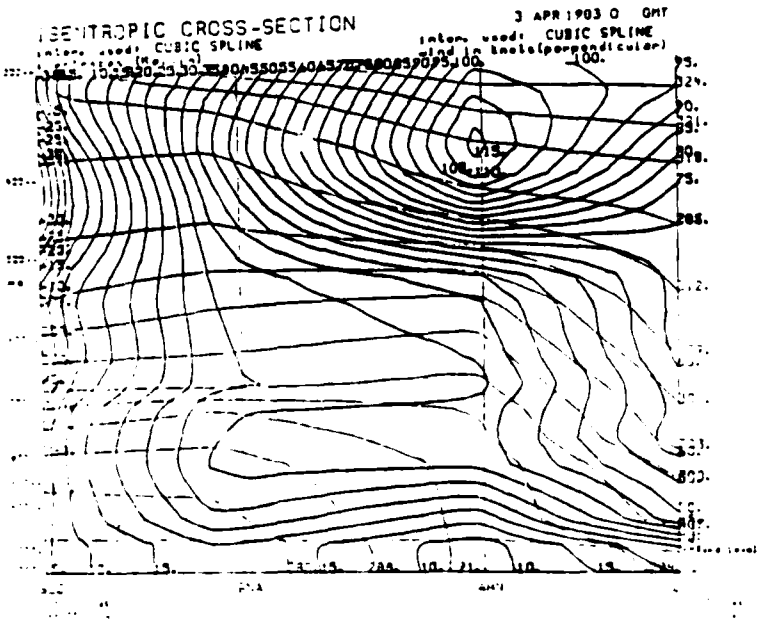

Figure 23. Isentropic cross section normal to jet axis using a cubic spline interpolation scheme: heavy dark lines, across-plane windspeed in knots; thin lines, potential temperature.

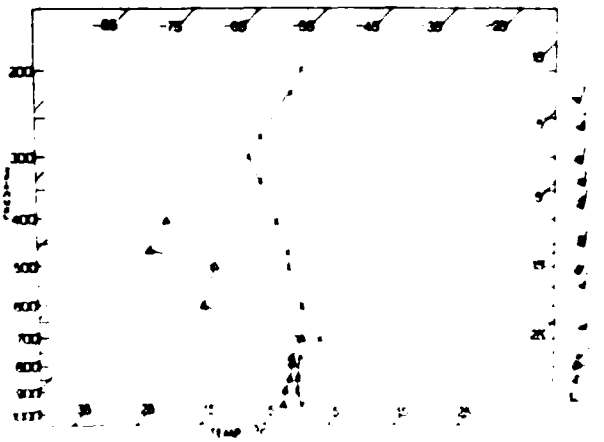

Figure 24. Upper air sounding of temperature and dewpoint for Nashville TN at 0000 GMT 3 Apr 1983 Wind barbs are expressed in knots

invalidating any diagnostic computations. Streamlines were able to be lower and were selected for the midway point in the vertical depth CMCB since no computations were taken on these surfaces.

4. DISCUSSION OF RESULTS

4.1 Case Study I

4.11 Synoptic Overview

This situation deals with a strong extratropical cyclone which formed in the Panhandle of Texas on 1 April 1983, moved northeast and became occluded over southeastern Missouri on 00 GMT 2 April (Fig. 25a). The cold moist conveyor belt is the east to southeast flow extending near Mobile, AL in the south to Norfolk, VA in the north. The CMCB reaches a point due north of the surface low, perpendicular to a line from central Missouri to Minnesota and then turns cyclonically southward reaching south central Texas. Cloud cover extends along the flow from just east of the Appalachains to central Texas with precipitation occurring in the Mississippi Valley indicating rising motions. Hence the flow is bounded to the south by the surface warm front and to the north by the cold anticyclone as outlined and discussed by Carlson (1980).

The upper air flow at 250mb for the same period (Fig. 25b) shows a well defined jet streak in New Mexico

(a)

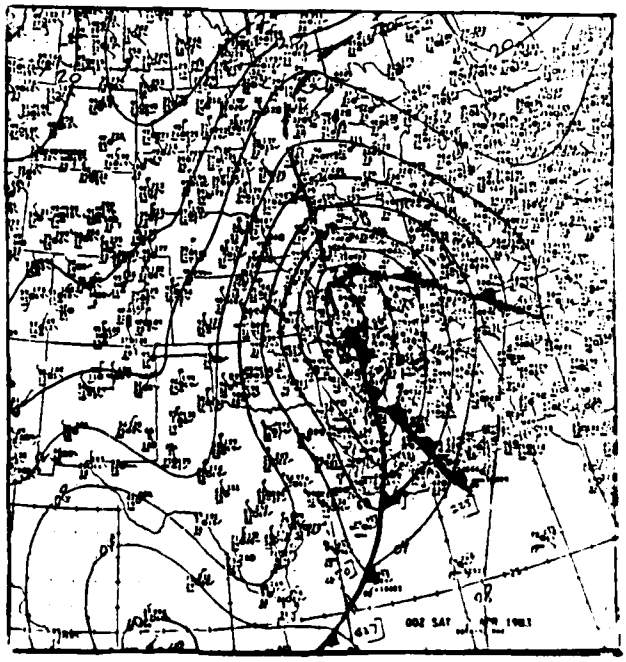

(b)

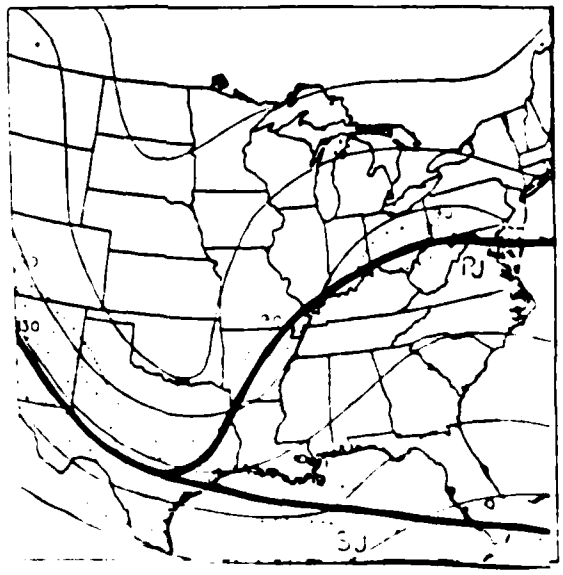

Figure 25. Synoptic illustration of the (a) surface and (b) 250mb features at 00Z 2 April 1983. Thin solid lines are pressure contours in (a) height contours in (b) dots indicate isotachs. Heavy line is jet axis

and west central Texas just upstream of the main trough extending across the Great Plains. This approximates a position somewhere between the depictions illustrated in Fig. 12b and c. Of importance is the presence of secondary jet streaks, one located in the base of the trough near Victoria, Texas. The flow then splits into two branches with the south branch extending across Florida. The northern branch moves northeast where another jet streak is located over Indiana. Also of note are the diffluent streamlines ahead of the trough over the Mississippi valley. Manual analysis of all upper air charts for all cases studied became a necessity due to the significant smoothing associated with National Weather Service charts missing many secondary jet streaks whose influence became obvious in calculations.

During the next 12 hours (Fig. 26a, b) the cyclone reaches full occlusion with the upper air flow closely approximating the schematic depiction by Shapiro (1983) and shown in Fig. 11c. At the surface we see the main low located near St. Louis, Missouri with an occluded front extending southeastward to Georgia. The CMCB has expanded extending from the warm front to near New York City. It then flows around the low reaching the deep

(a)

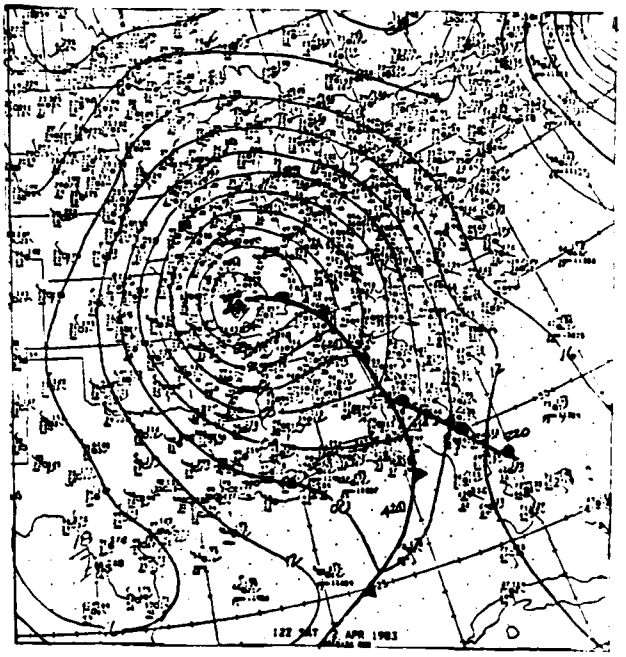

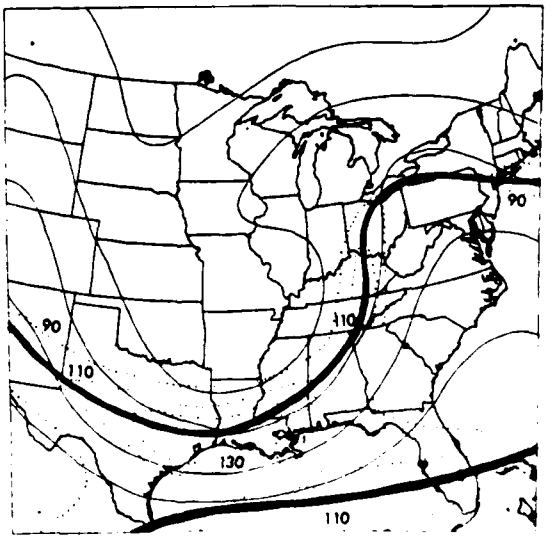

(b)

Figure 26. Synoptic overview for the period 1200 GMT 2 April 1983. Annotations are the same as in Fig 24.

south. The upper air flow indicates the main jet streak in the base of a strongly cyclonically curved trough in southeast Texas very similar to Fig. 12c. Significant secondary jet maxima are also located in New Mexico and eastern Kentucky.

4.12 Locating the CMCB on an Isentropic Surface

Selecting an isentropic surface in the CMCB required the use of soundings and isentropic cross sections. Cross sections at 0000 GMT and 1200 GMT 2 April were selected that would most closely parallel the flow in the CMCB while crossing the jet entrance and exit region ahead of and behind the trough respectively (Fig. 27). Then soundings were taken for the station furthest upstream along each line (Fig. 28). Using the basic properties of each air mass defined by Harrold (1973), Carlson (1980), and Browning (1986) and expanded on in section 2.4 we can identify the location of each conveyor belt. In Fig. 28a, at 0000 GMT the CMCB can be seen to extend up to 580mb at Nashville, TN where an inversion exists and the air is near saturation above this point which is indicative of the presence of the WMCB. For Topeka, KS at the same time period (Fig.

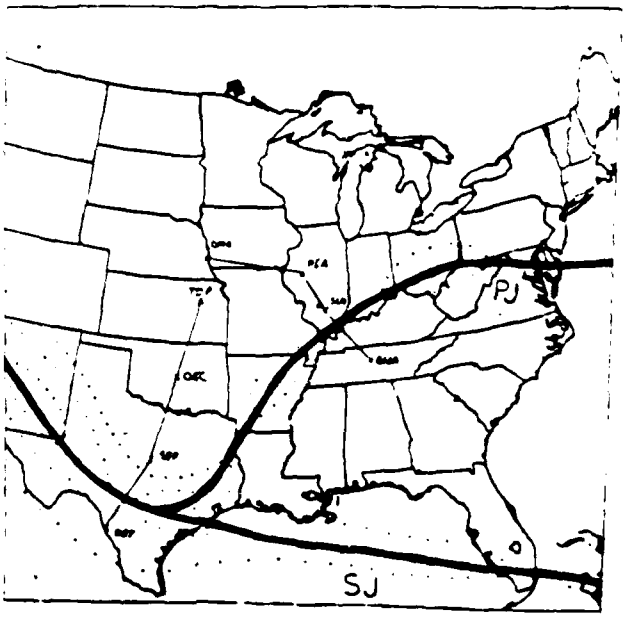

(a)

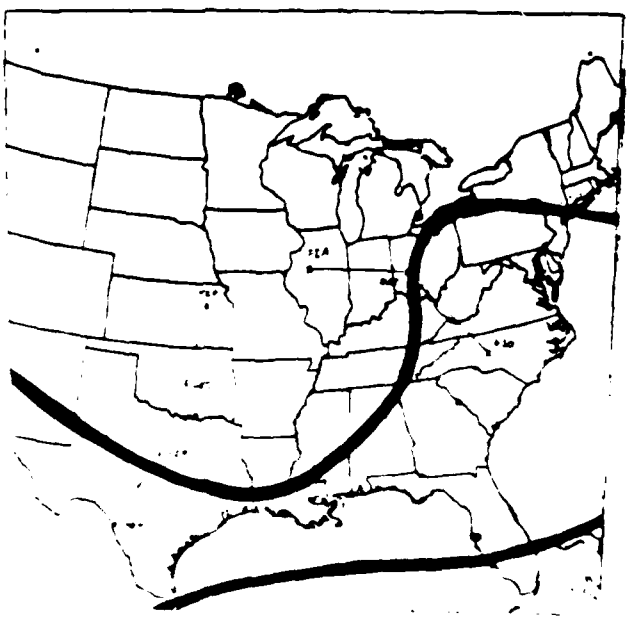

(b)

Figure 27. Schematic illustration of the cross-sectional profile used in determining heights of CMCB. Crosses indicate rawinsonde station used, heavy dark line, jet axis, dots, isotachs (a 0000 GMT b 1200 GMT 2 April 1983.

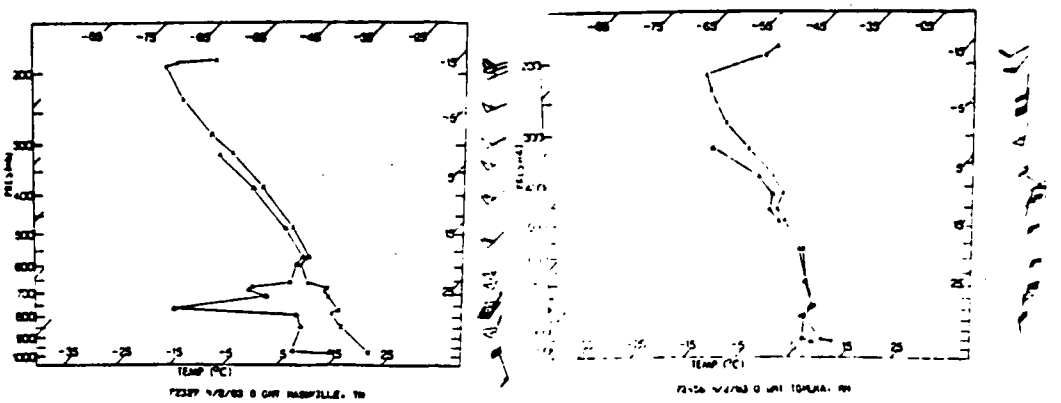

(a) (b)

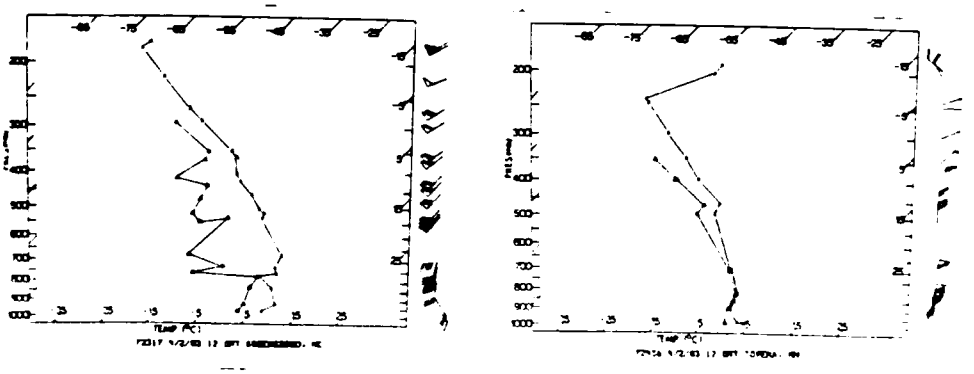

(c) (d)

Fig 28. Soundings used for determination of top levels of CMCB at (a), (b) 0000 GMT and (c), (d) 1200 GMT 2 April 1983.

28b) the top of the inversion is near 450 mb as noted by the inversion and near 180° shift in wind direction; also note the significant drying above this level caused by the penetration of the CDCB at these levels. At 1200 GMT (Fig. 28c, d) we can mark the tops of the CMCB using the inversions located near 550mb and 480mb for Greenesboro, NC and Topeka, KS respectively.

The relative positions of these soundings to the cyclone generally correspond to points B and D in Fig. 17 where point B marks the beginning of the saturation of the ascending CMCB while point D represents the point in the flow of the CMCB where it becomes fully saturated and reaches its greatest vertical depth. The general characteristics of each sounding at point B and D as shown in Fig. 19 will be used as a guideline to determine the top of the CMCB for each sounding. For point B then, we look for a marked veering of wind with height, with an inversion at or above this level with generally moist air above the inversion indicative of the WMCB. For point D, a weak inversion will be present with significant drying above this level along with sharp backing of the wind with height indicating cold air advection.

The corresponding isentropic cross-sections for

0000 GMT (Fig. 29a and b) indicate the top of the CMCB at 312°K at Nashville, TN and Topeka, KS based upon the heights of the top of CMCB obtained for the applicable soundings. This is indicative of the same airmass since the potential temperature values are constant. Looking at Fig. 29a we note generally ascending isentropic surfaces to the left. This corresponds closely to warm air advection as shown in Fig. 11d, 12c, and 13c as applied to the exit region. Inspection of Fig. 29b indicates a slope toward DRT indicative of descending motions since the general flow of the CMCB is from TOP to DRT, this most closely approximates Fig. 12b. A value of 312°K was also obtained for the second time period (Fig. 29c, d) for Greenesboro and Topeka. Little change in in the isentropic temperature indicates the system is not undergoing any total change in temperature but is remaining near steady state. The relatively constant elevation of the lower isentropic surfaces across the jet streak exit region as in Fig. 29c is attributed to the slight crossing of the plane selected with the actual flow pattern. This is due to the limited amount of stations available to produce cross sections. The jet stream axis across the plane is nearly perpendicular

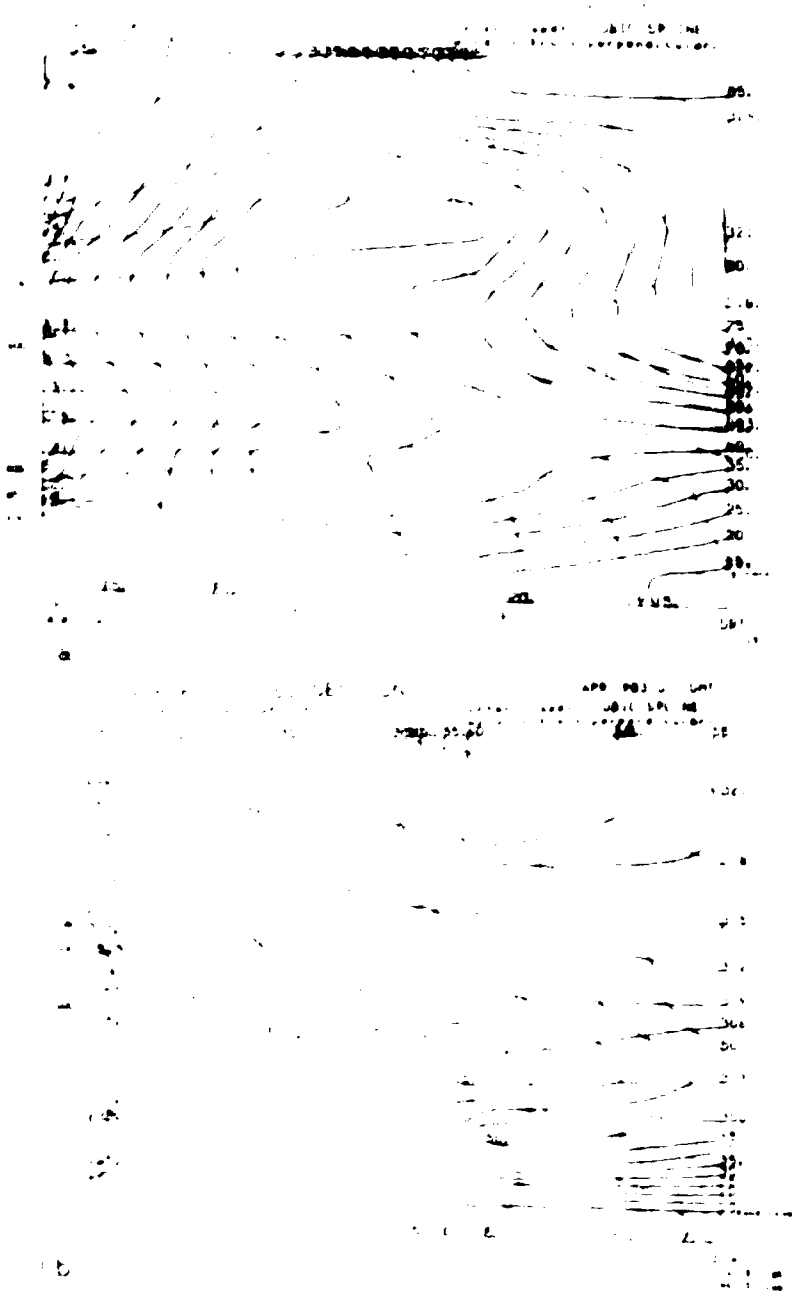

Figure 29 Isentropic cross section across the exit and entrance regions of jet for 0000 GMT 2 April 1983. Heavy dark lines indicate wind speed perpendicular to the plane with positive values into the paper. Thin lines are isentropic temperatures. Cubic Spline interpolation used.

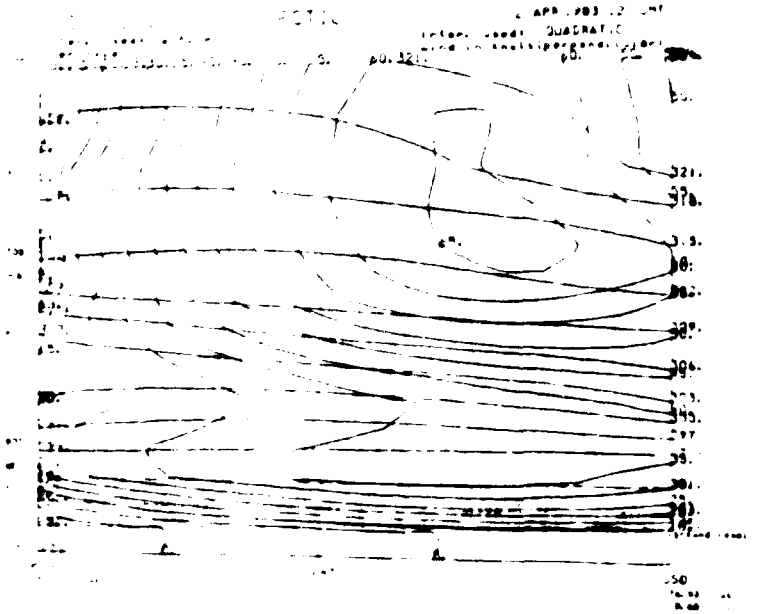

(c)

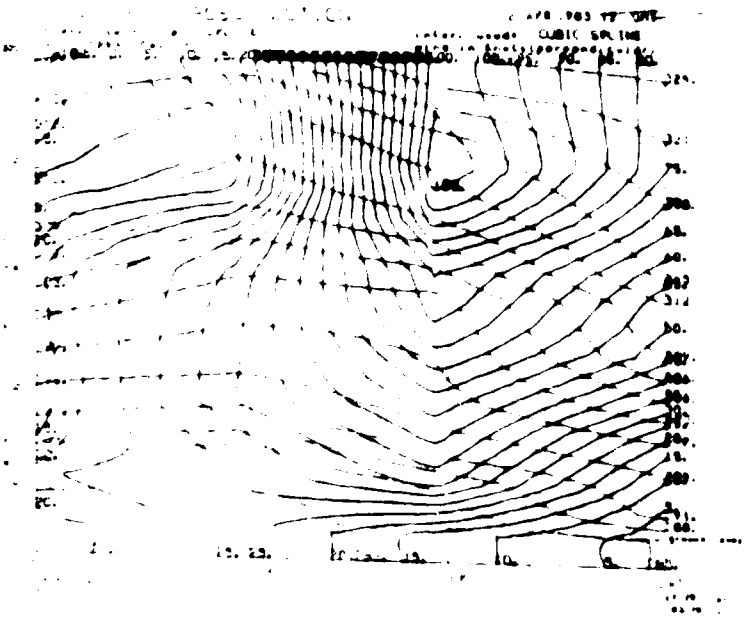

(d)

Fig. 29 (c), (d) Same as Fig. 28 (a), (b) except for 1200 GMT 1983

and is located between Dayton, OH and Greenesboro, NC with positive values indicating flow into the page

In Fig. 27 the plane across the jet streak entrance region for both time periods ends near the jet streak axis and is due to the lack of available upper air data in the Gulf of Mexico This predicament occurs several times in the other cases as well but does not have a significant effect on our results Flow along the isentropic surface indicates an increasing downward vertical motion as the jet axis is approached and is similar to the cross section illustrated in Fig 13b

Selection of an isentropic surface for trajectories and streamlines was chosen with the objective of obtaining a surface as close to the middle of the CMCB while limiting the diabatic effects associated near the surface From Fig 29, 290°K for trajectories was selected, the same value was also used for streamlines at 0000 GMT while 286°K was used for 1200 GMT due to the cooler diurnal temperature at this time This allowed for an average height near 825mb which should be low enough to demonstate the lower branch of the transverse circulations in jet streaks Since these isentropic temperatures are well below the 313°K surface determined as the top of the CMCB, a... flow

shown will be representative ofthe flow in the CMCB

4 13 Location and Orientation of CMCB to Jet Streaks

Fig 30a and b represents streamlines for the appropriate isentropic level at 0000 GMT and 1200 GMT The outline of the CMCB is marked by the heavy dark dashed line In Fig 30a, note that the southeast flow is similar to Fig 8a which demonstrates the isallar flow for a cyclonically curved jet streak As the CMCB moves toward the low, one branch turns away from the low, as described by Carlson (1980 while the other branch turns around the low as discussed by Browning (1986) This latter branch recrosses the jet axis as in Fig 8b By 1200 GMT (Fig 30b the low has deepened and the flow has increased in width and backed slightly flow from the anticyclonic center to the north as depicted in Fig 18b Comparison of the two figures indicates that, as the low strengthens and deepens during its occlusion process, more and more of the CMCB turns cyclonically behind the center As the orientation of the CMCB turns cyclonically with time

Trajectories for selected gridpoints in the CMCB are shown in Fig 31 for the 12 hour period from

(a)

(b)

Figure 30 Relative streamlines for (a) 00Z and (b) 12Z 2 April 1983 Heavy dashed line indicates boundary of CMCB The heavy line is the jet axis. It is represent isotachs

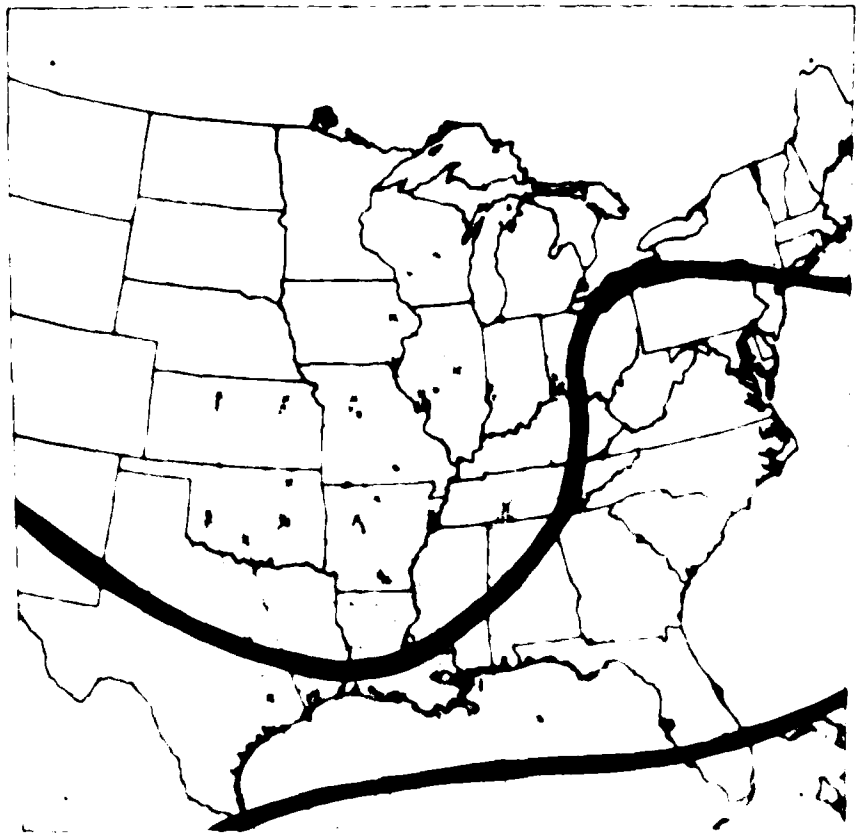

Figure 31 Trajectories of selected gridpoints covering 0000-1200 GMT 2 April 1983 for a 290°K isentropic surface. The heavy dark line is the jet axis while the dotted line represents isotachs.

0000 GMT-1200 GMT 2 April 1983 The paths along these trajectories can be subdivided into the three flows analagous to Fig 17 Parcels 13 and above indicate motion toward the low, either turning anticyclonically away or cyclonically behind the low center Parcels 5, 7, 9, and 11 represent flow very close to the low turning cyclonically around it Parcels 1 and 3 are taken further to the southwest of the low center and show anticyclonic veering of the flow as it moves south showing the effect of the CDCB

4 14 Relationship of CMCB to Lower Transverse Circulations in Jet Streaks

Streamline flow overlain on various kinamatic fields is one way to illustrate the properties in the CMCB. Fig 32a and b represents the streamline flow across isobars as indicated by dashed lines. As the flow approaches the low we can see rising motion since lower values of pressure are reached. Then, as the flow turns south toward Texas, descending motion is noted as the higher values of pressure are reached. This is to be expected for the bottom half of flow in the jet exit (indirect thermal circulation) and entrance

(a)

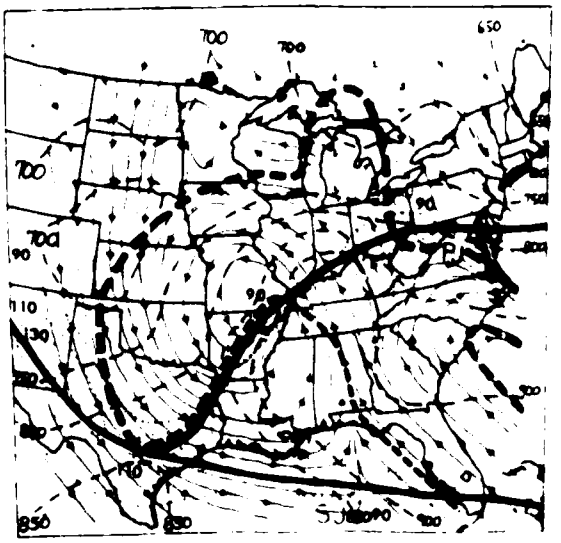

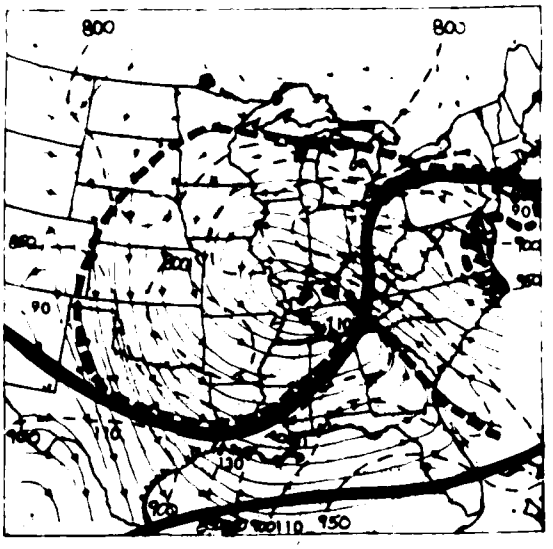

(b)

Figure 32. Cross-contour flow of streamlines at (a)0000 GMT on 290°K surface and (b)1200 GMT on 286°K surface: dashed line, pressure; heavy dashed line, boundary of CMCB; thick line, jet axis; dots, isotachs.

region (direct thermal circulation) as shown in Fig 4 and 5. We can note that the strongest pressure gradient is on the cyclonic side of the jet axis similar to the depiction shown for Fig 14d illustrating cold air advection in the jet entrance region and warm air advection in the exit region for a cyclonically curved trough. This is especially true for the latter period.

Flow across the Montgomery Streamfuntion, (psi) is shown in Fig. 33. As the flow approaches the low, lower values of psi are reached indicating an ageostrophic component of the flow to the northwest, as the flow turns cyclonically progressively higher values of psi are reached indicating an ageostrophic component toward the south and across the jet streak axis. Both fields are in agreement with the theoretical ageostrophic component found in the lower half of the Fig 4. This would indicate that the CMCB is a participant in the transverse circulations present in the flow thru jet streaks.

Langrangian computations of the change in potential energy, omega, and psi are illustrated in Fig. 34 with positive values of potential energy across the jet exit region and negative values across the jet entrance

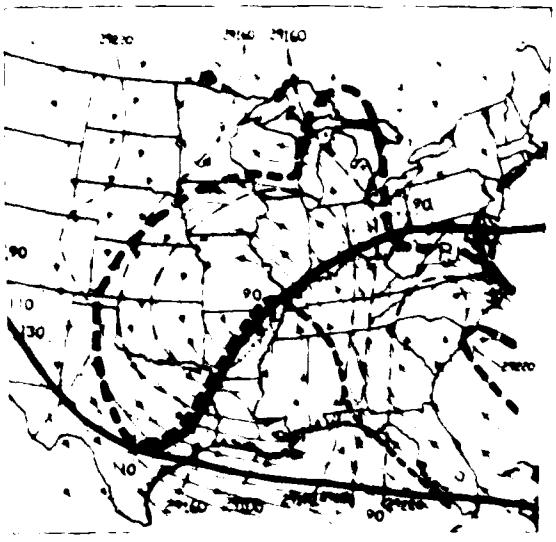

(a)

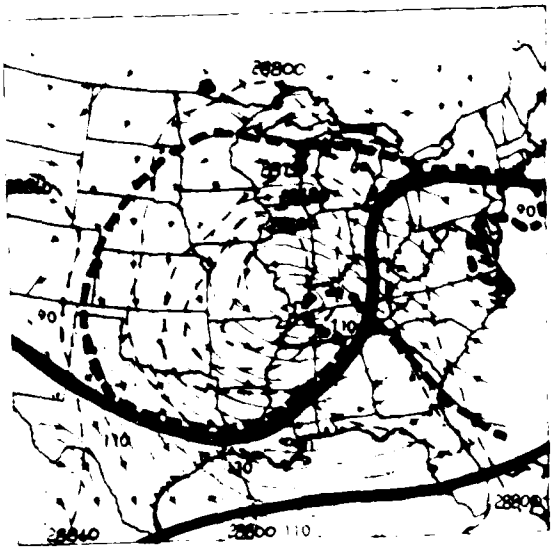

(b)

Figure 33. Same as Fig. 32 except dashed lines represent Montgomery Streamfunction. (psi).

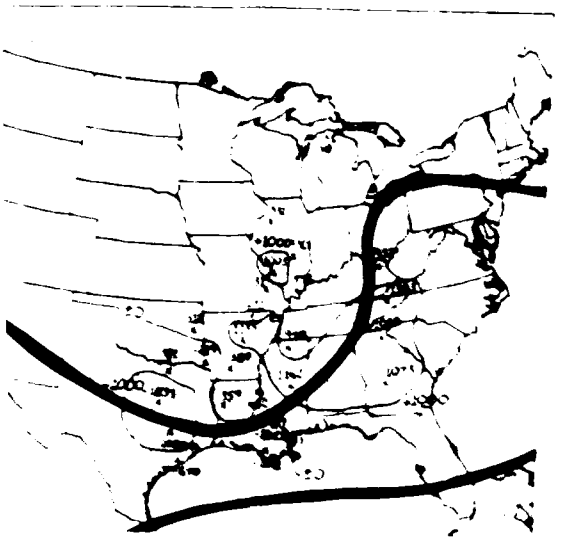

(a)

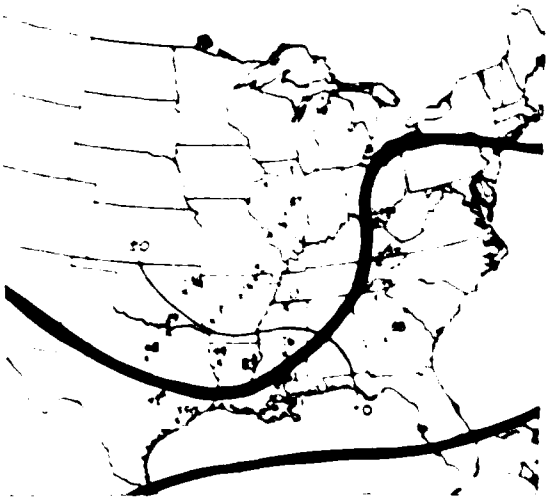

(b)

Figure 34. Computations at the midway point of all parcels in a preselected grid for the period of 0000 GMT-1200 GMT 2 April showing the change of (a) potential energy and (b) psi. Dashed lines are isopleths of for each computed paramenter.

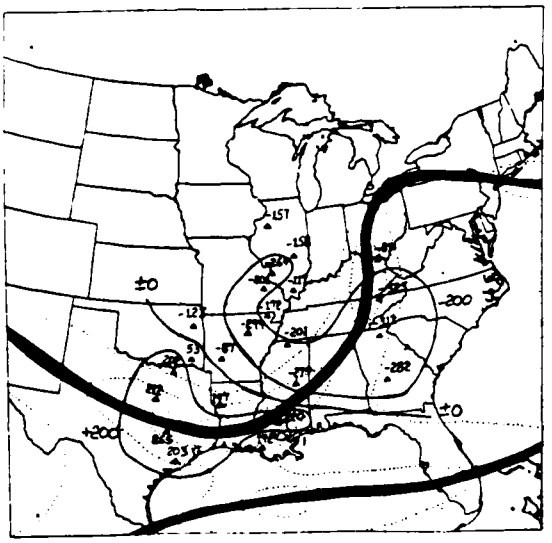

(c)

Figure 34 (c) cont.) Same as 34 (a) (b) except for changes in pressure (omega).

AD-A186 774 INTERACTION OF THE COLD CONVEYOR BELT WITH POLAR JET STREAKS(U) AIR FORCE INST OF TECH WRIGHT-PATTERSON AFB OH W D NICHOLAS 1987 AFIT/CI/NR-87-44T 2/2

UNCLASSIFIED F/G 4/2 NL

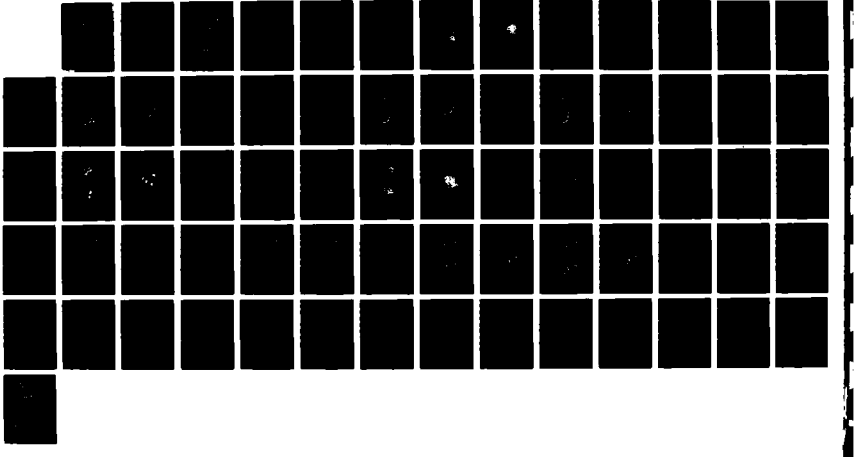

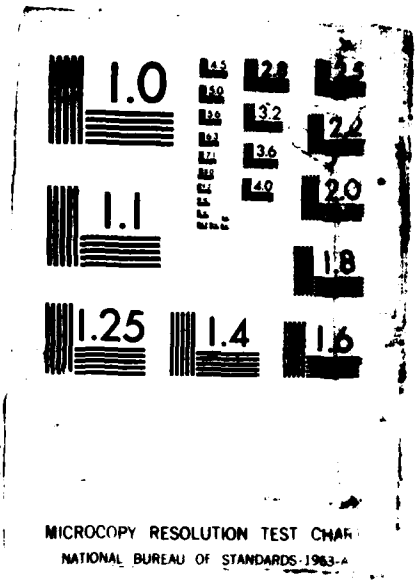
1.0
1.1
1.25
1.4
1.6
1.8
2.0
2.2
2.8
3.2
3.6
4.0
MICROCOPY RESOLUTION TEST CHAR
NATIONAL BUREAU OF STANDARDS-1963-A

region which is to be expected for indirect (direct) circulation in the jet exit (entrance) regions. Fig. 34b represents changes in psi with negative values noted across the jet exit region and positive values in the jet entrance region. This correlates well with Fig. 33b with the same conclusions of an ageostrophic component to the northwest under jet exit and to the south across the jet entrance region. Changes in pressure (Fig. 34c) correlate positively with theoretical values expected with strongest positive values just on the cyclonic side of the jet axis exit region and strongest negative values near the jet axis entrance region similar to the theoretical model shown in Fig. 15. These results support the observation that the CMCB plays a part in the lower transverse circulation of curved jet streaks.

4.15 Identification of Forcing Terms prevalent in CMCB.

Eularian computations of omega in the CMCB are shown in Fig. 35a and b for the two time periods. The heavy dashed line indicates the outline of the CMCB for both respective time periods. Cross-hatched regions are areas of strongest upward and downward vertical motion

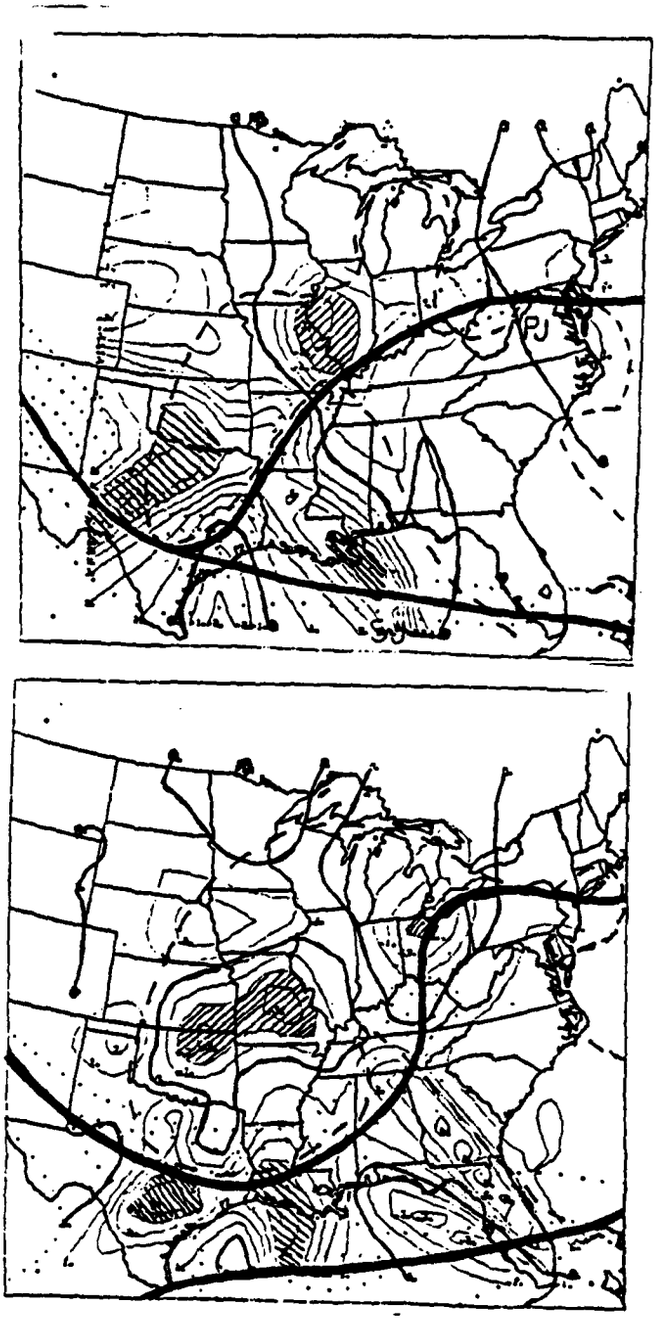

(a)

(b)

Figure 35. Calculations of omega (a) on 290°K isentropic surface at 0000 GMT (b) on 286°K isentropic surface at 1200 GMT. Right/Left Stippled regions indicate enhanced areas of rising/sinking motion. Heavy dashed lines represent outer boundary of CMCB.

within the CMCB. Strong upward vertical motions are noted over Missouri well to the left of the jet axis. In Fig. 35a, the location of the maximum upward vertical motion appears to be a consequence of curved flow and diffluence since it is to the cyclonic side of the cyclonically curved trough near the inflection point. Hence, the effects of warm air advection on the actual jet streak appear to be limited since it would put the area over the jet axis and well to the southwest of its actual location.

Areas of strongest downward vertcal motion appear to occur near and just to the cyclonic side of the jet axis similar to the observations of Krishnamurti (1968) and Mudrick (1974) and to theoretical results for frontogenesis for curved jet streaks by Newton and Trevisan (1984). This would indicate the effects of curvature and cold air advection as discussed by the aforementioned authors in their previous studies.

Vertical motion measurements in the CMCB at 1200 GMT (Fig. 35b) indicate areas of maximum vertical motion. One area is located over Ohio and appears in the left front quadrant of the jet streak located over Kentucky and is very similar to Fig. 4a. The second larger area is over central Missouri and is located well to the

to the cyclonic side of the jet axis. It appears due north of the main jet streak located in the trough over southeast Texas. This comes close to the left front quadrant of a jet streak. However the extreme cyclonic side appears to be feedback from a combination of mechanisms, diffluence, curvature and possible enhancement from the jet streak over Kentucky. Comparison of vertical motion fields to divergence fields (not shown) at 290°K and near tropopause at 320°K revealed good agreement with low/high level convergence/divergence in areas of upward vertical motion and divergence/convergence in areas of downward vertical motion.

4.2 Case Study II

4.21 Synoptic Overview

The second cyclone discussed occurred over the central and eastern United States during the period from 25 to 29 February 1984. The specific time periods covered are 0000 GMT 27 February to 0000 GMT 28 February 1984 and were selected since the storm became a mature occlusion with a well developed CMCB and an upper air pattern similar to Fig. 12c during this time. Inspection of Fig. 36 depicts the surface and upper air features of the storm during these time periods.

On 27 February at 0000 GMT the center of the surface low was situated over extreme northeastern Texas with a warm front extending eastward to northern Georgia and a cold front southward and westward to Northern Mexico. A large anticyclone is located 1300 km north near Duluth, Minnesota. The CMCB extends from Charleston, SC northward to Norfolk, VA and is evidenced by the easterly winds. It extends westward to a Minnesota - Texas line bounded by the respective anticyclone and cyclone. It then turns southward to central Texas as a northerly wind. Widespread cloudiness and

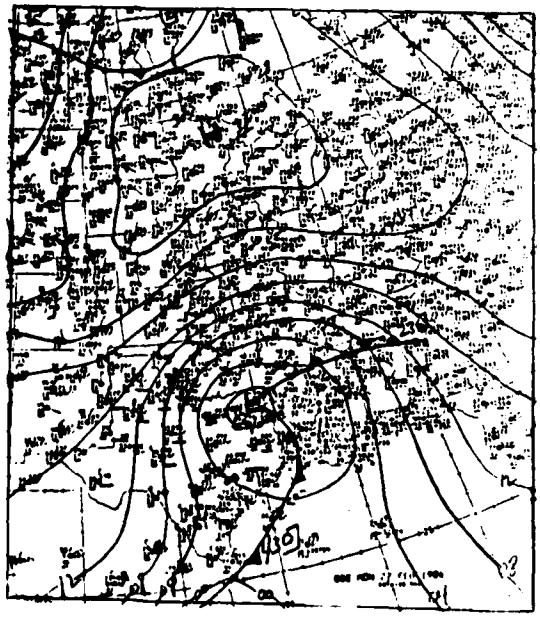

(a)

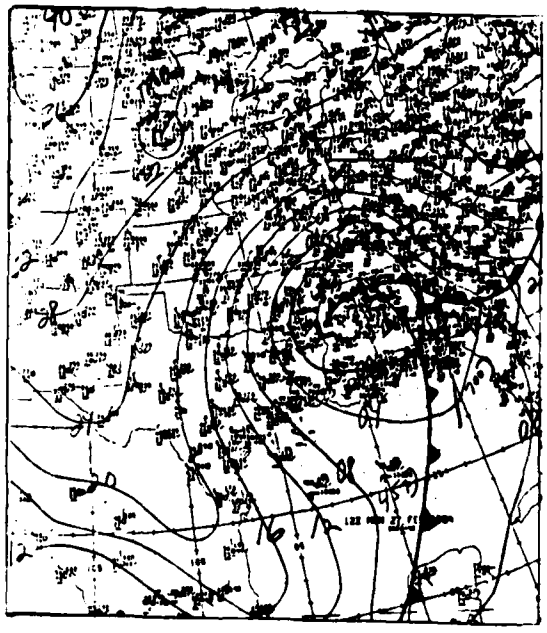

(b)

Figure 36. (a) Surface pattern for the period 0000 GMT 27 February 1984. Thin solid lines indicate pressure height contours. All symbols have usual metorological meanings; (b) same as above except for 1200 GMT 27 February

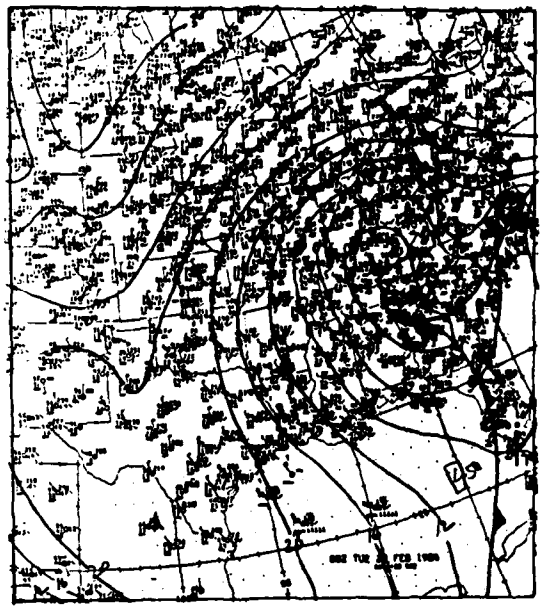

(c)

Figure 36 (c) cont.) Same as Fig. 36 (a) and (b) except for time of 0000 GMT 28 February 1984

precipitation indicative of rising vertical motions are characteristic of the flow peaking in the area due north of the low in central Missouri where moderate snow is reported. Both the precipitation and cloudiness diminishes as the flow turns south reaching an area of fair skies in central Texas indicating sinking motion. Fig. 36b and c are for the following two time periods indicating the movement of the storm during the period studied. During this time period the low moves northeast reaching full occlusion in central Kentucky by 0000 GMT on the 28th of February.

Upper air features related to the system indicate (Fig. 37a) a curved jet maximum of 110 kts at the base of the trough near Del Rio, TX similar to Fig. 12c. Two other embedded jet streaks are noted with one nearly straight at over 90 kts in western Missouri and second stronger maximum of 110 kts in the anticyclonic ridge near Chicago. This indicates a more complex pattern than schematically shown earlier in the figures of sections 1 and 2. Thick solid lines indicate the jet axis with windspeeds 70 kts or greater. By 1200 GMT (Fig. 37b), the main jet maximum has reached the southeast quadrant of the trough with a wind maximum of over 130 kts. A second anticyclonic jet maximum is now

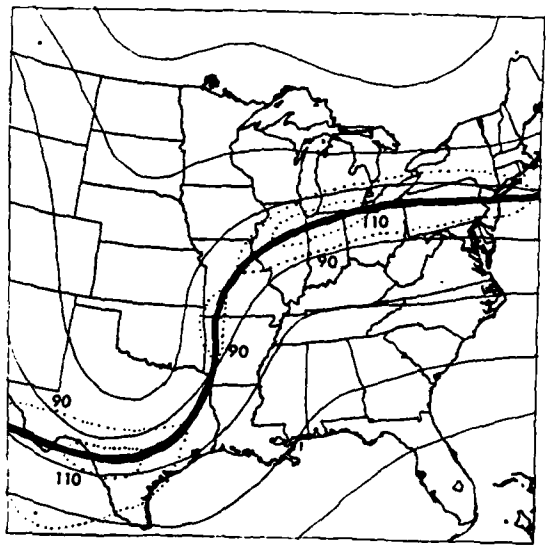

(a)

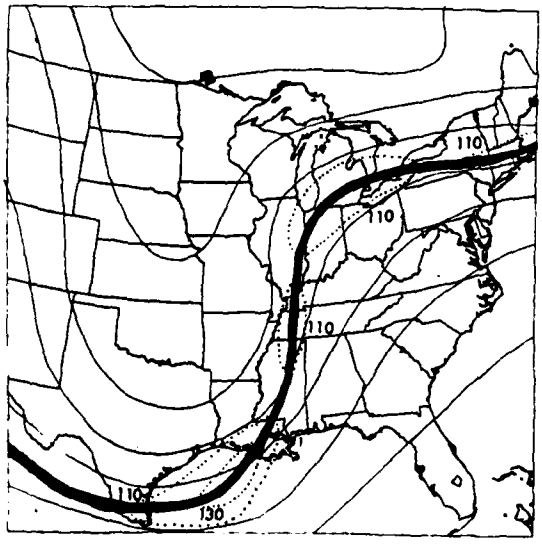

(b)

Figure 37. 250mb analysis for (a) 0000 GMT and (b) 1200 GMT 27 February 1984. Thick solid line, jet axis; thin solid lines, height contours; dotted lines, isotachs.

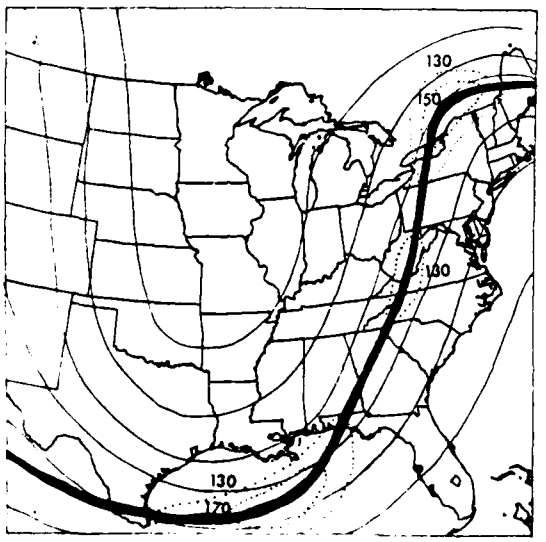

(c)

Figure 37 (c) cont.) Same as Fig. 37 (a) and (b) except for 0000 GMT 28 February 1984.

located over the Great Lakes. Finally at 0000 GMT on the 28th, the main jet maximum of170 kts has moved steadily eastward to a position just south of New Orleans, LA with a second maximum of over 150 kts running from West Virginia northward to near Montreal, Quebec. For all these time periods it appears that the main jet streak stays "locked" in to the bottom of the trough with various speed maximum running through them. Therefore it appears to act more like a continuous jet shown in Fig. 4b than a single jet streak as in Fig. 4a. As indicated by Fig. 37, manual analysis became necessary since corresponding NWS upper air charts missed many of the secondary jet streak maximums.

4.22 Locating the CMCB on an isentropic surface

Cross sections and soundings in the CMCB through the jet exit and entrance regions of the jet streak trough were taken using the same procedures outlined for case study I. Good cross-sections were obtained for the jet exit region at all three time periods (not shown). A good cross section was also obtained for the first jet entrance time period but as the jet moved slowly southeast over the next two time periods only the

area around and to the north of the jet axis was well represented with areas well to the south unobtainable due to lack of upper air data over Mexico and the Gulf of Mexico.

Sounding data for the stations furthest upstream of each cross-section (not shown) illustrated features generally synonomous to points B and D in Fig. 17 and Case study I. They showed that the top of the CMCB in the jet exit region were at 750, 780, and 650 mb for the three time periods. Their existence was indicated by the expected inversion and veering of the winds at these levels. In the jet entrance region for the CMCB the top was analyzed at 600, 550, and 400 mb and was evidenced by an inversion and a sharp backing of the winds at these levels.

Corresponding isentropic cross-sections (not shown) of the heights selected from the aforementioned soundings indicated the top of the CMCB was at about 297°K in both the jet entrance and exit regions for 0000 GMT 27 February. At 1200 GMT, the top remained near 297°K while by 0000 GMT the top had risen to near 306°K indicating significant cooling of the system had occurred. This can also be noted by the raising of the analyzed heights with time for the top of the CMCB.

Selection of the preferred isentropic surfaces fo further computations was done with same purposes outlined in case I. After inspecting all isentropic cross-sections, values of 292°K for trajectories and 288°K for streamlines were determined most desirable. This provided an average height of near 830 mb and 860 mb for computations with maximum heights of 650 mb or below which would keep all computations in the lower half of the transverse circulations related to jet streaks. Only at surfaces well to the anticyclonic side of the jet axis for 0000 GMT 27 February did the isentropic surface actually encounter the ground. Since this is out of the area of the CMCB, it provided no problems.

4.23 Location and orientation of CMCB to jet streaks

Analysis of streamlines on 288°K and 292°K surfaces for the 1200 GMT and 0000 GMT time periods are shown in Fig. 38. Again the location of the CMCB is outlined by a thick dashed line. The stippled region is an area where isentropic surface reaches the ground. In Fig. 38a, we note the east-southeast flow outlined in Fig. 8a for cyclonically curved jet streak. The parent

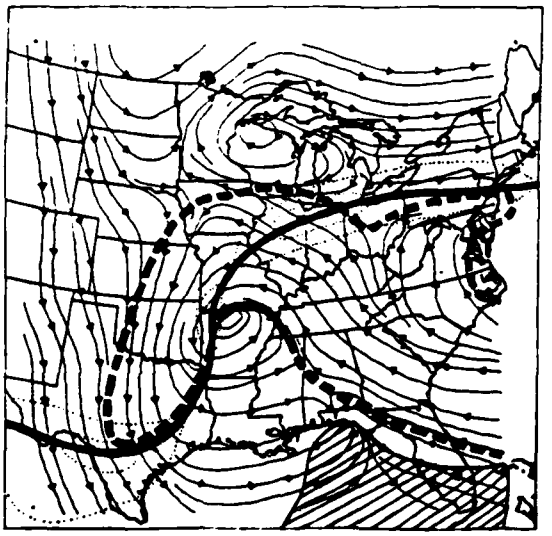

(a)

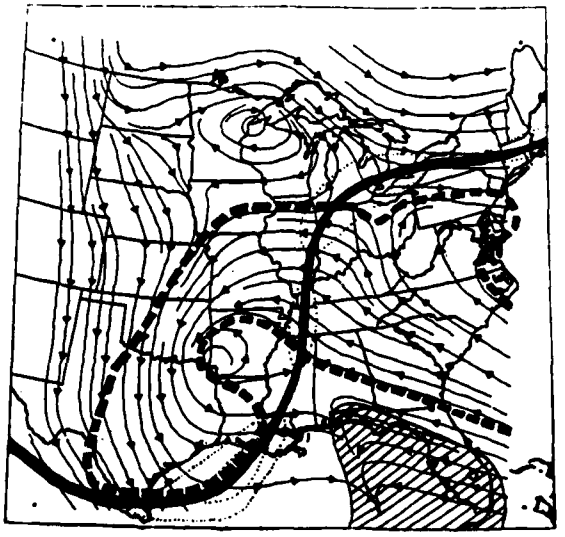

(b)

Figure 38. Relative streamlines for (a) 0000 GMT (b) 1200 GMT 27 February 1984. Heavy dashed lines indicates the boundary of the CMCB. A thick lines depicts jet axis; dots represent isotachs. Stippled area is where isentropic surface intersected the ground.

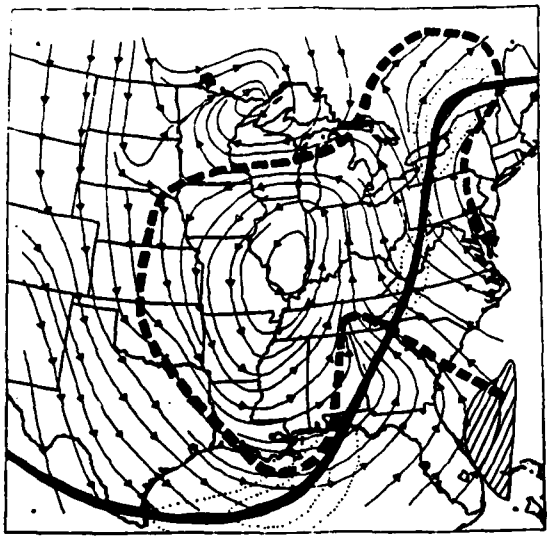

(c)

Figure 38 (c) cont.) Same Fig. 38 (a) and (b) except for 0000 GMT 28 February 1984.

low at this level is near the inflection point of the jet axis with flow ahead (north) of low crossing nearly perpendicular to the jet axis from east to west and flow behind crossing from north to south which is more similar to a straight jet streak. Again we see both branches of the CMCB as one ascends and turns cyclonically away while the other turns cyclonically behind the storm center. These features are repeated for the ensuing two time periods except the cyclone center moves well to the left (cyclonic) side of the jet axis. Flow ahead of the main trough remains almost 90° to the jet axis ahead of low while flow behind it backs with time angling across the axis similar to Fig. 8b indicating effects of curvature.

Selected trajectories in the CMCB illustrate the flow within the CMCB at different stages. In Fig. 39a, covering the period 0000 to 1200 GMT 27 February, we see strong southward flow toward the jet axis in parcels 10 and less representing the terminal portion of the closed CMCB. Parcels 12 and 16 represent flow very close to storm center. Parcels 14 and 18 and to some extent 10 show flow turning cyclonically around storm center while the remaining parcels indicate an anticyclonic turning away from storm center as in the "open wave" portion.

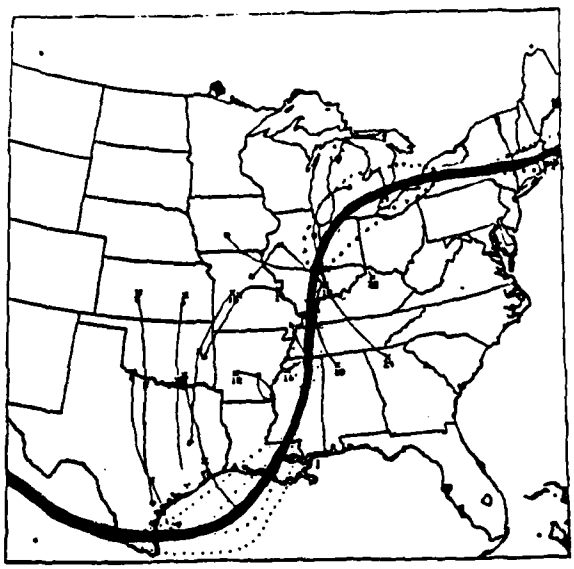

(a)

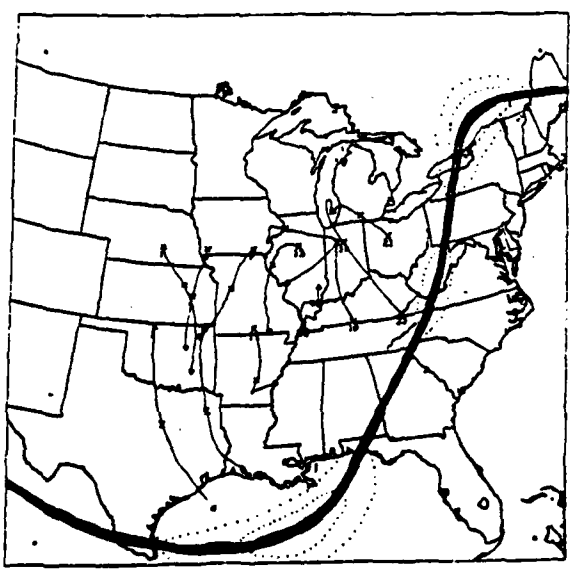

(b)

Figure 39. Trajectories of selected gridpoints on a 290°K for the periods (a) 0000-1200 GMT 27 February 1984, (b) 1200 GMT 27 February to 0000 GMT 28 February 1984. Crosses at beginning indicate starting point of each parcel, crosses at center of line illustrate position at 6 hour point, arrow shows ending position.

In the second time period (Fig. 39b), the same general pattern is repeated except no turning away from the storm center analogous to the "open wave" is noted. This is problably due to the closeness of the preselected points with the storm center and the fact that storm center was intensifying with time.

4.24 Relationship of CMCB to lower transverse circulations in jet streaks

In this case, flow of the streamlines across the contours of Montgomery Streamfunction (psi) (Fig. 40) for all three time periods illustrate the flow across the contours to lower values of psi for the easterly flow ahead the main jet streak trough. After the CMCB turns southward and heads back toward the jet axis generally higher values of psi are reached. Hence this indicates an ageostrophic component from east to west for the jet exit region and northwest to southeast in the jet entrance region. This is consistent with the indirect circulation in jet exit regions and direct circulations in entrance regions as proposed by Uccellini and Johnson (1979) and others.

Analysis of the streamline flow across contours of

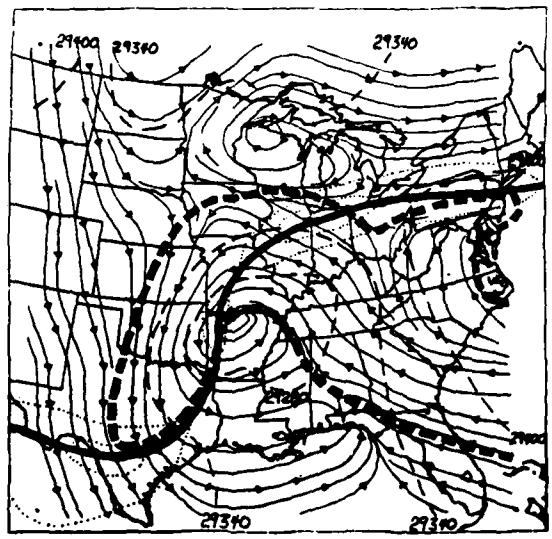

(a)

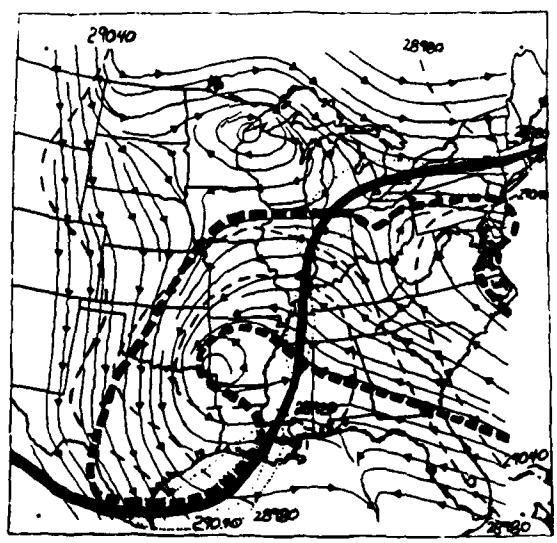

(b)

Figure 40. Cross-contour flow of streamlines at (a) 0000 GMT 27 February on 292°K surface and (b) at 1200 GMT on 288°K surface. Dashed lines indicate contours of Montgomery Streamfunction (psi). Thick line, jet axis; dots, isotachs.

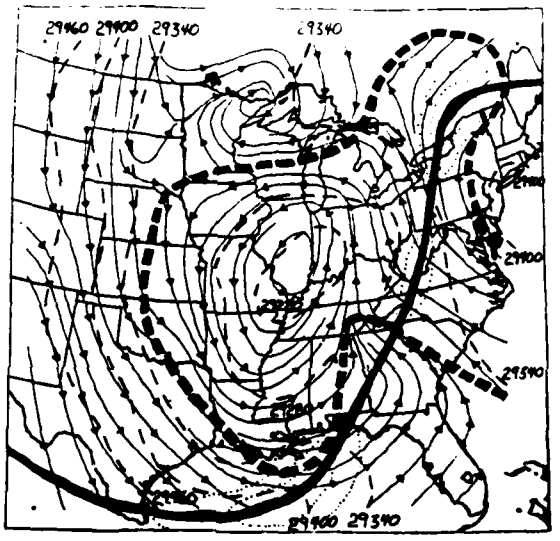

(c)

Figure 40 (c) cont.) Same as Figure 40 (a) and (b) except for 0000 GMT 28 February on an 292°K surface.

constant pressure is another avenue of cross-checking the implied vertical motions fields of streamlines across jets with the theoretical fields (Fig. 41). Looking at the vertical motion field as the CMCB crosses the jet axis from the east we note an increased cross-contour gradient to lower pressure indicative of upward vertical motion along and to the cyclonic side of the jet axis. This then is consistent with the results outlined by Cahir (1971) in Fig. 6 and modified by curved jet streak with diffluence as shown by Newton and Trevisan (1984) in Fig. 14. As the CMCB reaches the jet axis from the north we note increasing pressure values are reached indicative of sinking motions. This is similar to findings for the jet entrance region with a direct thermal circulation as shown in Fig. 11a and c and Fig. 14.

Computations of the change in potential energy for parcels in the CMCB (Fig. 42) illustrate a positive correlation with the theoretical results of increasing potential energy in the jet exit region and decreasing in the entrance region as outlined by Johnson (1970). For all three time periods we note maximum positive values over the Midwest near the jet entrance region with crosses representing the midpoints of the

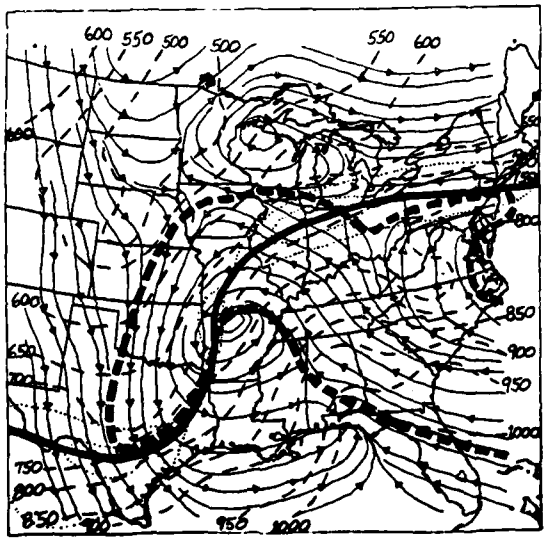

(a)

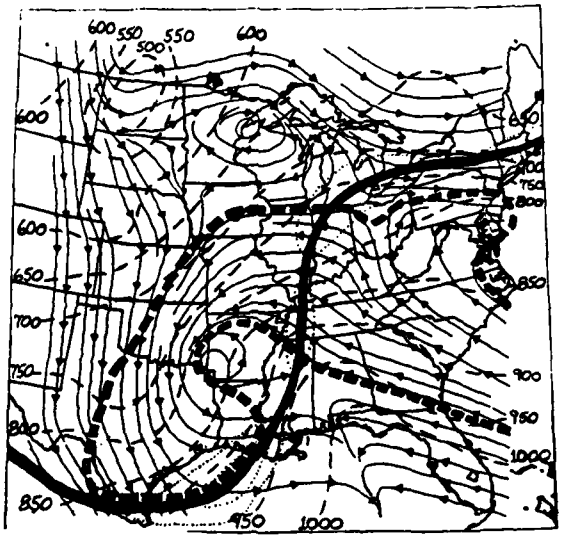

(b)

Figure 41. Same as Fig. 40 (a) and (b) except for pressure.

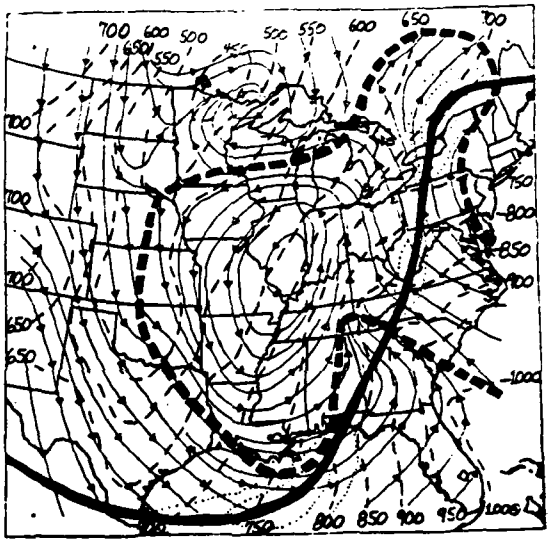

(c)

Figure 41 (c) cont.) Same as Fig. 40 (c) except for pressure

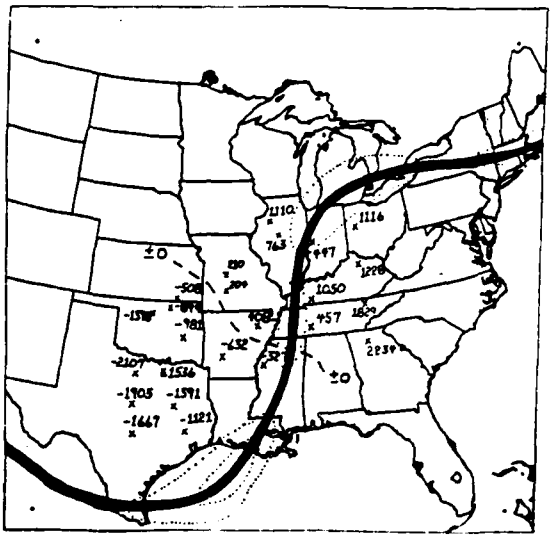

(a)

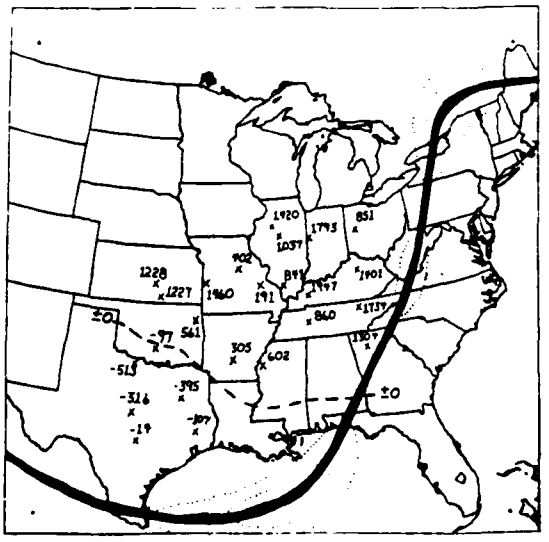

(b)

Figure 42. Computations at the midway point of all parcels in the preselected grid for the period of (a) 0000-1200 GMT 27 February 1984 and (b) 1200-0000 GMT 27-28 February 1984, for changes in potential energy. Dashed line is isopleth between positive and negative values.

shown in Fig. 42 for each corresponding time period. Negative values are located in Texas near the jet entrance region.

Computation of the change of psi as shown in Fig. 43 demonstrate clearly the negative values obtained ahead of the low in the jet exit region and positive values behind the low in the jet entrance region giving further support to involvment of the CMCB in the lower component of the transverse circulations. Respective values of the change in pressure (omega) in Fig. 44 give us a good cross reference to the vertical motion field obtained by isentropic cross-contour flow as well as by Eularian computations. Rising motions are obtained in the jet exit region with sinking motions for the entrance region giving us a general pattern similar to that obtained by isentropic cross-contour flow.

4.25 CMCB and Forcing Mechanisms

Computations of omega for the three streamlined surfaces are used to relate which possible forcing mechanisms outlined in section 2 appear to be important for this case study. Fig. 45 shows the vertical motion fields in microbars per second with most significant

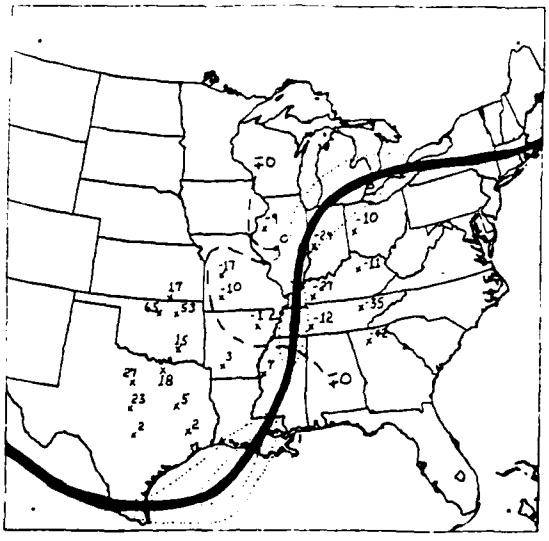

(a)

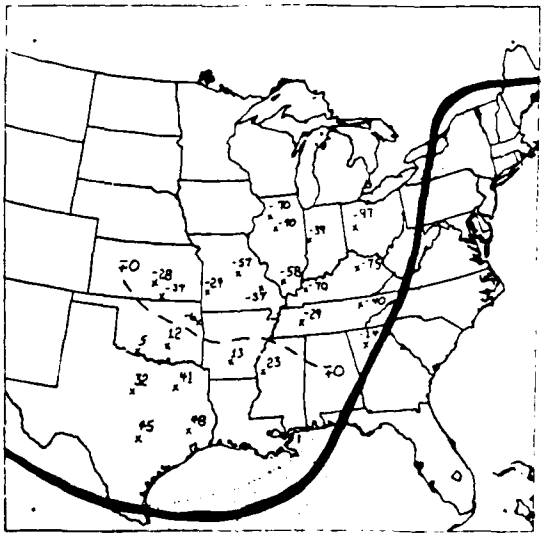

(b)

Figure 43. Same as Fig. 42 except for change in psi.

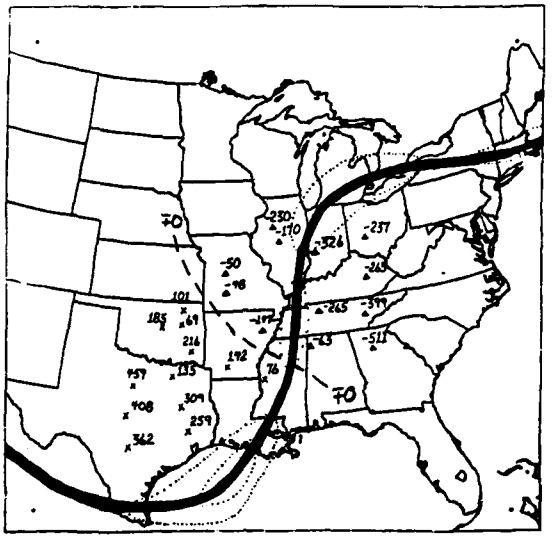

(a)

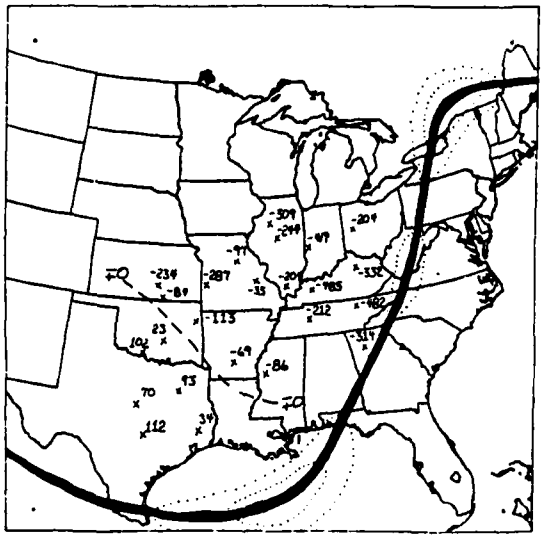

(b)

Figure 44. Same as Fig. 42 except for change in pressure (omega).

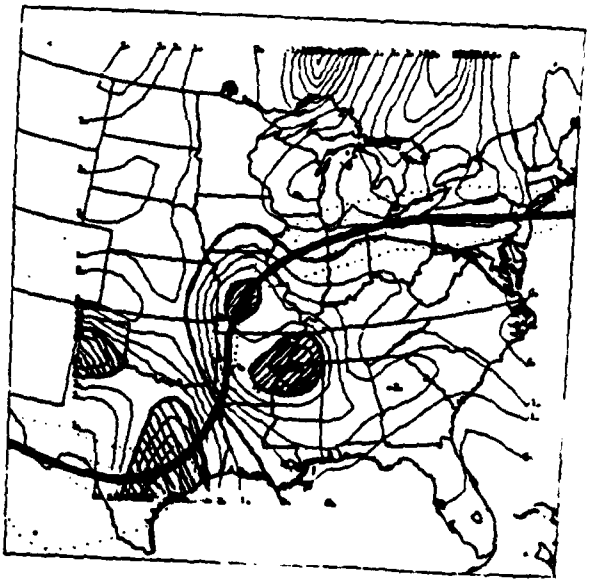

(a)

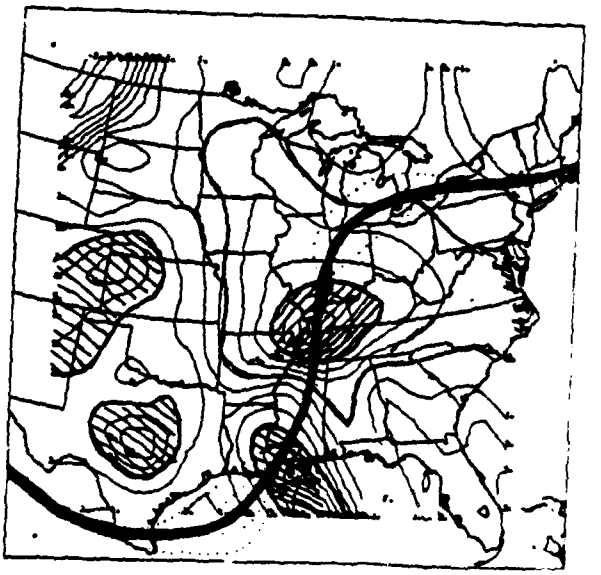

(b)

Figure 45. Calculations of omega (a) on a 292°K isentropic surface at 0000 GMT 27 February (b) on a 288°K isentropic surface at 1200 GMT. Right/Left stippled regions are enhanced areas of rising/sinking motions.

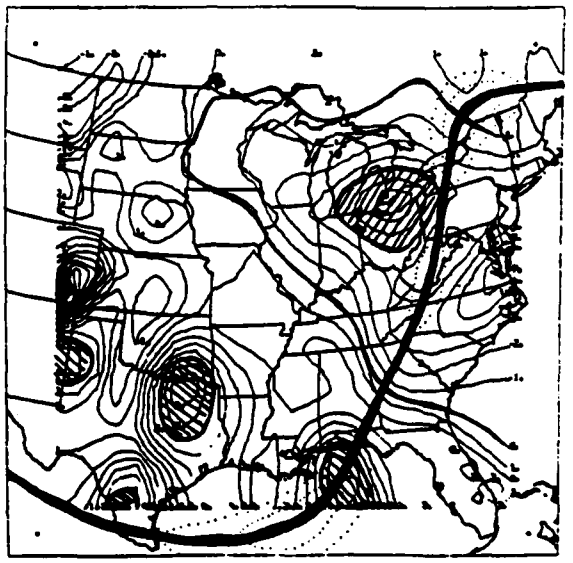

(c)

Figure 45 (cont.). (c) for 0000 GMT 28 February 1984.

areas cross-hatched. Comparing these areas with the location of the curved jet axis and associated jet streaks provides some interesting differences with case I. For the first time period we can note two areas of strong upward motion. One area is well to the right of the jet axis and is located near Memphis with a second maximum straddling the axis in central Missouri. The first area is near the triple point of the storm and is an area of convective showers which would help to destroy the isentropic surface giving us some questionable values. The second area was free of these effects and appears reliable as stratified rain and snow was falling in the area. Comparing its location with the jet axis, it is situated just downstream from the inflection point of the trough which would be the desired area for upward vertical motion for a curved jet. Also of significance is warm air advection since it would provide for enhanced upward vertical motion along the jet axis.

The area of enhanced downward vertical motion lies underneath the bottom of the jet axis trough which correlates well with the findings of Mudrick (1974) and others. In the second time period, this general pattern is repeated. In the last time period, two upward

vertical motion areas are noted again with the one over Norfolk, VA related to convective precipitation. The second area near Lake Erie is now left of the jet axis and appears to be related to the jet streak over West Virginia as well as the larger scale forcing related to the curved trough. Another possible participant for this location could be diffluence since it would create upward vertical motion on the cyclonic side of the jet axis in the exit region. An important side note is the fact that wind speeds throughout the jet axis were at least 110 kts which means the difference in magnitude of the jet streaks was less than what is normally considered standard for a typical jet streak. Hence in this case, the jet streak acted more like a continuous jet (with small embedded maxima) than a single large jet streak.

4.3 Case Study III

4.31 Synoptic Overview

This extratropical storm occurred during the period of 1200 GMT 17 March to 1200 GMT 18 March 1987 and was chosen because of its very strong CMCB ahead of the low pressure system. Inspection of the synoptic situation shows a very strong high presure system just north of the Great Lakes which remained nearly stationary (Fig. 46) while a strong low presure system moved slowly northeast over the time period. This caused a tightening of the pressure gradient across the region producing surface winds of 20 kts or more across much of the Midwest. The flow around the low pressure system is significantly different than the other two cases in that the CMCB appears to lose its strength as it turns cyclonically around the low since the pressure gradient weakens considerably.

Analyis of the upper air (Fig. 47) indicates a strongly curved jet across the southern plains with strong northwesterly jet extending from the Great Lakes to east of Cape Hatteras. Three jet streaks are observed for all three time periods with the first a

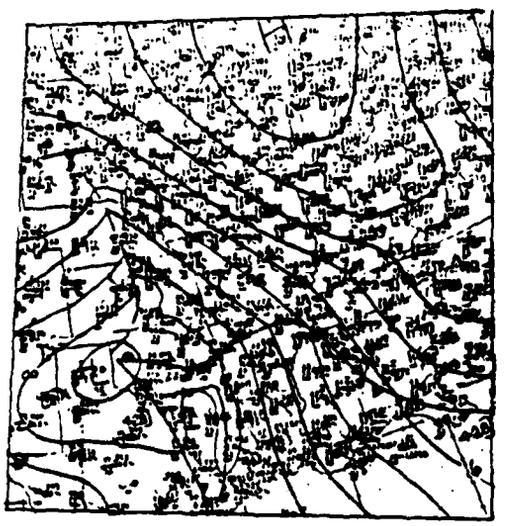

(a)

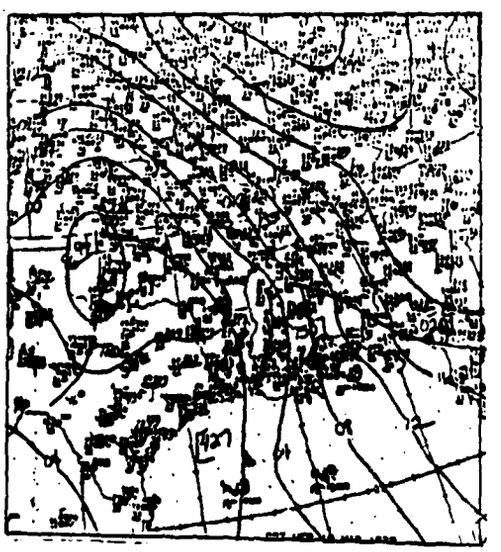

(b)

Figure 46 (a) and (b). Same as Fig. 38 except for the period 1200 GMT 17 March 1987 to 1200 GMT 18 March 1987.

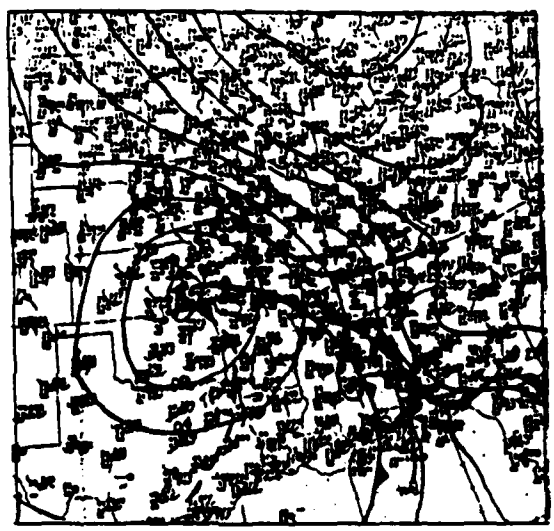

(c)

Figure 46 (c) cont.) Same as Fig. 46 (a) and (b) except for 1200 GMT 18 March 1987.

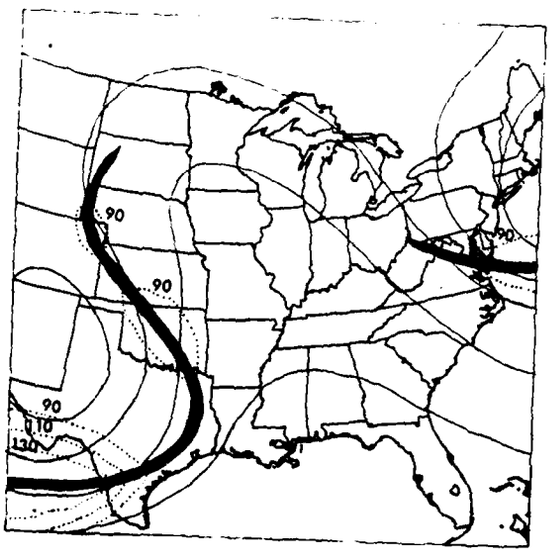

(a)

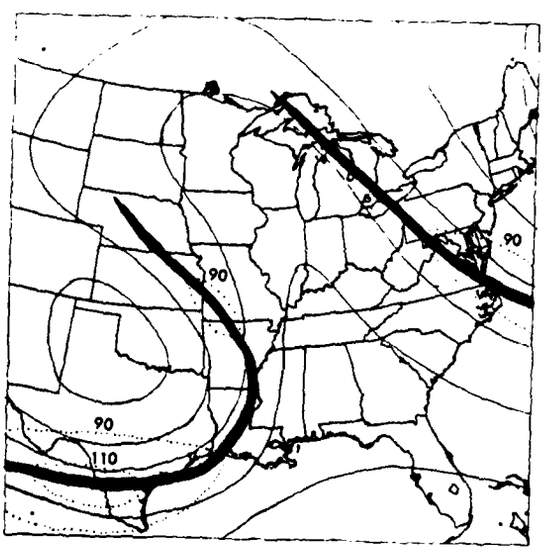

(b)

Figure 47 (a) and (b). Same as Fig. 39 (a) and (b) except for the time periods 1200 GMT 17 March to 1200 GMT 18 March 1987.

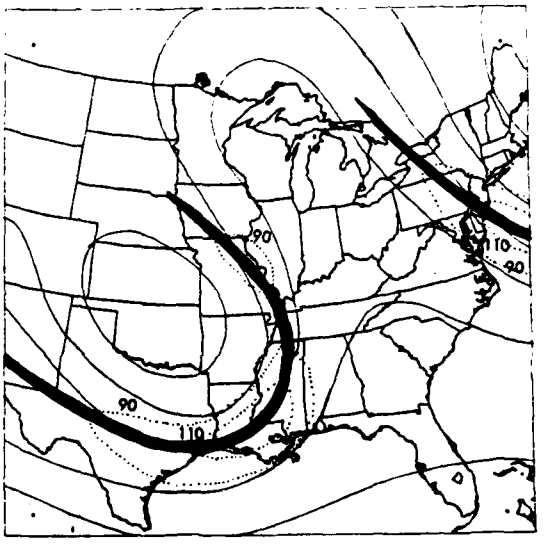

(c)

Figure 47 (c) cont.) Same as Fig. 39 (c) except for time period of 0000 GMT 18 March 1987.

curved jet located in the base of the trough, another nearly straight near the inflection point downstream of the trough and a third also nearly straight located in the northwesterly flow over the northeast.

4.32 Identification Of the CMCB and selection of Isentropic Surfaces

Isentropic cross-sections and soundings were taken in jet entrance and exit regions using the same criteria outlined in case study I. Cross-sections across the jet entrance region were again limited by lack of upper air data south of Texas. Profiles of the isentropic cross-sections (not shown) showed the same general features shown in the first two cases with the jet entrance region resembling Fig. 13b while the exit region generally resembled the exit regions of Fig. 11a and c which illustrate diffluence and along-jet warm advection.

Analysis of the soundings taken for the station furthest upstream from each cross-section(not shown) illustrated all the features outlined at points B and D in Fig. 17. Further analysis revealed one interesting item for the soundings located near point B in the jet

exit region. A very strong inversion was present in the lowest 50mb of the surface with very strong winds for these levels of up to 30 kts. This indicates there is a strong supply "new" CMCB air entering the system from the large anticyclone over the Great Lakes.

Selection of isentropic surfaces for computation of isentropic streamlines and trajectories was accomplished in the same manner as the preceding two cases. Streamline surfaces of 290°K were calculated , while 296°K was used for trajectories which enabled us to get below all inversions found on the preceding soundings for the tops of the CMCB.

4.33 Locating CMCB and its relationship to Jet Steaks

Inspection of the streamline analysis for all three time periods (Fig. 48) indicates a large influx of air into the CMCB from the anticyclone to the north. This helped "feed" the CMCB as the flow turned to the east and southeast. Further inspection indicates that for this case very little, if any of the CMCB turns behind the low center at this level but continues northwest in the "open wave". Also noteworthy, is the apparent parallel flow of the CMCB at this level with the jet

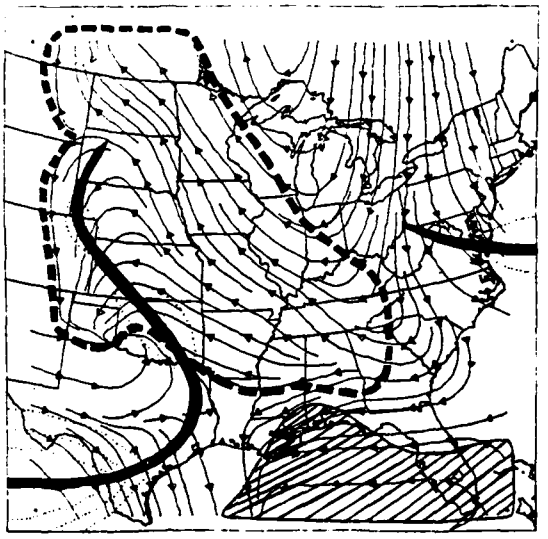

(a)

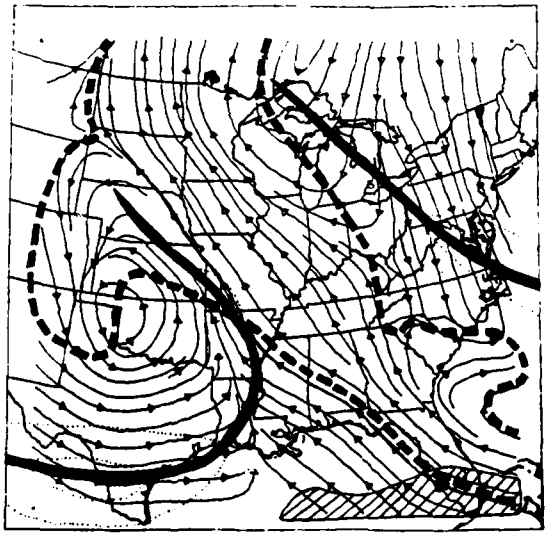

(b)

Figure 48. Relative streamlines for (a) 1200 GMT 17 March 1987, (b) 0000 GMT 18 March 1987. Heavy dashed line indicates the boundary of the CMCB. Thick black line is jet axis, dots represent isotachs.

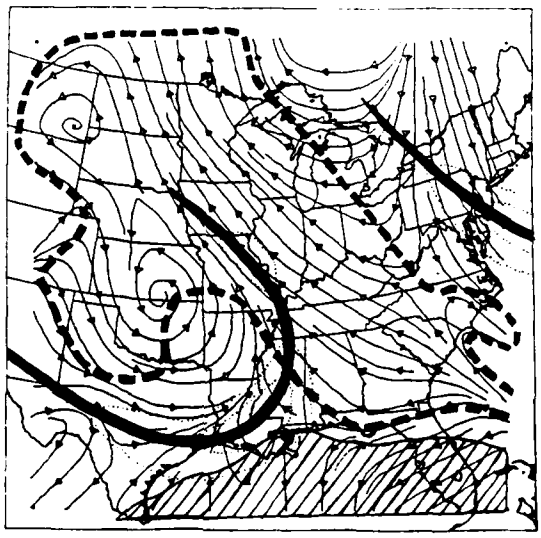

(c)

Figure 48 (c) cont.) Same as Fig. 48 (a) and (b) except for 0000 GMT 18 March 1987.

axis indicating strong effects of curvature. The flow that goes around the low parallels the upper-level jet axis. Also of note is the strong crossing of the northerly streamlines out of the anticyclone across the jet axis in the northeast which appears to be part of the lower direct thermal circulation for the jet entrance region of that jet streak. This might be significant due to its proximity to the cyclone and associated CMCB.

Evidence of the "open wave" CMCB is shown in Fig. 49 as almost all the selected parcels show movement away from the actual low center. Only parcel 2 in Fig. 49a and parcel 1 in Fig. 47b show significant components back behind the parent surface low center. Almost all the other parcels are caught in the fast southeasterly flow. Most of the parcels parallel the jet axis with some crossing of the jet axis noted as they reach the end of the jet axis.

4.34 The CMCB and its relationship to transverse circulations in jet streaks

Computations of the change in potential energy for the gridded parcel network is shown in Fig. 50. In Fig.

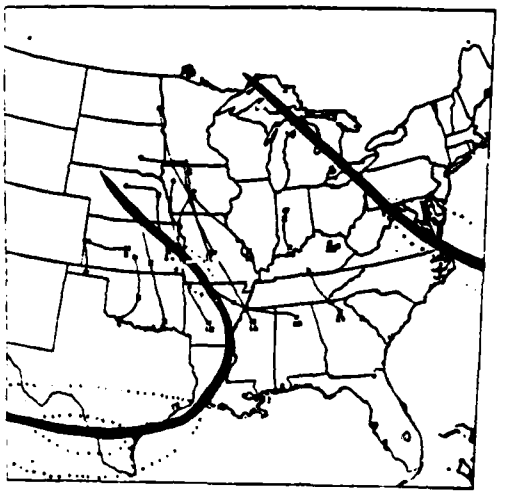

(a)

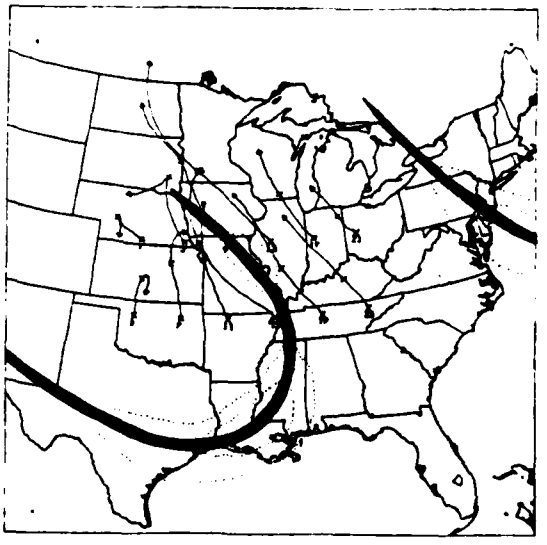

(b)

Figure 49. Trajectories of selected gridpoints on 296°K surface, crosses at one end represent starting points, crosses in the middle are positions of the parcel at 6 h point, arrows at the end are the ending 12 h positions of the selected parcel. (a) for 1200 GMT 17 March 1987 to 0000 GMT 18 March 1987, (b) for 0000 - 1200 GMT 18 March 1987.

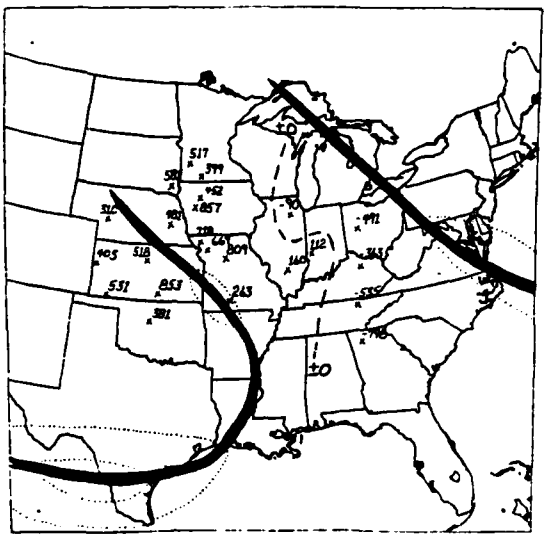

(a)

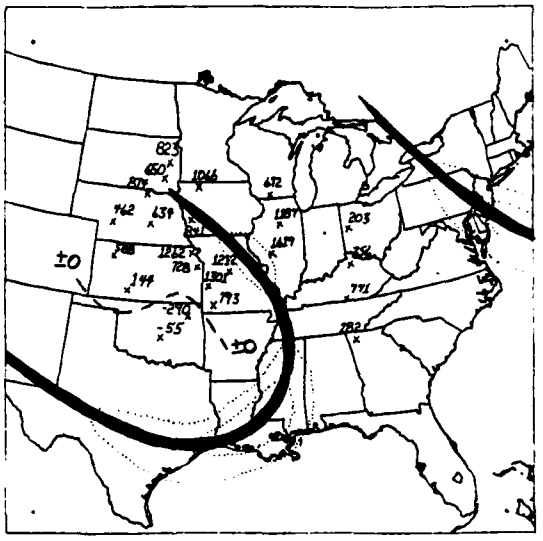

(b)

Figure 50. Computations at the midway point of all parcels in the preselected grid for changes in potential energy for the period of (a) 1200 GMT 17 March to 0000 GMT 18 March 1987, (b) 0000-1200 GMT 18 March 1987. Dashed line reresents isopleth seperating positive and negative values.

50a, high positive values are shown for all but the extreme eastern points which appear to be experiencing the effects of the direct thermal circulation related to the jet streak near Maryland. For the second time period (Fig. 50b), as the trough moves eastward even the easternmost points indicate positive values. Three points of weak negative values are noted near the surface low associated with the weak flow around the center. Looking at the change in psi (Fig. 51) across the CMCB supports evidence that the entire CMCB is linked with the indirect circulation of the jet exit region ahead of the trough. Since the flow is apparently very weak behind the surface low diagnosing the direct portion of the curved jet streak is not attainable. Again note the positive values of psi for the early time frame indicative of the direct circulation of the jet streak over the northeast.

Calculations of Langrangian omegas for the same time periods (Fig. 52) support indirect circulation with nearly all parcels showing rising motions with the maximum values along and to the anticyclonic side of the inflection point of the curved jet axis. Negative values are shown for the early time period for the four easternmost stations supporting the direct circulation

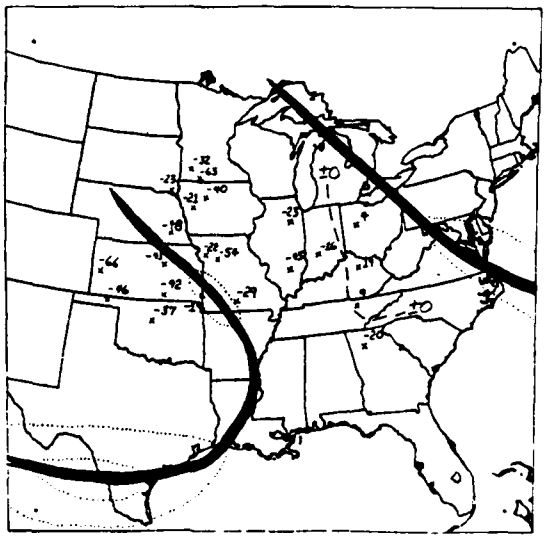

(a)

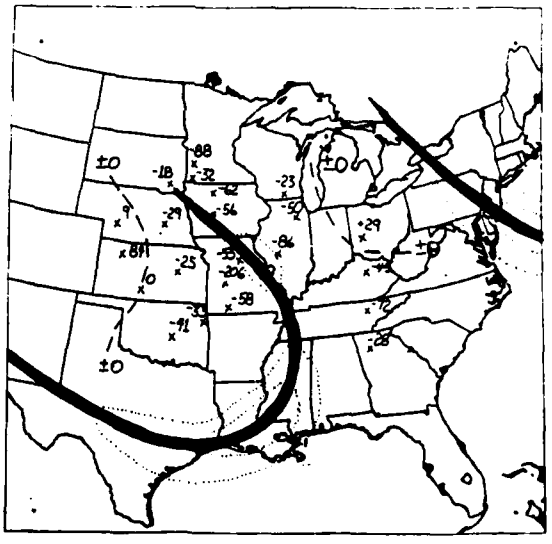

(b)

Figure 51. Same as Fig. 50 except for changes in the Montgomery Streamfunction, (psi).

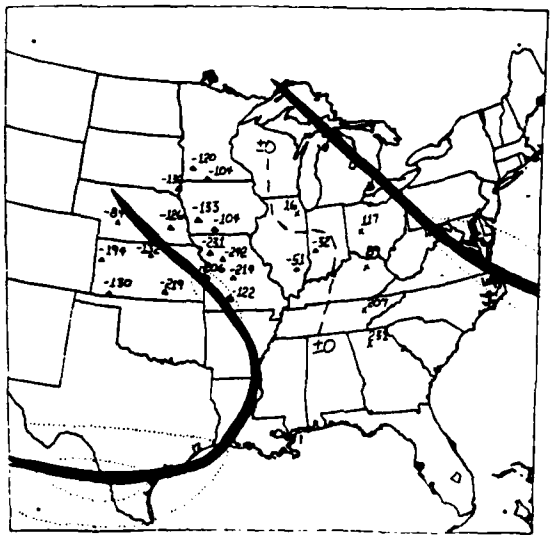

(a)

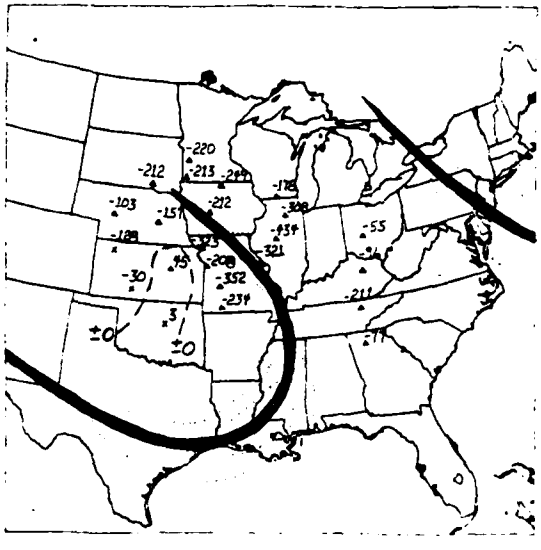

(b)

Figure 52. Same as Fig. 50 except for changes in omega.

associated with that jet streak while three positive values are obtained for the area near the surface in the disorganized weak flow around and behind the surface low.

Cross-contour flow of the streamlines and psi support the Langragian computations of the parcels as rising values of psi are reached for the northerly flow around the high near the jet streak in the northeast (Fig. 53). Meanwhile lower values of psi are reached for the three time periods in the fast moving CMCB. Very little cross contouring to higher psi values is notable in the weak branch behind the surface low.

Looking at the flow across the contour of constant pressure (Fig. 54), reveals apparent strong downward vertical motion across the jet entrance region of the northeastern jet associated with the direct circulation expected there. Strong flow across lower values of pressure are consistent in all three time periods in the southeastern flow of the CMCB. This upward verical motion appears to occur on both sides of the curved jet axis. Some downward vertical motion is apparent in the weak flow behind the low over Texas which appears to strengthen as the low intensifies toward the latter period.

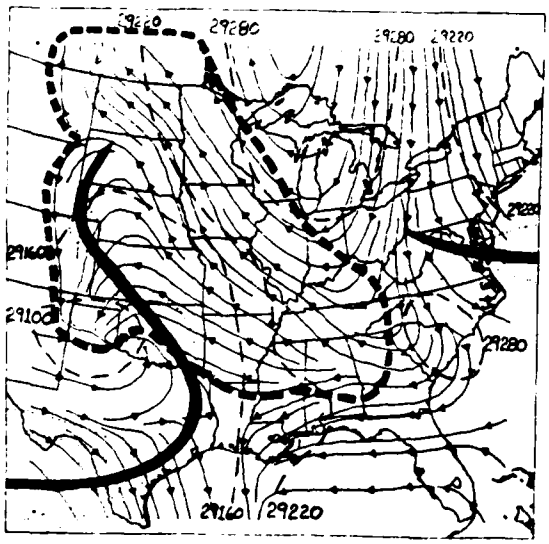

(a)

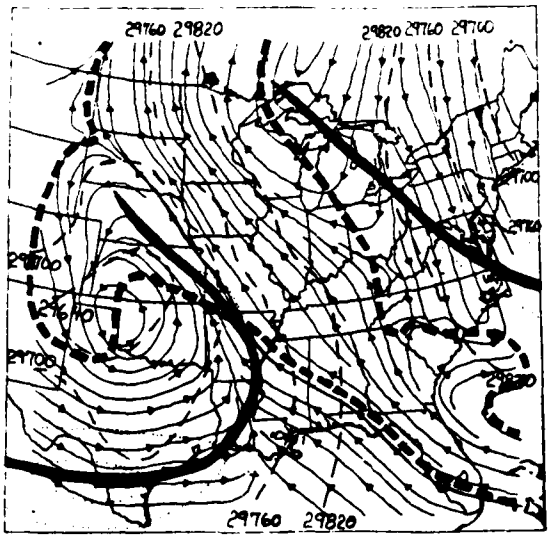

(b)

Figure 53. Cross-contour flow of streamlines at (a) 1200 GMT 17 March on 290°K surface (b) 0000 GMT 18 March on 296°K surface. Dashed lines are psi, heavy dashed line represents boundary of CMCB, Thick line is jet axis, dots are isotachs.

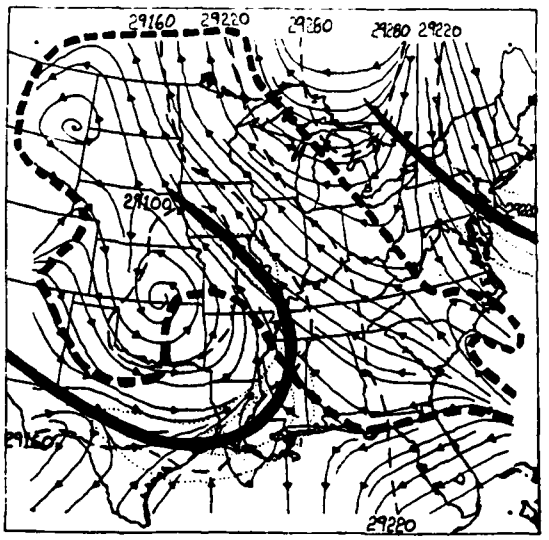

(c)

Figure 53 (c) cont.) Same as Fig. 53 (a) and (b) except for time period of 1200 GMT 18 March 1987 on a 290°K surface.

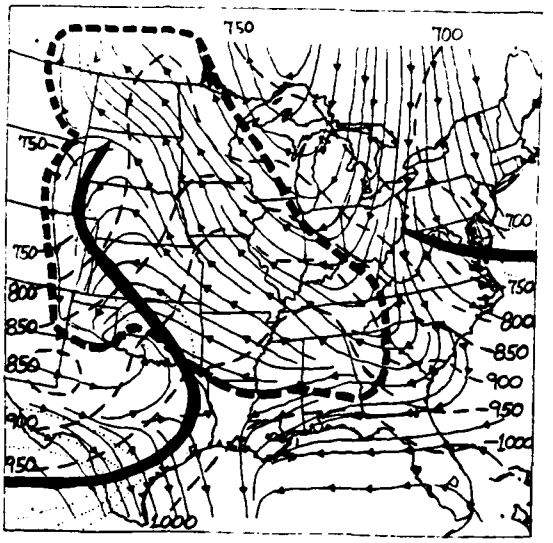

(a)

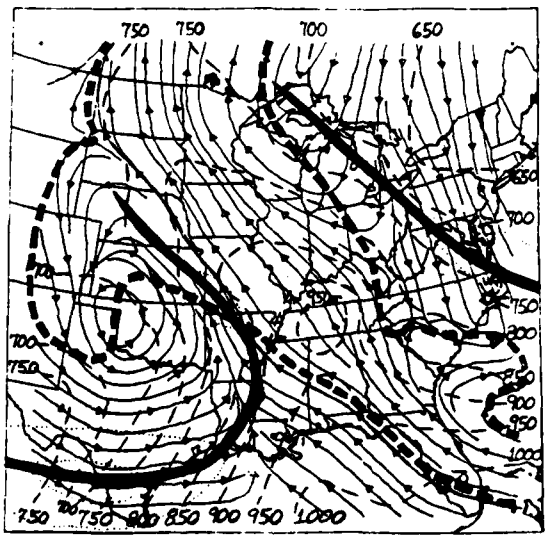

(b)

Figure 54 (a) and (b). Same as Fig. 53 (a) and (b) except dashed lines represent pressure.

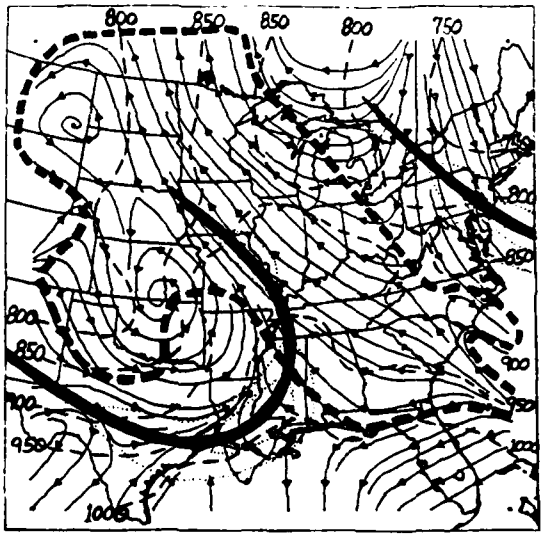

(c)

Figure 54 (c) cont.) Same as Fig. 53 (c) except dashed lines represent pressure.

4.35 CMCB and possible forcing mechanisms of jet streaks

Careful examination of the vertical motion fields for the isentropic levels of 290°K and 296°K show several interesting observations (Fig. 55). For the three time periods we note that the areas of strongest upward vertical motions are to the right of the inflection point of the curved jet. Looking at the vertical motion field around the jet streak axis of the northeast we also see strong downward vertical motions along and to the left of the jet streak in the right rear quadrant similar to the findings expected in Fig. 4a and 5. That would put the upward vertical motion for the right rear quadrant in the Ohio valley. Thus, the location of the upward vertical motion field may be a combination (interaction) of the curved flow jet which would put the flow over the inflection point in the plains and the right rear quadrant of the preceeding jet streak (Ohio valley). This would seem plausable since actual vertical motions appear to be inbetween these two areas and all other calculations have indicated some feedback with the downstream system. The area of strong upward and downward vertical motions over Texas at 0000 GMT are

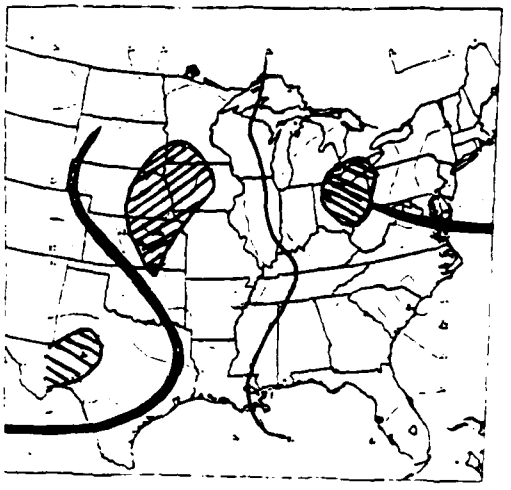

(a)

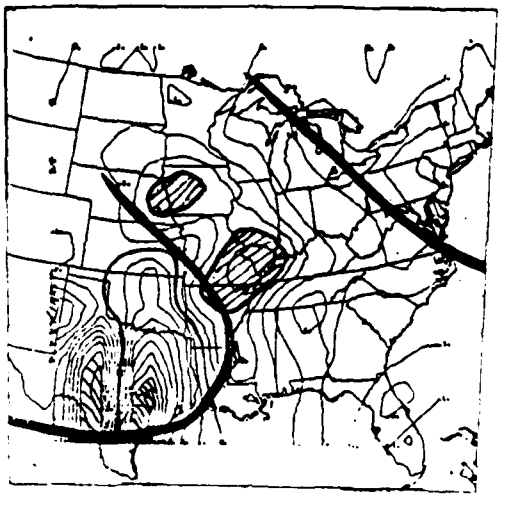

(b)

Figure 55. Calculations of omega (a) on 290°K surface at 1200 GMT 17 March (b) on 296°K surface for 0000 GMT 18 March 1987. Right/Left stippled regions indicate enhanced areas of rising/sinking motion. Heavy dashed lines represent outer boundary of CMCB.

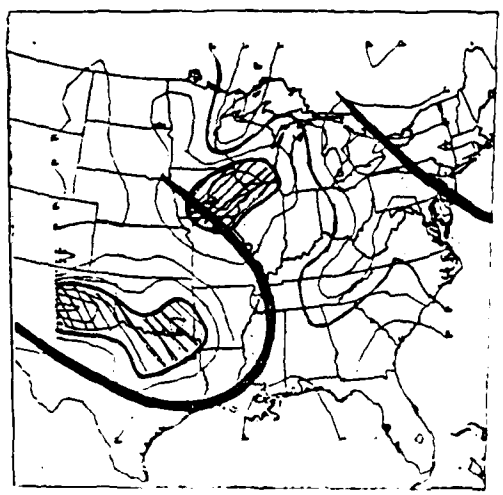

(c)

Figure 55 (c) cont.) Same as Fig. 55 (a) and (b) except for time period of 1200 GMT 18 March 1987 on 290°K surface.

due to a squall line. For the final period some strong downward vertical motion is shown for the cyclonic side of trough which is consistent with our other two cases.

5. CONCLUSIONS AND INTERPRETATIONS

Analysis of the adiabatic flow around the north side of three extratropical cyclones, referred to in this article as the CMCB, revealed two branches. One branch turned anticyclonically away from the low center after it reached a point northeast of the surface low, similar to Carlson's model. The second branch turned cyclonically behind the cyclone center gradually mixing with the CDCB near the jet axis in the bottom of the trough.

Each of the three cyclones analyzed demonstrated its own unique characteristics concerning these two flows. In case I, the cyclonic branch became the major flow pattern which backed with time. In the second case, the two branches appeared to maintain their resective magnitudes well through the time period studied. In this case the orientation of the CMCB appeared to back with time. In the final case, the CMCB demonstrated a weak cyclonic branch while the "open" branch was the prime particpant. The 'open wave' flow appeared to be enhanced by the interaction of a surface cyclone with a strong anticyclone to the northeast.

Exploration of various kinematic parameters revealed support for a direct relationship between the CMCB and upper level jet streaks. Using Langrangian changes of psi, similar to the method outlined by Uccelliini and Johnson (1979), negative changes of psi were diagnosed in the CMCB ahead of the cyclone center with positive values dominating to the west and southwest of the parent low. Hence parcels crossed to lower heights as the CMCB crossed the jet axis from east to west. This supports an ageostrophic component in the same direction and along with the position of the upper level curved jet axis indicates an indirect thermal circulation for the jet exit region. With positive changes in psi for parcels in the northerly component of the CMCB, the reverse is seen as it recrossed the jet axis supporting a direct thermal circulation in the jet entrance region.

Computations from a Langrangian perspective of changes in potential energy and omega revealed support for these two circulations. Computed changes in potential energy and omega revealed values in direct agreement with the expected values for indirect/direct thermal circualtions of jet streaks outlined by Johnson (1970).

Indications from the orientation of the CMCB to the

jet streak axis in both the jet streak entrance and exit region illustrate the effects of curvature of upper level jet streaks. A striking similarity of the CMCB flow and upper-level jet streaks is revealed when compared with the isallobaric flow for curved jet streaks which is assumed to dominate in lower levels as outlined in Fig. 9.

Evaluations of which modifying effects, as outlined by Keyser and Shapiro (1986) for jet streaks and shown in Fig. 11 would hold dominance in the area of the CMCB revealed inconsistent results for the jet exit region. Applications of vertical motion areas in the CMCB to the upper level jet streaks for all three cases indicated varying degees of dominance of the four physical parameters: 1) confluence, 2) diffluence, cold advection, and 4) warm advection along with curvature. Some terms appeared to dominate at certain time periods for certain cases while others did for other cases. A consistent pattern was not evident for the jet exit region as each pattern deviated from the others for all three cases. Also, in the third case, the jet exit region of the storm trough and jet entrance region of the downstream jet streak trough appeared to be

interacting to enhance the low level flow pattern.

In the jet entrance region, consistent strong dowmward vertical motion was obtained along and to the cyclonic side of jet axis for all three cases indicating the effects of confluence, cold air advection and curvature as shown by Krishnamurti (1968) for a developing wave cyclone and Mudrick (1974) and Newton and Trevisan (1984) in their upper level frontogenisis models for curved flow.

Further studies in the relationship of low level flow to jet streaks is necessary to better understand this "coupling". It is not clear as to whether one produces the other or they enhance each other. More studies of the CMCB flow and jet streaks in other cyclones are needed to possibly identify and catagorize certain dynamical effects to certain types of storms.

Other areas to be considered is the possible enhancement of the CMCB due to latent heat release from precipitation as explained by Cahir (1971). Also possible strengthening of the storm circulation due to differential heating of the system caused by high albedos of the clouds in the CMCB compared to the low albedos of the relatively cloud-free areas to the south needs further attention. Finally, a better resolution

of upper air data is needed to reduce possible errors and to better resolve jet streak characteristics, including the effects of multiple jet streaks.

REFERENCES

Astling, E. G., 1982: Some Aspects of Cloud and Precipitation Features Associated with a Mid-latitude Cyclone. Monthly Weather Review, 110, 1466-1473.

Barr, S., M. B. Lawrence, and F. Sanders, 1966: TIROS Vortices and Large-Scale Vertical Motion. Monthly Weather Review, 94, 675-696.

Bergeron, R., 1952: The Distribution of Temperature and Wind Connected with Active Tropical Air in the Higher Troposphere and Some Remarks Concerning Clear Air Turbulence at High Altitude. Tellus, 4, 43-53

Bjerknes, J., 1922: Life Cycle of Cyclones and the Polar Front Theory of Atmospheric Circulation. Geofys. Publ., 3, 1-18.

Bjerknes, J., 1951: Extratropical Cyclones. Compendum of Meteorology, T. F. Malone, Ed. Amer. Meteor. Soc., 577-598.

Browning, K. A., 1971: Radar Measurements of Air Motion Near Fronts. Weather, 20, 320-340.

_____, M. E. Hardman, T. W. Harrold, and C. W. Pardoe, 1973: The Structure of Rain Bands Within A Midlatitude Depression. Quarterly Journal of the Royal Meteorological Society, 99, 215-231.

_____, 1984: Structure and Evolution of a Mesoscale Convective System near the British Isles. Quarterly Journal of the Royal Meteorological Society, 110, 897-913.

_____, and F. F. Hill, 1985: Mesoscale Analysis of a Polar Trough Interacting with a Polar Front. Quarterly Journal of the Royal Meteorological Society, 111, 445-462.

_____, 1986: Conceptual Models of Precipitation Systems. Weather and Forecasting, 1-2, 23-41.

Buzzi, A., T. Nanni and M. Tagliazucca, 1977: Mid-Tropospheric Frontal Zones: Numerical Experiments with an Isentropic Coordinate Primitive Equation Model. Arch. Meteor. Geophys. Bioklim., A26, 155-178.

_____, A. Trevisan and G. Salustri, 1981: Internal Frontogenesis: A Two-Dimensional Model in Isentropic, Semi-geostrophic Coordinates. Monthly Weather Review, 109, 1053-1060.

Byers, H. R., 1974: General Meteorlogy (Fourth Edition). McGraw-Hill, Inc., 461 pp.

Cahir, J. J. 1971: Implications of Circulations in the Vicinity of Jet Streaks at Subsynoptic Scales. Ph.D. Thesis, The Pennsylvania State University, University Park, PA 16802 170 pp.

Cahn, A., 1945: An Investigation of the Free Oscillations of a Simple Current System. Journal of Meteorology, 2, 113-119.

Carlson, T. N., 1980: Airflow through Midlatitude Cyclones and the Comma Cloud Pattern. Monthly Weather Review, 108, 1498-1509.

Carr, F. H. and J. P. Millard, 1985: A Composite Study Of Comma Clouds And Their Association With Severe Weather Over The Great Plains. Monthly Weather Review, 113, 370-387.

Danielson, E. F., 1961: Trajectories: Isobaric, Isentropic and Actual. Journal of Meteorology, 18, 479-486.

Duquet, R. T., 1964: Data Processing for Isentropic Analysis. Tech. Rep. No. 1, Contract At(30-1)-3117, Pennsylvania State University, 36 pp. (Available from Pennsylvania State University, Dept. of Meteorology, University Park, PA 16802.)

Eliassen, A., 1962: On the Vertical Circulation in Frontal Zones. Geofys. Publ., 24, 147-160.

Emanuel, K. E., 1985: Frontal Circulations in the Presence of Moist Symmetric Stability. Journal of the Atmospheric Sciences, 42, 1062-1071.

Endlich, R. M. and G. S. McLean, 1960: Geostrophic and Gradient Departures in Jet Streams. Journal of Meteorology, 17, 135-147.

Fawbush, E. J. and R. C. Miller, 1953: The Tornado Situation of 17 March 1951. Bulletin of the American Meteorological Society, 34, 139-145.

_____, and _____, 1954: The Types of Airmasses in which North American Tornadoes Form. Bulletin of the American Meteorological Society, 35, 154-165.

Green, J. S. A., F. H. Lundlam J. F. R. McIvan, 1966: Isentropic Relative-Flow Analysis and the Parcel Theory. Quarterly Journal of the Royal Meteorological Society, 92, 210-219.

Harrold, T. W., 1973: Mechanisms Influencing the Distribution of Precipitation of Within Baroclinic Disturbances. Quarterly Journal of the Royal Meteorological Society, 99, 232-251.

Hovanic, R. D., and L. H. Horn, 1975: Static Stability and the 300 mb isotach field in the Colorado cyclogenetic area. Monthly Weather Review, 103, 628-638.

Johnson, D. R., 1970: The Available Potential Energy of Storms. Journal of the Atmospheric Sciences, 27, 727-741.

Keyser, D. and M. J. Pecnick, 1985: A Two-Dimensional Primative Equation Model of Frontogenesis Forced by Confluence and Horizontal Shear. Journal of the Atmospheric Sciences, 42, 1259-1282.

_____, and M. A. Shapiro, 1986: A Review of the Structure and Dynamics of Upper Level Frontal Zones. Monthly Weather Review, 114, 452-499.

Koch, S. E., M des Jardins, and P. J. Kocin, 1981: The Gempack Barnes Analysis Scheme. NASA Technical Memorandum 83851, NASA/GLAS, Greenbelt, MD 20771, 56 pp.

Kreitzberg, C. W. and H. A. Brown, 1970: Mesoscale Weather Systems Within an Occlusion. Journal of Applied Meteorology, 9, 417-432.

Krishnamurti, T. N., 1968: A Study of a Developing Wave Cyclone. Monthly Weather Review, 96, 208-217.

Leese, J. A., 1962: The Role of Advection in the Formation of Vortex Cloud Patterns. Tellus, 4, 409-421.

Matsumoto, S., K. Ninomiya, R. Hasegawa and Y. Miki, 1982: The Structure and the Role of a Subsynoptic-Scale Cold Vortex on the Heavy Precipitation. Journal of the Meteorological Society of Japan, 60, 339-354.

Mudrick, S. E., 1974: A Numerical Study of Frontogenesis, Journal of the Atmospheric Sciences, 31, 869-892.

Murray, R. and S. M. Daniels, 1953: Transverse Flow at Entrance and Exit to Jet Streams. Quarterly Journal Royal Meteorological Society, 79, 236-241.

Newton, C. W., 1959 Axial Velocity Streaks in the jet stream: ageostrophic "inertial" oscillations. Journal of Meteorology, 16, 638-645.

_____, 1964: Severe Convective Storms. Advances in Geophysics, Vol 12. Academic Press, 257-303.

_____, and A. V. Persson, 1962: Structural Characteristics of the Subtropical Jet Stream and Certain Lower-Stratospheric Wind Systems. Tellus, 14, 221-241.

_____, and A. Trevisan, 1984a: Clinogenesis and Frontogenesis in Jet Stream Waves. Part I: Analytical Relations to Wave Structures. Journal of Atmospheric Science, 41, 2717-2734.

_____, and _____, 1984b: Clinogenesis and Frontogenesis in Jet Stream Waves. Part II: Channel Model Numerical Experiments. Journal of Atmospheric Sciences, 41, 2735-2755.

Palmen, E. and C. W. Newton, 1969: Atmospheric Circulation Systems: Their Structure and Physical Interpretation. Int. Geophys. Ser., 13, Academic Press, 603 pp.

Peterson, R. A. and L. W. Uccellini, 1979: The Computation Of Isentropic Atmospheric Trajectories Using a "Discrete Model" Formulation. Monthly Weather Review, 107, 566-574.

Petterssen, S., 1956: Weather Analysis and Forecasting. Vol 1. Motion and Motion Systems. Second Edition. McGraw-Hill, Inc., 428 pp.

Reiter, E. R., 1969: Jet Stream Meteorology. University of Chicago Press. 515 pp.

_____, 1972: Atmospheric Transport Processes-Part 3: Hydrodynamic Tracers (AEC Critical Review Series), 212 pp.

Riehl, H., and Collaborators, 1952: Forecasting in the Middle Latitudes. Meteorological Monograph 5. American Meteorological Society, 80 pp.

_____, 1963: Tropopause Circulation and Jet Streams. World Survey of Climatology. Vol 4. Climate of the Free Atmosphere. D. F. Rex, Ed., 85-193.

Rossby, C. G., 1949: On the Nature of the General Circulation of the Lower Atmosphere. The Atmosphere of the Earth and Planets. G. P. Kuiper, Ed.. University of Chicago Press, 16-48.

Sawyer, J. S. 1956: The Vertical Circulation at Meteorological Fronts and its Relation to Frontogenesis, Proc. Roy. Soc. London, A234, 346-362.

Shapiro, M. A., 1974: A Multiple Structured Frontal Zone-Jet Stream System as Revealed by Meteorologically Instrumented Aircraft. Monthly Weather Review, 102, 244-253.

_____, 1981: Frontogenesis and Geostrophically Forced Secondary Circulations in the Vicinity of Jet Stream-Frontal Zone Systems. Journal of the Atmospheric Sciences, 38, 954-973.

Shapiro, M. A., 1983: Mesoscale Weather Systems of the Central United States. The National STORM Program: Scientific and Technical Bases and Major Objectives. R. A. Anthes, Ed. University Corporation for Atmospheric Research, P.O. Box 3000, Boulder CO 80307, 3.1-3.77.

_____, and P. J. Kennedy, 1981: Research Aircraft Measurements of Jet Stream Geostrophic and Ageostrophic Winds. Journal of the Atmospheric Sciences, 38, 2642-2652.

_____, A. J. Krueger and P. J. Kennedy, 1982: Nowcasting the Position and Intensity of Jet Streams Using A Satellite Borne Total Ozone Mapping Spectrometer. Nowcasting, K. A. Browning, ed. Academic Press, 137-145.

Uccellini, L. W., 1976: Operational Diagnostic Applications of Isentropic Analysis. National Weather Digest, 1, 4-12.

_____, 1980: On the Role of Upper Tropospheric Jet Streaks and Leeside Cyclogenesis in the Development of Low-Level Jets in the Great Plains. Monthly Weather Review, 108, 1689-1696.

_____, and D. R. Johnson 1979: The Coupling of Upper and Lower Tropospheric Jet Streaks and Implications For the Development of Severe Convective Storms. Monthly Weather Review, 107, 682-703.

_____, D. R. Johnson and R. E. Schlesinger, 1979: An Isentropic and Sigma coordinate Hybrid Numerical Model: Model Development and some Initial Tests. Journal of the Atmospheric Science, 36, 390-414.

_____, P. J. Kocin, R. A. Peterson, C. H. Wash and K. F. Brill, 1984: The President's Day Cyclone of 18-19 February 1979: Synoptic Overview and Analysis of the Subtropical Jet Streak Influencing the Precyclogenetic Period. Monthly Weather Review, 107, 962-988.

Weldon, R. B., 1979: Satellite Training Course Notes. Part 4. Cloud Patterns and the Upper Air Wind Field. Applications Division, NESS (NOAA), Washington D. C.. 80 pp.

Wetzel, P. J., W. R. Cotton, and R. L. McAnelly, 1983: A Long-Lived Mesoscale Convective Complex. Part II: Evolution and Structure of the Mature Complex. Monthly Weather Review, 111, 1919-1937.

Whitney, L. F., 1977: Relationship of the Subtropical Jet Stream to Severe Local Storms. Monthly Weather Review, 105, 398-412.

BIOGRAPHY OF THE AUTHOR

William D. Nichols was born in Aurora, Colorado on May 9, 1955. The son of an Air Force officer, he spent his childhood years in 13 locations including West Germany and Okinawa. He graduated from Southwest High School in Dallas, Texas in 1973. He attended Texas A&M University in College Station, Texas where he graduated with a Bachelor of Science degree in Meteorology in 1977. Upon his graduation, he was commissioned a second lieutenant in the United States Air Force and attended Undergraduate Navigator Training at Mather AFB, California, graduating in 1979.

The author flew for four years as a navigator aboard Air Force B-52G aircraft. In 1983, the author was reassigned as a weather forecaster/briefer to Seventh Weather Wing at Scott AFB, Illinois. In August, 1985, he entered graduate school at Saint Louis University at St. Louis, Missouri and began his studies toward a Master of Science degree in Meteorology.

He is married to the former Patricia Elaine Bante, and they have a daughter, Kathryn Anne. The author's parents, Colonel and Mrs. Carl B. Nichols, Jr., currently reside in DeSoto, Texas.

END

JAN.

1988

DTIC